

SAND80-2813

~~CONFIDENTIAL~~

SAND80-2813

Unlimited Release

RETURN TO R. W. LYNCH, NNWSI
PROJECTS DEPARTMENT LIBRARY

2737

PROPERTY OF WMT LIBRARY

PRELIMINARY THERMAL ANALYSES FOR A NUCLEAR WASTE REPOSITORY IN TUFF

David K. Gartling, Roger R. Eaton, Robert K. Thomas

Prepared by Sandia Laboratories, Albuquerque, New Mexico 87185
and Livermore, California 94550 for the United States Department of
Energy under Contract DE-AC04-76DP00780

Printed April 1981



Sandia National Laboratories

SF 2900-G(3-80)

1.2.4.2.1.1

REPORTS REMOVED FROM LIBRARY MUST BE SIGNED
SIGN LOG SHEET TO BORROW REPORT.

Issued by Sandia Laboratories, operated for the United States
Department of Energy by Sandia Corporation.

NOTICE

This report was prepared as an account of work sponsored by the United States Government. Neither the United States nor the Department of Energy, nor any of their employees, nor any of their contractors, subcontractors, or their employees, makes any warranty, express or implied, or assumes any legal liability or responsibility for the accuracy, completeness or usefulness of any information, apparatus, product or process disclosed, or represents that its use would not infringe privately owned rights.

Printed in the United States of America

**Available from
National Technical Information Service
U.S. Department of Commerce
5285 Port Royal Road
Springfield, VA 22161**

Price: Printed Copy \$8.00; Microfiche \$3.00

CONTENTS

	<u>Page</u>
INTRODUCTION	7
PROBLEM DESCRIPTION	8
Stratigraphy and Thermal Properties	8
Repository Geometry	10
Wasteform	10
ANALYSIS AND RESULTS	19
Far Field Models	19
Room and Pillar Models	19
Near Field Models	22
SUMMARY	23
REFERENCES	24
APPENDIX A: ROOM AND PILLAR ANALYSIS FOR HLW	25
APPENDIX B: ROOM AND PILLAR ANALYSIS FOR SF	60
APPENDIX C: NEAR FIELD ANALYSIS FOR HLW	95

LIST OF FIGURES

	<u>Page</u>
Figure 1. Mine Design Working Group Specifications -- Room Design, HLW	15
Figure 2. Mine Design Working Group Specifications -- Room Design, SF	16
Figure 3. Repository Modeling -- Room and Pillar Models	21

LIST OF TABLES

	<u>Page</u>
Table 1. Assumed Stratigraphy and Material Thermal Properties -- Tuff Mine Design Activity	9
Table 2. Heat of Vaporization of H ₂ O, Addition to Heat Capacity	11
Table 3. Backfill Properties	12
Table 4. Wasteform Material Properties	13
Table 5. Repository Geometry and Initial Conditions	14
Table 6. Canister Dimensions and Initial Power Output	17
Table 7. Normalized Waste Power as a Function of Waste Form and Time After Emplacement	18

INTRODUCTION

The potential use of welded tuff as an isolation medium for nuclear waste material is the subject of a continuing investigation at Sandia National Laboratories. A central issue in assessing the suitability of tuff as a repository medium is the thermal response of the rock due to the emplacement of heat producing waste. The purpose of the present document is to provide some results of the initial thermal analysis for a generic waste repository sited in welded tuff and located below the water table at the Nevada Test Site (NTS). The parametric analyses presented here were intended to provide order-of-magnitude bounds on the thermal response of a repository environment; the results are not to be interpreted as the expected thermal environment in a repository.

The work outlined in the following sections was carried out at the request of a working group that was organized to support the tuff study program. The Mine Design Working Group (MIDES) was chartered to act generally as a focal point for research activities associated with the tuff program and specifically to address issues and data needs associated with the conceptual design of a mined repository. In developing the initial thermal analysis program, the MIDES group chose to divide the task into a series of six subtasks. These subproblems were defined according to the type of waste form considered (high level waste, HLW, or spent fuel, SF) and the geometric scale of the analysis (far field or entire repository scale, room and pillar scale, and waste canister or very near field scale). Responsibility for the analysis of these six problems was divided between members of the working group as shown below:

<u>Waste Form</u>	<u>Geometric Scale</u>	<u>Responsible Organization</u>	<u>Principle Investigator</u>
High Level	Far Field	Texas A&M University	J. Russell
High Level	Room and Pillar	SNLA/Division 5511	D. Gartling
High Level	Very Near Field	SNLA/Division 5511	R. Eaton
Spent Fuel	Far Field	RE/SPEC	W. McLain
Spent Fuel	Room and Pillar	SNLA/Division 5521	R. Thomas
Spent Fuel	Very Near Field	RE/SPEC	P. Gnirk

This present report is limited to the presentation of results obtained at SNLA; results for the remaining cases may be found in References 1-3.

PROBLEM DESCRIPTION

The problem considered in the present work concerns the thermal response of a mined, room and pillar repository to the emplacement of high level (HLW) or spent fuel (SF) nuclear waste. A primary objective of the analysis was the determination of changes in the thermal response of the repository due to variations in parameters such as gross thermal loading (GTL) of the repository, extraction ratio (ER), type of room backfill and potential dry-out of the initially saturated rock. In essence, this work was designed to provide a preliminary thermal "data base" for future work in the tuff repository program.

Detailed specifications for a generic repository geometry, stratigraphic location, material properties, waste configuration, etc., were provided by the MIDES group. These specifications are outlined here for completeness.

Stratigraphy and Thermal Properties

The assumed stratigraphy for the repository location is given in Table 1. This data is taken from UE25A-1, a fully cored drill hole in the Southwest section of the NTS and immediately adjacent to Yucca Mountain. Also shown are the relevant thermal properties for each layer. The repository horizon is assumed to be at a depth of 800 m and lies in the welded tuff Bullfrog member below 711 m. The water table is located 500 m below the surface.

TABLE 1

ASSUMED STRATIGRAPHY AND MATERIAL THERMAL PROPERTIES--TUFF MINE DESIGN ACTIVITY *

Depth-m (ft)	Porosity	(Mg/m ³)		(cal/cm ³ °C)		K (W/mK)		T (°C) T _{boil} (hydrostatic)
		Bulk Density	Grain Density	ρC_p	ρC_p	< T _{boil}	> T _{boil}	
0-53 (0-173)	0.11	2.38	2.56 (m)	0.66	0.46	1.4	2.3	100°C
53-63 (173-208)	0.28	2.07	2.53 (m)	0.82	0.36	1.9		100°C
63-84 (208-276)	0.50	1.53	2.46 (m)	0.84	0.25	0.9	0.7	100°C
84-139 (276-457)	0.12	2.37	2.56 (a)	0.67	0.45	2.6	2.3	100°C
139-192 (457-631)	0.50	1.78	2.56 (a)	0.50	0.26	0.85	0.7	100°C
192-286 (631-939)	0.12	2.37	2.57 (m)	0.67	0.45	2.6	2.3	100°C
286-328 (939-1076)	0.50	1.78	2.56 (a)	0.50	0.26	0.85	0.7	100°C
328-388 (1076-1273)	0.11	2.38	2.56 (m)	0.67	0.46	2.6	2.3	100°C
388-401 (1273-1317)	0.13	2.26	2.43 (m)	0.68	0.43	1.2	1.0	100°C
401-416 (1317-1364)	0.28	2.05	2.45 (a)	0.86	0.35	1.10	0.7	100°C
416-545 (1364-1789)	0.31	1.97	2.40 (m)	0.89	0.33	1.05 (calc) 1.10 (meas)	0.67 (calc) 0.71 (meas)	100°C
545-560 (1789-1836)	0.25	2.12	2.50 (a)	0.85	0.37	1.1	0.8	175
560-578 (1836-1897)	0.29	2.15	2.61 (a)	0.92	0.37	1.55	1.0	187
578-594 (1897-1950)	0.25	2.21	2.61 (m)	0.88	0.39	1.65	1.1	189
594-614 (1950-2014)	0.18	2.34	2.62 (m)	0.80	0.43	1.80 (meas) 1.80 (calc)	1.39 (calc) 1.33 (meas)	195
614-643 (2014-2110)	0.32	2.13	2.55 (m)	0.98	0.36	1.90	1.2	203
643-697 (2110-2288)	0.29	2.10	2.55 (a)	0.90	0.36	2.0	1.3	214
697-711 (2288-2333)	0.29	2.17	2.65 (a)	0.93	0.38	2.1	1.4	221
711-- (2333--)	0.23	2.28	2.66 (m)	0.87	0.41	2.4 (meas) 2.35 (calc)	1.65 (meas) 1.7 (calc)	223

(a) - assumed

(m) - measured

* Data is taken from the Mine Design Working Group - Activity
Work Package dtd. 12/4-5/79.

Since consideration was given to the possibility of vaporization of pore fluid in the tuff layers, data on the heat of vaporization was required. This data for the assumed stratigraphy is given in Table 2. Thermal property data was also required for the various room backfill materials and for the two wasteforms; this data is summarized in Tables 3 and 4, respectively.

Repository Geometry

Specifications for the overall repository geometry and the ambient conditions at the repository location are given in Table 5. The repository is assumed to be of a conventional room and pillar type. For analysis purposes, it is then required to have the geometry of the room cross-section defined. Figures 1 and 2 show the geometric description of the rooms for the HLW and SF, respectively.

Wasteform

The waste material is assumed to be encapsulated in a cylindrical container and buried in the floors of the repository rooms. The canister geometries and initial thermal power outputs for both HLW and SF are summarized in Table 6. The thermal output from each canister is a function of time due to the radioactive decay process. A tabulation of the normalized power output for each wasteform as a function of time is given in Table 7.

TABLE 2
HEAT OF VAPORIZATION OF H₂O, ADDITION TO HEAT CAPACITY *

Depth-m (ft)	For boiling @ 100°C		For Boiling @ 220°C (assumed conservative above this depth)	
	Total ($\frac{\text{cal}}{\text{cm}^3}$)	Avg. Spread Over 20°C ($\frac{\text{cal}}{\text{cm}^3 \text{ } ^\circ\text{C}}$)	Total ($\frac{\text{cal}}{\text{cm}^3}$)	Avg. Spread Over 20°C ($\frac{\text{cal}}{\text{cm}^3 \text{ } ^\circ\text{C}}$)
0- 53 (0- 173)	51	2.55	35	1.76
53- 63 (173- 208)	131	6.55	89	4.47
63- 84 (208- 276)	233	11.65	160	7.98
84-139 (276- 457)	56	2.80	38	1.91
139-192 (457- 631)	43	2.15	29	1.44
192-286 (631- 939)	56	2.80	38	1.91
286-328 (939-1076)	43	2.15	29	1.44
328-388 (1076-1273)	51	2.55	35	1.76
388-401 (1273-1317)	68	3.40	46	2.31
401-416 (1317-1364)	145	7.25	99	4.96
416-545 (1364-1789)	161	8.05	110	5.50
545-560 (1789-1836)	130	6.50	89	4.43
560-578 (1836-1897)	150	7.50	103	5.14
578-594 (1897-1950)	130	6.50	89	4.43
594-614 (1950-2014)	93	4.65	64	3.19
614-643 (2014-2110)	166	8.30	113	5.67
643-697 (2110-2288)	150	7.50	103	5.14
697-711 (2288-2333)	150	7.50	103	5.14
711-- (2333--)	120	6.00	82	4.08

* Data is taken from the Mine Design Working Group - Activity
Work Package dtd. 12/4-5/79.

TABLE 3
BACKFILL PROPERTIES *

<u>Case I</u>	<u>Fully saturated</u>
	$\rho_b = 1.64 \text{ g/cm}^3$
	$\phi = 0.62$
	$K = 1.18 \text{ W/mK}$
	$\rho_b C_p = 1.14 \text{ cal/cm}^3\text{K}$
<u>Case II</u>	<u>Fully dehydrated</u>
	$\rho_b = 1.01 \text{ g/cm}^3$
	$\phi = 0.62$
	$K = 0.48 \text{ W/mK}$
	$\rho_b C_p = 0.20 \text{ cal/cm}^3\text{K}$

Assumptions

1. Material is crushed tuff, matrix properties of Bullfrog Member of Crater Flats Tuff (i.e., from 711 m to = , see table)
2. 50% compaction

* Data is taken from the Mine Design Working Group - Activity Work Package dtd. 12/4-5/79

TABLE 4
WASTEFORM MATERIAL PROPERTIES*

HLW (vitrified)

$$\begin{aligned}\rho_b &= 187 \text{ lb/ft}^3 \\ C_p &= 0.2 \text{ BTU/lb}^\circ\text{F} \\ K &= 0.7 \text{ BTU/hr ft}^\circ\text{F}\end{aligned}$$

<u>SF(UO₂)</u>	<u>UO₂</u>	<u>Zircalloy</u>
ρ_b (lb/ft ³)	684	412

	<u>T(°F)</u>	
UO ₂	300	1000
C _p (BTU/lb°F)	4.05	2.37
K (BTU/hr ft°F)	0.056	0.067

	<u>T(°F)</u>		
Zircalloy	200	600	1000
C _p	0.073	0.081	0.086
K	8.42	9.42	10.9

SF - 1 assembly/can,

assume: 289 pins, in 17 x 17 array

pitch/diameter ratio between pins: 1.36

rod diameter: 0.38"

cladding thickness: 0.021"

pin O.D.: 0.32"

carbon steel, air filler

* Data is taken from the Mine Design Working Group - Activity Work Package dtd. 12/4-5/79.

TABLE 5
REPOSITORY GEOMETRY AND INITIAL CONDITIONS*

Repository Depth (to top of heat-producing zone): 800 m
Thickness of Heat-Producing Zone for Generalized Repository: 10 m
Repository Area: 2000 acres
Geothermal Heat Flux: $1.6 \mu\text{cal}/\text{cm}^2\text{s}$
Static Water Level (depth): 470 m
Air Surface Temperature: 20°C
Initial Temperature at Disposal Horizon: 35°C

* Data is taken from the Mine Design Working Group - Activity
Work Package dtd. 12/4-5/79.

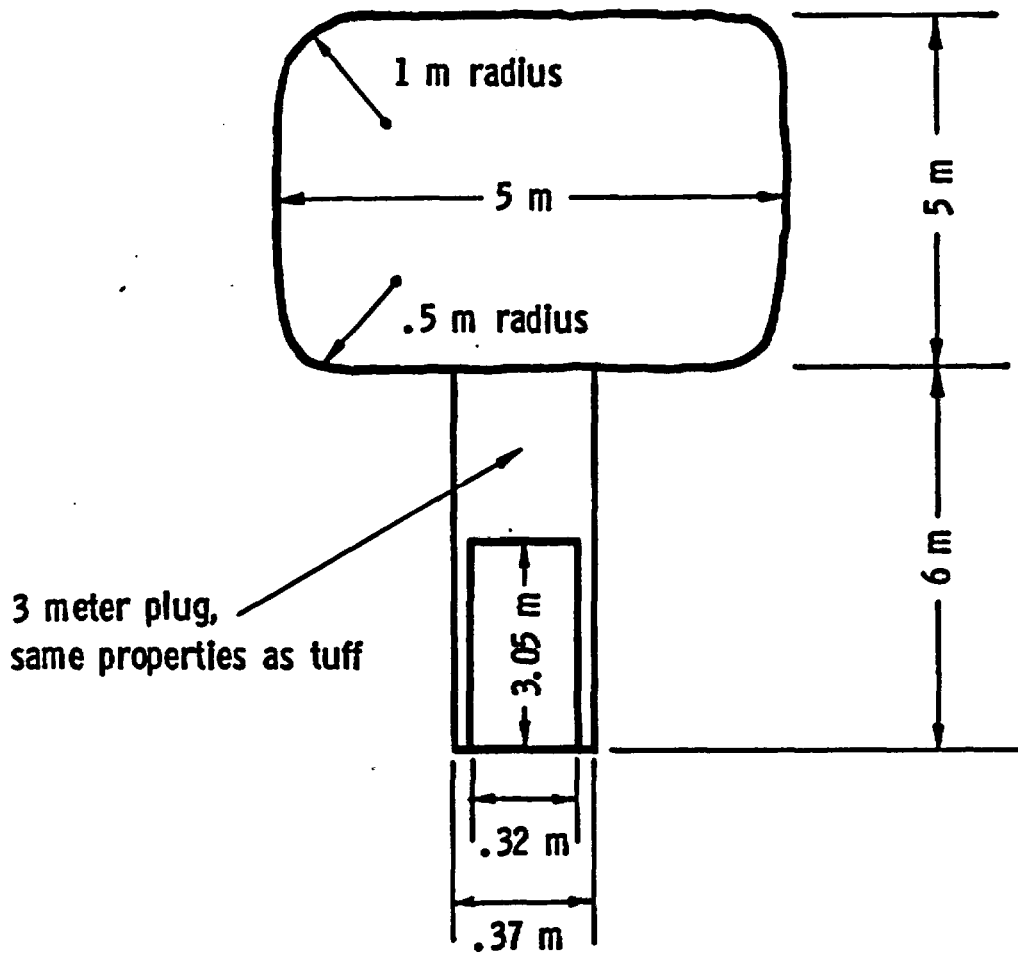


FIGURE 1. Mine Design Working Group Specifications--
Room Design, HLW

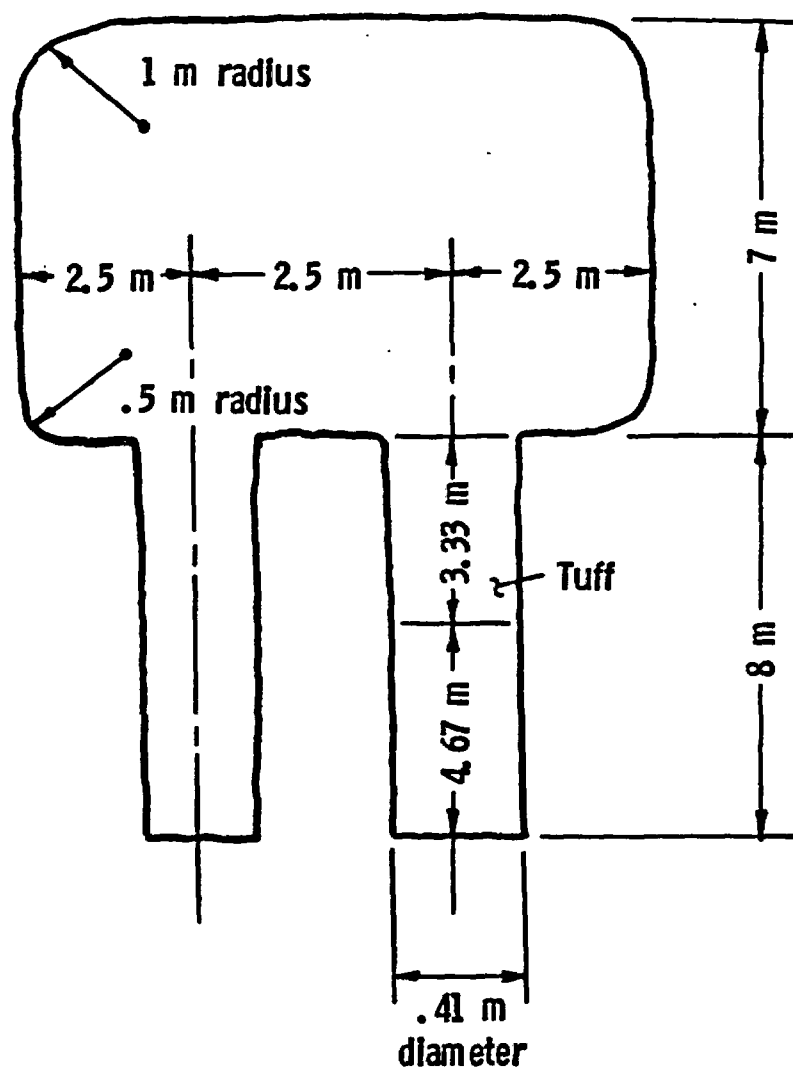


FIGURE 2. Mine Design Working Group Specifications--
Room Design, SF

TABLE 6
CANISTER DIMENSIONS AND INITIAL POWER OUTPUT *

Spent Fuel Canister Dimensions

Total Length, 4.67 m
Outside Diameter, 0.355 m
Inside Diameter, 0.30 m
Heated Length, 3.66 m
Air-Filled
Canister Material--Carbon Steel

HLW Canister Dimensions

Total Length, 3.05 m
Outside Diameter, 0.32 m
Inside Diameter, 0.30 m
Heated Length, 3.0 m
Canister Material--Stainless 304

Power at Time of Emplacement; Waste Assumed 10 Years Old

HLW: 3.5 kW/can
SF: 0.55 kW/can

* Data is taken from the Mine Design Working Group - Activity
Work Package dtd. 12/4-5/79.

TABLE 7
NORMALIZED WASTE POWER AS A FUNCTION OF WASTE
FORM AND TIME AFTER EMPLACEMENT*

Waste Age After Emplacement (Assume 10 yrs old at emplacement)	HLW (UO ₂) Q/Q ₀	SF (UO ₂) Q/Q ₀
0	1.0	1.0
1	0.95	---
2	0.907	---
3	0.871	---
4	0.851	---
5	0.810	0.848
6	0.783	---
7	0.769	---
8	0.734	---
9	0.714	---
10	0.692	0.758
15	0.600	---
20	0.529	0.625
30	0.402	0.521
40	0.313	0.439
55	---	0.347
70	0.157	0.282
90	---	0.224
100	0.0864	---
190	0.0296	0.152
290	0.0215	0.102
390	---	0.0884
400	0.0167	---
490	---	0.0778
590	0.127	---
649	---	0.0651
690	0.0113 *	---
990	0.00810 *	0.0455
1990	0.00404	0.0238
2990	---	0.0184
3990	---	0.0165
4990	---	0.0153
6490	---	0.0139
9990	---	0.0112
14990	---	0.00851
19990	---	0.00670
29990	---	0.00445

* These values
being checked

* Data is taken from the Mine Design Working Group - Activity
Work Package dtd. 12/4-5/79.

ANALYSIS AND RESULTS

As noted previously, the thermal analysis of the repository was divided into six subproblems based on type of wasteform and a geometric scaling for the analysis. The present section provides a brief description of the analyses carried out for each subproblem.

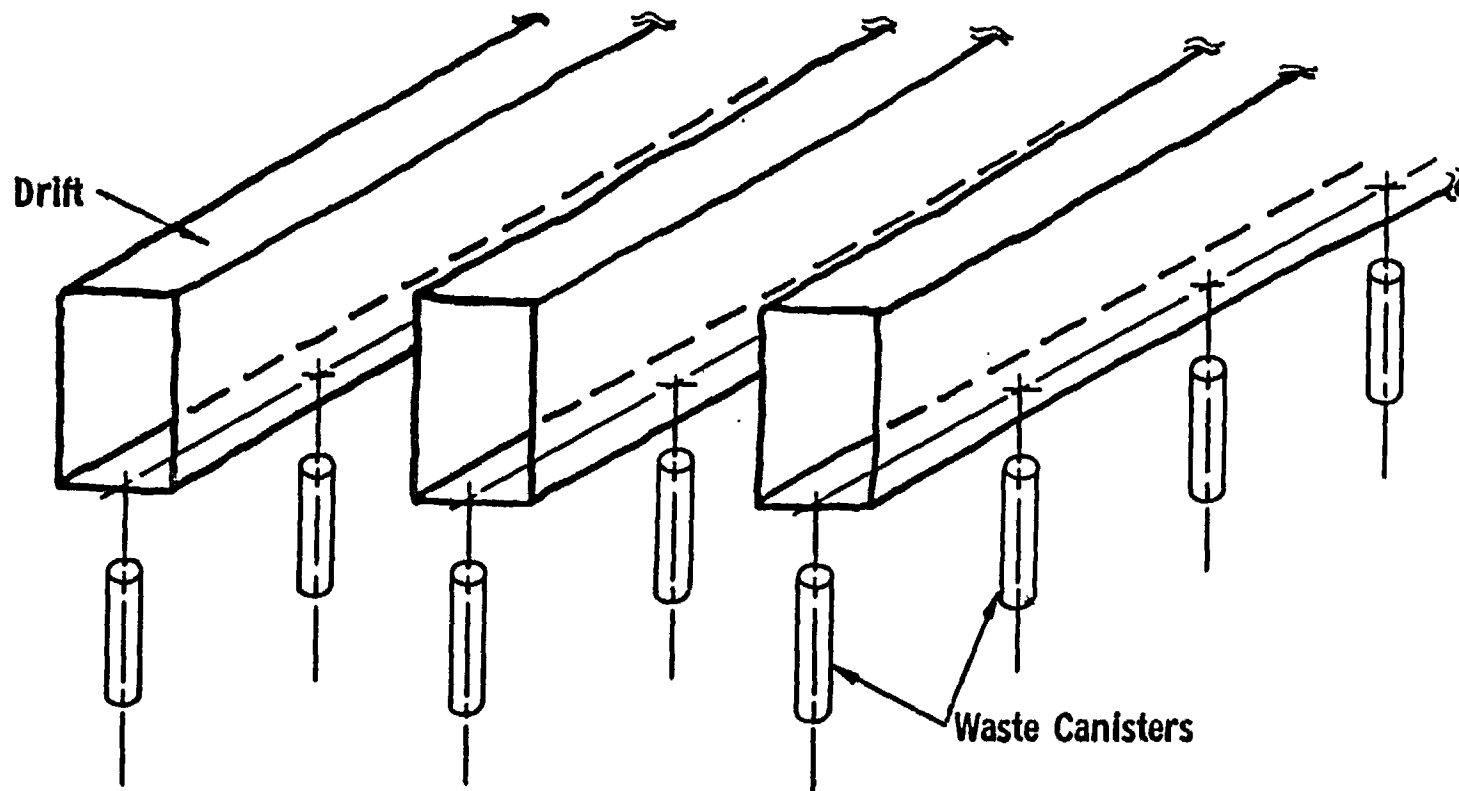
Far Field Models

The far field or global repository analyses assume that the repository and its thermal output can be modeled as a heat producing disc located at the appropriate horizon in the assumed geologic stratigraphy. Typically, these far field models attempt to estimate the temperature field over horizontal and vertical dimensions of several kilometers. The far field calculations for the present repository configuration were carried out by several contractors to Sandia National Laboratories. These results may be found in References 1 and 2.

Room and Pillar Models

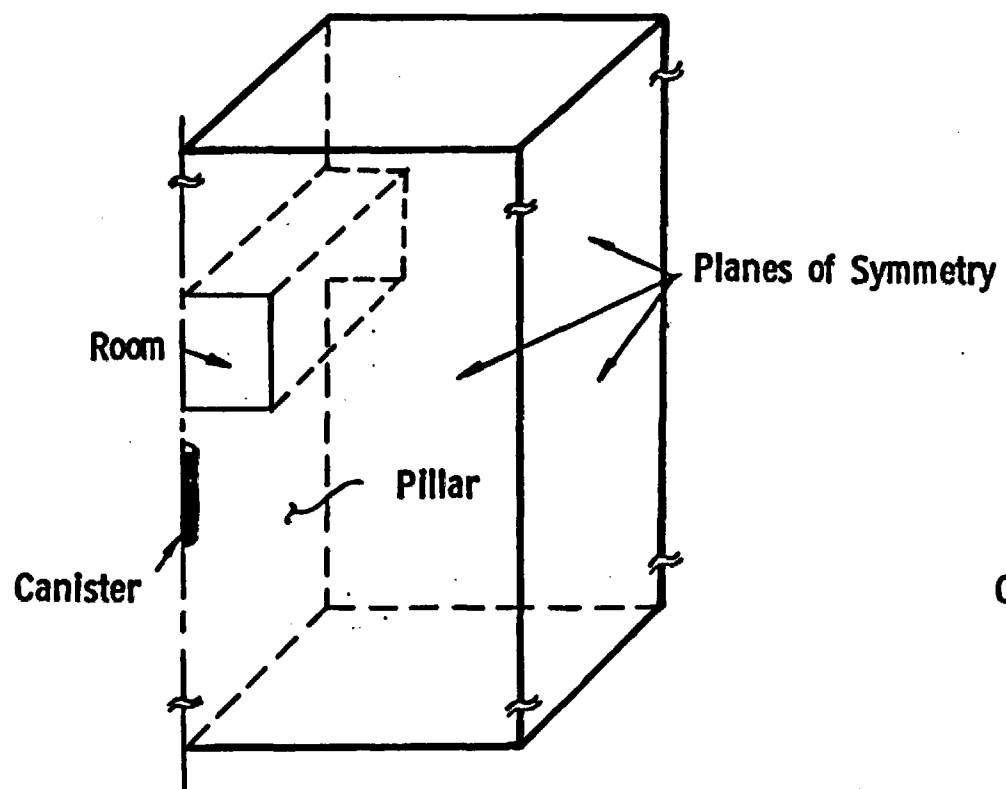
The second level of analysis considered the temperature field on the scale of an individual repository room and pillar. Invoking the usual arguments regarding the multiplicity of identical drifts in a full repository and identifying the existing planes of symmetry allowed the problem sketched in Figure 3a for HLW to be reduced to the simpler geometry shown in Figure 3b. The three-dimensional problem illustrated in Figure 3b may be simplified to a two-dimensional model if the cylindrical waste canister is idealized as an "equivalent" planar heat source. This technique was used in both the HLW and SF room and pillar analyses. A typical (HLW) model is shown in Figure 3c.

The room and pillar computations were carried out at Sandia using two general purpose (finite element) heat conduction computer codes. The program COYOTE⁴ was used for the HLW geometry while the ADINAT⁵ program was used to

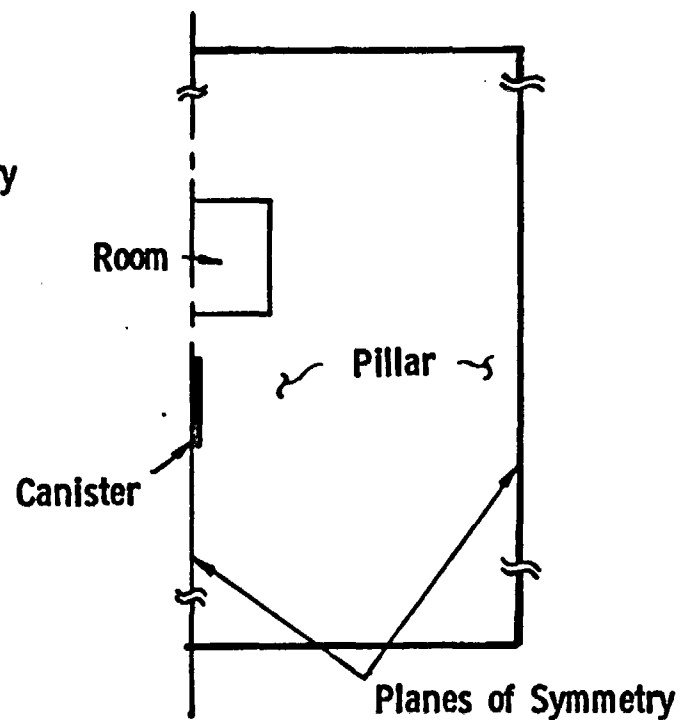


a) Schematic of Typical Room and Pillar Waste Storage, HLW

Figure 3. Repository Modeling - Room and Pillar Models



**b) Schematic of 3-Dimensional
Unit Cell Model, HLW**



**c) Schematic of 2-Dimensional
Unit Cell Model, HLW**

Figure 3. Repository Modeling - Room and Pillar Models

model the SF case. In both instances the programs were employed to model the transient temperature response of a typical room and pillar due to the imposed heat load.

The analyses were carried out in a parametric fashion with the independent variables being the repository gross thermal loading (i.e., canister spacing or thermal power density for the planar source), mine extraction ratio (i.e., pillar width), type of backfill material and vaporization temperature of the pore fluid. The specifications for the parameter variations were provided by the MIDES group and are reproduced in Appendices A and B for HLW and SF, respectively. Details of the thermal models and results of the numerical computations are also provided in the Appendices.

Near Field Models

The third and final level of thermal analysis considered the temperature response in the immediate vicinity of the waste canister. The models for this case were intended to be of sufficient detail to include the major features of the waste package structure (e.g., air gaps between canister and tuff borehole). Like the room and pillar models the basic geometry for the near field model is inherently three-dimensional. However, for the HLW geometry the effective radius concept was used to simplify the problem to a two-dimensional (axisymmetric) geometry. This idea is more fully described and justified in Appendix C. The SF waste geometry could not be reduced to a simpler model and therefore was analyzed as a three-dimensional problem.

The near field HLW analysis was carried out using the finite element conduction code, COYOTE.⁴ The independent variables in the parametric study of this problem were specified by the MIDES group and are reproduced in Appendix C. Details of the thermal models and results of the computations are also collected in Appendix C. The results of the near field SF analysis can be found in Reference 3.

SUMMARY

Under the direction and guidance of the MIDES working group a series of scoping thermal calculations were carried out for a generic nuclear waste repository sited in tuff. The thermal analyses were performed on three geometric scales that included far field or global repository models, individual room and pillar models and near field single canister models. Both HLW and SF waste-forms were considered in the computations. The present document serves to collect the results of those thermal calculations performed at Sandia National Laboratories, i.e., room and pillar analyses of HLW and SF and the near field analysis for HLW. The remaining thermal calculations may be found in the previously referenced documents.

REFERENCES

1. M. L. Klasi, J. E. Russell, W. C. McClain, and T. Brandshaug, Far Field Thermal Analysis of a High Level Waste Repository in Tuff, RSI-0137, RE/SPEC, Inc., Rapid City, South Dakota, January, 1981.
2. M. L. Klasi, W. C. McClain and T. Brandshaug, Far-Field Thermal Analysis of a Spent Fuel Repository in Tuff, RSI-0128, RE/SPEC, Inc., Rapid City, South Dakota, November, 1980.
3. D. Parrish, Very Near Field Thermal Analysis of a Spent Fuel Repository in Tuff, RSI-0144, RE/SPEC, Inc., Rapid City, South Dakota, in preparation.
4. D. K. Gartling, COYOTE - A Finite Element Computer Program for Nonlinear Heat Conduction Problems, SAND77-1332, Sandia National Laboratories, Albuquerque, New Mexico
5. K. J. Bathe, ADINAT - A Finite Element Program for Automatic Dynamic Incremental Nonlinear Analysis of Temperatures, MIT Report 82448-5 May, 1977 (Revised December 1978).

APPENDIX A
Room and Pillar Analysis for HLW

- Part I: MIDES Working Group - Work Package
- Part II: Tuff Mine Design Thermal Analysis - High Level Waste
(Memo, D. K. Gartling, 5511, to Distribution, dtd. 2/4/80)
- Part III: Further Results for Tuff Mine Design Thermal Analysis - High Level Waste
(Memo, D. K. Gartling, 5511, to Distribution, dtd. 2/19/80)
- Part IV: The Effect of Thermal Radiation in the Disposal of High Level Waste in Tuff
(Memo, O. L. George, 5511, to D. F. McVey, 5511, dtd. 1/4/80)
- Part V: Further Results Concerning the Effect of Thermal Radiation and Free Convection in the Drift of a High Level Waste Repository in Tuff
(Memo, O. L. George, 5511, to D. F. McVey, 5511, dtd. 1/22/80)

TUFF MINE DESIGN WORKING GROUP

ACTIVITY WORK PACKAGE

TITLE: Room-and-Pillar Thermal Analysis - High Level Waste

INVESTIGATOR: D. F. McVey (SLA, Div. 5511)

PHONE NUMBER: (505) 264-4949

OBJECTIVE: To model room temperatures as a function of extraction ratio, power densities, and resultant pitches

DESCRIPTION:

1. Model Geometry - 2-D planar
2. Room Initial Conditions - see specifications (5)
3. Room and Canister Dimensions, Hole Geometry, Initial Canister Power - see specifications (7 & 8)
4. Waste - HLW, instantaneous emplacement; for waste thermal output history see specification (9); for waste material and thermal properties see (10)
5. Backfill - assume room open 50 years, with radiative heat transfer, but no active cooling; for backfill properties - see specification (4)
6. Temperature-Dependent Rock Properties (K, ρC_p , etc.) - use properties for tuff layer at greater than 711 m depth, see specifications (2 & 3)

PARAMETERS:

1. Extraction Ratio and Power Densities
 - a. 10% extraction ratio - 75 kW/acre
 - b. 20% extraction ratio - 25, 75, 150 kW/acre
 - c. 30% extraction ratio - 75 kW/acre
2. Boiling Temperature
 - Case I - 100°C
 - Case II - hydrostatic-head - potential boiling (223°C), see specification (2)(Case II run at discretion of modeler)

DUE DATE: February 5, 1980

REPORTING: 1. Technical Memo (letter form) to Working Group Members
2. Presentation of Results

Sandia Laboratories

Albuquerque, New Mexico
Livermore, California

date: February 4, 1980

to: Distribution

D. K. Gartling

from: D. K. Gartling - 5511

subject: Tuff Mine Design Thermal Analysis - High Level Waste

At the request of the mine design working group, the thermal analysis of a high level waste repository was undertaken. The specifications for the problem of interest were outlined in the work package section of Reference 1. The primary objectives of the analysis were the prediction of peak room and pillar temperatures as a function of mine extraction ratio, thermal power loading and type of backfill material.

Thermal Model

The two-dimensional room and pillar geometry for the case of a high level waste repository is shown schematically in Figure 1. Canister dimensions, burial depth, and drift dimensions were maintained as shown in the figure; pillar width (S_2) was varied to produce the extraction ratios ($ER = S_1/S_2$) of interest. The vertical dimension of the model was carried to $\pm 250m$ from the drift floor.

The assumption of a two-dimensional planar model for the mine required that the thermal energy produced by an array of cylindrical canisters be converted into an "equivalent" planar heat source. This conversion was effected by uniformly distributing the energy in each canister over a rectangular slab with dimensions corresponding to the canister height, diameter and canister pitch. The canister pitch was varied between cases in order to maintain an initial canister power of 3.5 KW in conjunction with the assumed gross thermal loading (GTL) for the repository. In all cases, the heat source varied with time according to the decay law for high level waste as specified in Reference 1.

The repository was assumed to reside in a uniform layer of saturated tuff with material properties as specified in Reference 1. The drift was assumed to be opened for the first 50 years after canister emplacement. Heat transfer (i.e., radiation) across the air filled drift was simulated through the use of an "effective" material as defined in References 2 and 3. The drift was filled 50 years after canister emplacement with either a saturated tuff or dehydrated tuff backfill. The boiling point and latent heat of vaporization for the pore fluid in the tuff and backfill were taken as parameters in the study. Thermal conductivity and heat capacity for the tuff and backfill were assumed to vary with temperature as shown in Figure 2. Further details of the mine geometry, waste form, material properties, etc., may be found in Reference 1.

The thermal analysis of the model outlined above was carried out using the finite element conduction code, COYOTE (4). Figure 3 shows a typical element mesh for the problem which contains 320 elements and approximately 1000 temperature nodes. The transient analysis was performed using a modified Crank-Nicholson time integration scheme with quasilinearization (i.e., nonlinear coefficients are evaluated at the beginning of the time step - no equilibrium iterations are performed). Typically, approximately 100 time steps were used to carry the computation out to 250 years; time steps ranged in value from approximately six days to ten years. A check on the time integration was made by re-running several cases with the time steps reduced by a factor of 2. As the thermal response of the model was found to be independent of the choice of time step, the transient solution was judged to be of acceptable accuracy.

Results and Discussion

Fifteen cases were analyzed for the high level waste configuration and these are tabulated in Table I according to extraction ratio (ER). For the 10% and 30% ER's, the gross thermal loading (GTL) was held at 75 KW/acre while the type of backfill and boiling temperature were varied. The 20% ER was studied more extensively by allowing the GTL to take on values of 25, 75, and 150 KW/acre. As the data produced from these computations were quite voluminous, no attempt will be made to describe each case in detail. Rather, some typical results will be presented followed by a discussion of the trends inferred by the remaining cases.

Shown in Figures 4-6 are a series of isotherm plots for a 20% ER that was backfilled at 50 years with saturated tuff. The boiling point was 100°C. The GTL's for the three cases shown are 25, 75, and 150 KW/acre. The main point of interest in these figures is the variation in the volume of tuff near the heat source that exceeds 100°C and is therefore subject to dryout. With increasing GTL (decreasing canister pitch), the dryout zone is observed to increase rapidly in size for a given point in time. Similar trends were apparent for the cases where the GTL was fixed (at 75 KW/acre) and the extraction ratio (i.e., canister pitch) varied. The lower extraction ratios (smaller pitch) produced large dryout zones.

The effect of increasing the assumed boiling temperature on the isotherm pattern is shown in Figure 7 for the case of a 20% ER and GTL's of 75 and 150 KW/acre. Since the dryout process serves to extract energy from the system (through the heat of vaporization), it would be expected that a low boiling point would result in generally lower temperatures for a fixed power input. That this is the case may be seen in Figure 7 (especially the GTL of 150 KW/acre) where the volume of material at a temperature greater than 107°C is much smaller for the 100°C boiling point case than for the 220°C case. Further reference to this point will be made when peak temperatures in the room and pillar are discussed.

Of particular interest in this study were the temperatures of representative points in the mine drift and pillar. Shown in Figures 8-9 are temperature histories for points around the periphery of the drift and through the mid-height of the pillar. Also, shown in Figure 10 are temperature profiles (for selected times) taken through the mid-height of the room and pillar. The precise locations of these temperature computations are shown in Figure 1. All of the data presented in Figures 8-10 are for the "average" case of 20% ER, GTL = 75 KW/acre with saturated backfill and a 100°C boiling point.

Prior to backfill (time <50 years), the temperature of the room boundary (Figure 8) is very uniform due to the effectiveness of the radiative heat transfer across the drift. Also, just prior to backfilling the temperatures in the room and pillar are observed to reach a peak value and then decrease due to the decay of the heat source. Upon backfilling of the drift, the floor temperature (T_1) increases rapidly for a short period of time while the ceiling temperature (T_2) is reduced. The backfill produces a large thermal resistance (compared to radiation) across the room which in turn produces an appropriate temperature gradient in the backfill. The temperature difference across the filled drift decreases with time due to the decreasing energy output of the waste material. The temperatures through the pillar (Figures 9-10) are seen to be relatively uniform especially after backfill has occurred. Prior to backfill, the temperatures near the drift wall are affected by the radiative transfer in the room.

Examination of the room and pillar data for cases with other ER's and GTL's showed the results to be qualitatively similar to those illustrated in Figures 8-10. Quantitative differences between cases were observed primarily in the magnitude of the floor and ceiling temperature perturbations at the time of backfill and the degree of temperature non-uniformity in the pillar prior to backfill. For the lower thermal loadings (i.e., low GTL or high ER), the temperature change across the drift is reduced and the pillar temperatures are very uniform. At the higher thermal loads (i.e., high GTL or low ER), the temperature changes due to backfilling are increased and the temperature gradient through the pillar is larger. There was no significant effect on room and pillar temperatures due to the use of a dehydrated backfill in place of the saturated material.

In order to obtain a more quantitative idea of the variation in room and pillar temperatures with ER and GTL, Figures 11-13 were prepared. These figures show peak temperatures for the floor (T_1) room mid-height (T_3) and pillar centerline (T_4) plotted versus GTL with ER, boiling point and backfill material as parameters. Examining first the effect of ER (for a given GTL), it is seen that floor and room mid-height temperatures increase slightly with decreasing ER (decreasing canister pitch); pillar centerline temperatures decreased with a reduction in ER. Room temperatures are expected to vary inversely with canister pitch since for a fixed room/heat source orientation the canister pitch effectively determines the local thermal loading on the drift. However, the pillar centerline temperature varies directly with ER since the pillar width (distance from heat source) changes with ER.

Peak room and pillar temperatures are observed to vary linearly with GTL (fixed ER) when a 220°C boiling criteria is assumed. For the case of a 100°C boiling point, the temperature variation is linear with GTL up to 75 KW/acre; the departure from linearity at higher GTL's is a result of the significant loss of energy from the system due to dryout.

The data presented in Figures 11-13 showed no significant variation due to the type of material used in backfilling the drift. The lack of dependence on this parameter is felt to be due to several causes. For the lower GTL cases, room temperatures do not exceed a dryout temperature and as a result, the only difference between saturated and dehydrated backfill is the small variation in thermal properties. For the higher GTL cases where the room temperatures exceed the boiling point, some differences between backfills would be expected. However, in running the thermal model, the backfill was assumed to be emplaced with an initial temperature equal to the room temperature. Since room temperatures are above the boiling point at time of backfill, this assumption essentially reduced the saturated material to a dried out state and eliminated the difference between types

Distribution

-5-

February 4, 1980

of backfill. The use of this assumption also prevented both backfill materials from acting as a thermal sink as would be the case if the backfill was emplaced at a lower initial temperature.

DKG:5511:hm

Copy to:

Mine Design Working Group Members

4530	R. W. Lynch
4537	J. K. Johnstone
4537	A. R. Lappin
5500	O. E. Jones
5510	D. B. Hayes
5511	J. W. Nunziato
5511	R. R. Eaton
5520	T. B. Lane
5521	R. K. Thomas
5530	W. Herrmann

References

1. Mine Design Working Group, Activity Work Package, dtd. 12/4-5/79.
2. Memo, O. L. George, 5511, to D. F. McVey, 5511, dtd. 1/4/80, subject: The Effect of Thermal Radiation in the Disposal of High Level Waste in Tuff.
3. Memo, O. L. George, 5511, to D. F. McVey, 5511, dtd. 1/22/80, subject: Further Results Concerning the Effects of Thermal Radiation and Free Convection in the Drift of a High Level Waste Repository in Tuff.
4. D. K. Gartling, "COYOTE - A Finite Element Computer Program for Nonlinear Heat Conduction Problems," SAND77-1332, Sandia Laboratories, Albuquerque, New Mexico.

Distribution

-7-

February 4, 1980

Table I

Summary of Cases for Tuff Mine Design Analysis -
High Level Waste

	<u>Gross Thermal Loading (GTL) KW/acre</u>	<u>Pitch (metres)</u>	<u>Type of Backfill</u>	<u>Boiling Temperature °C</u>
10% Extraction Ratio ($S_1 = 2.5m$, $S_2 = 25.0m$)	75	3.777	Saturated	100
	75	3.777	Dehydrated	100
	75	3.777	Saturated	220
20% Extraction Ratio ($S_1 = 2.5m$, $S_2 = 12.5m$)	25	22.662	Saturated	100
	25	22.662	Dehydrated	100
	25	22.662	Saturated	220
	75	7.554	Saturated	100
	75	7.554	Dehydrated	100
	75	7.554	Saturated	220
	150	3.777	Saturated	100
	150	3.777	Dehydrated	100
	150	3.777	Saturated	220

Table I (cont)

	<u>Gross Thermal Loading (GTL) KW/acre</u>	<u>Pitch (metres)</u>	<u>Type of Backfill</u>	<u>Boiling Temperature °C</u>
30% Extraction Ratio ($S_1 = 2.5m$, $S_2 = 8.33m$)	75	11.331	Saturated	100
	75	11.331	Dehydrated	100
	75	11.331	Saturated	220

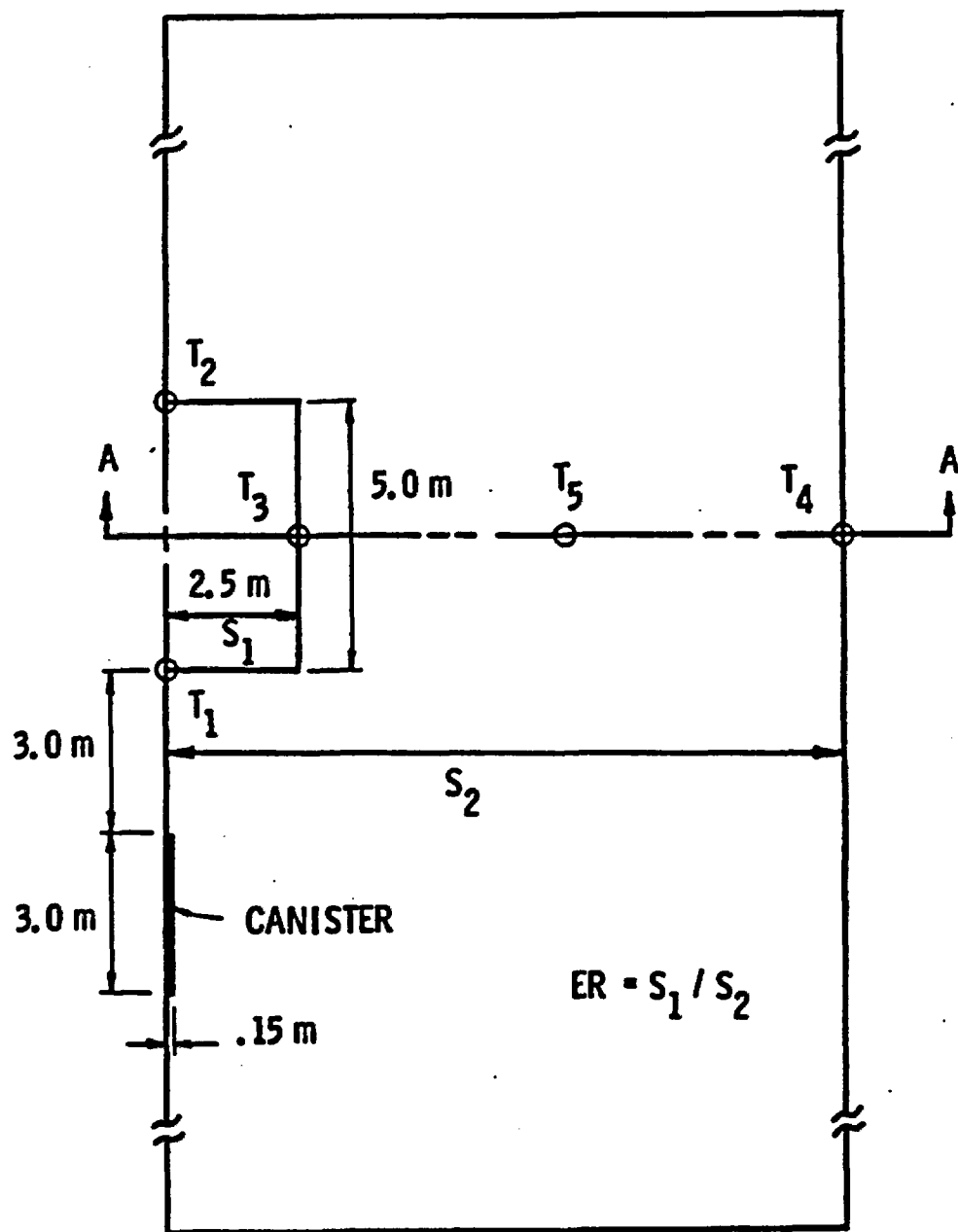


Figure 1 - Schematic of HLW Room and Pillar Design

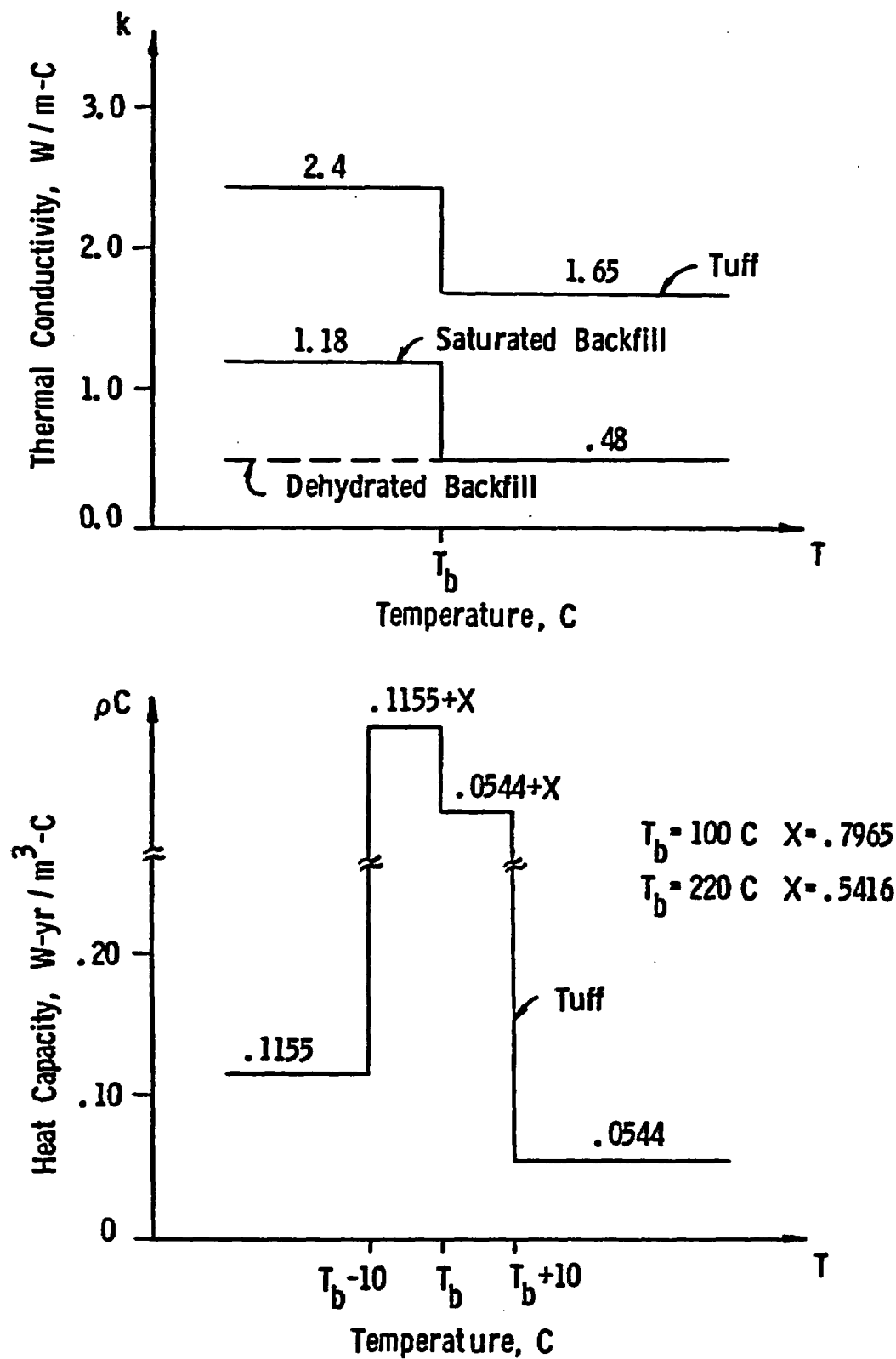


Figure 2 - Thermal Properties

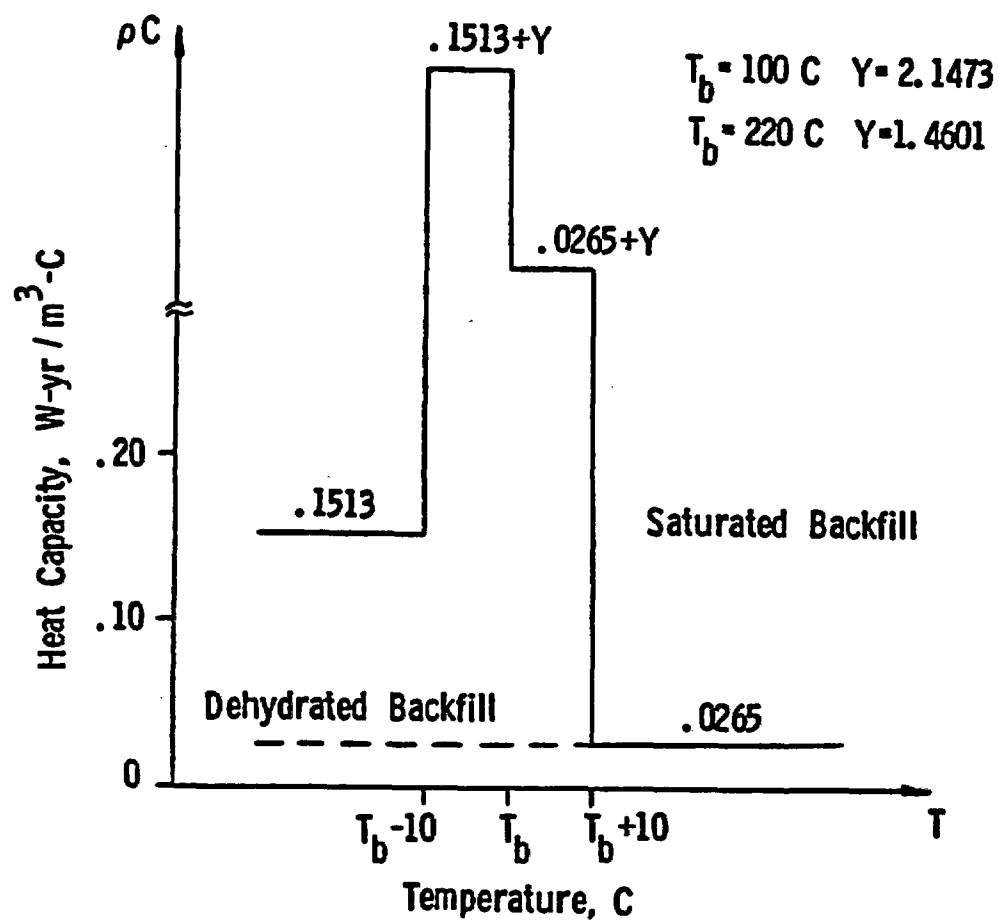


Figure 2 - continued

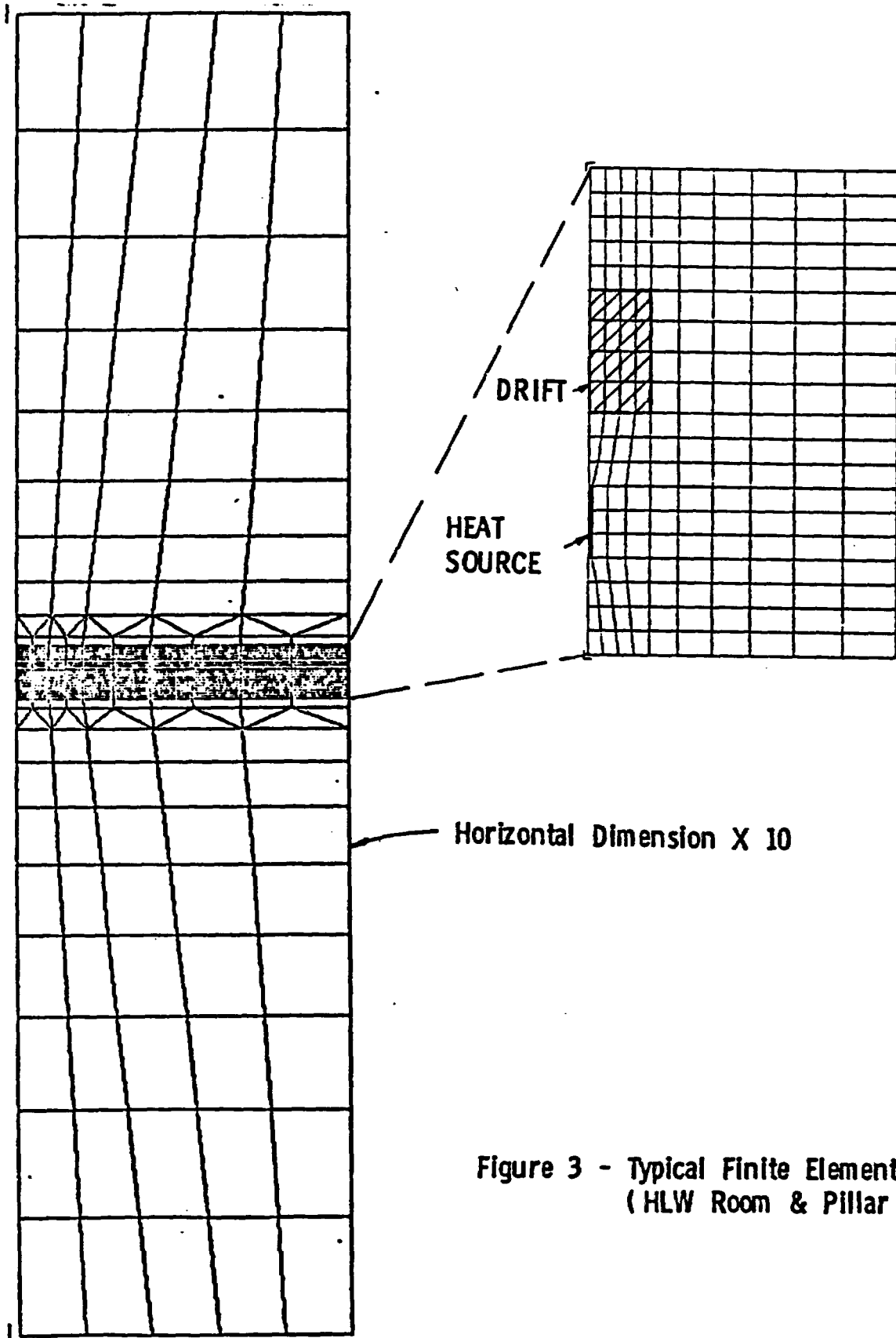


Figure 3 - Typical Finite Element Mesh
(HLW Room & Pillar)

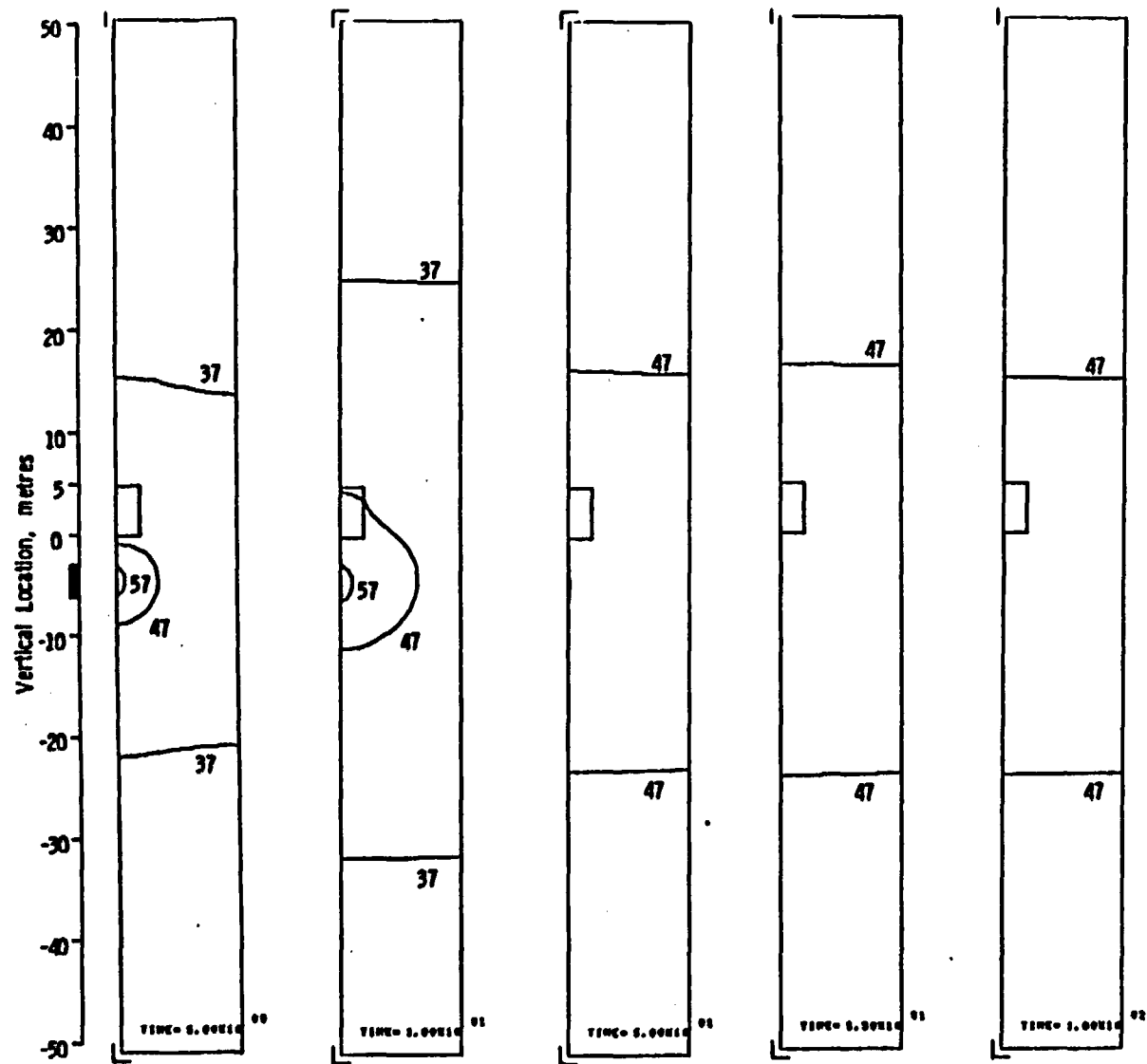


Figure 4 - Isotherms for Various Times
 ER = .20 , GTL = 25 KW / ACRE
 $T_0 = 100\text{ C}$, Saturated Backfill

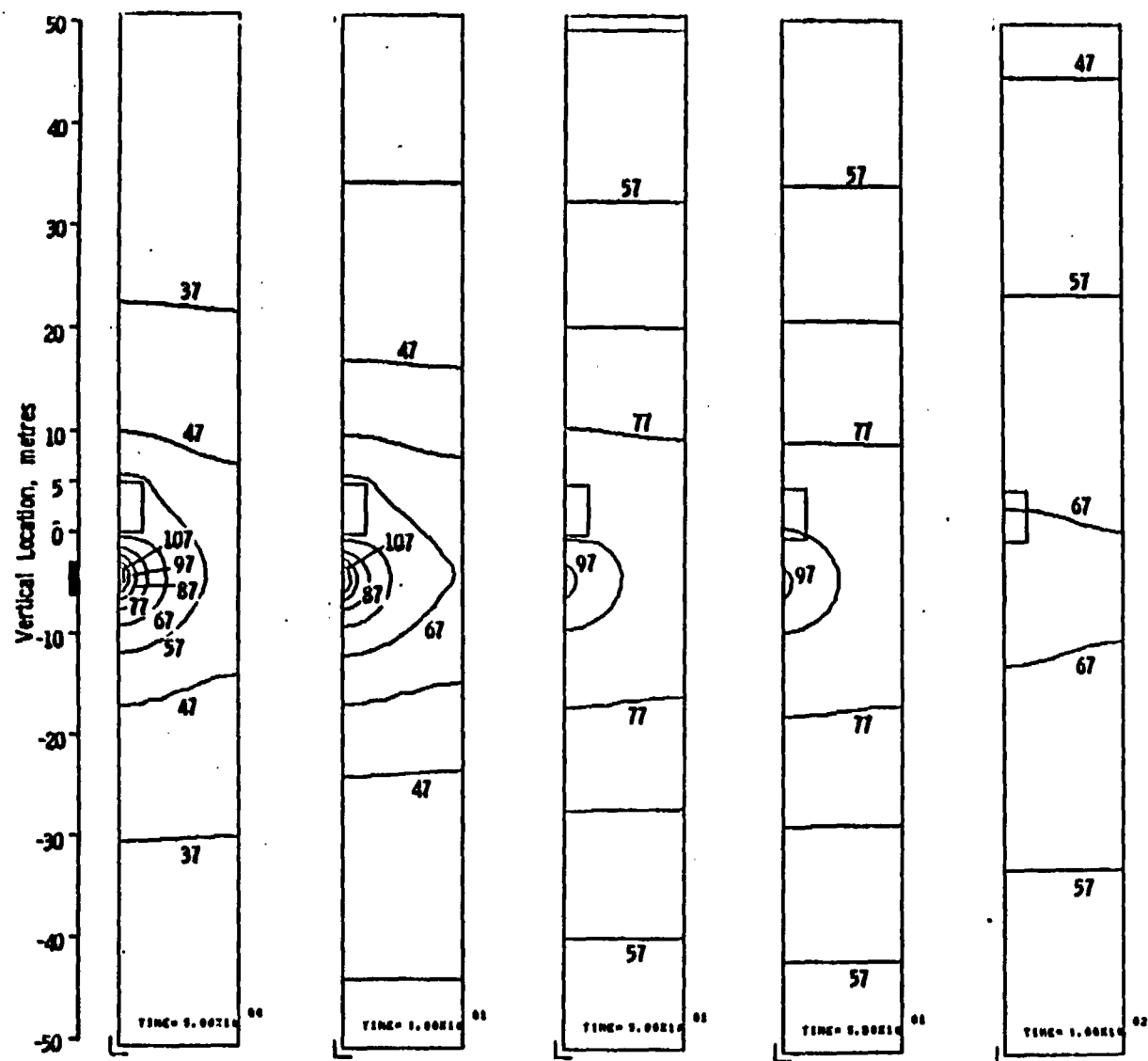


Figure 5 - Isotherms for Various Times
 $ER = .20$, $GTL = 75 \text{ KW / ACRE}$
 $T_b = 100 \text{ C}$, Saturated Backfill

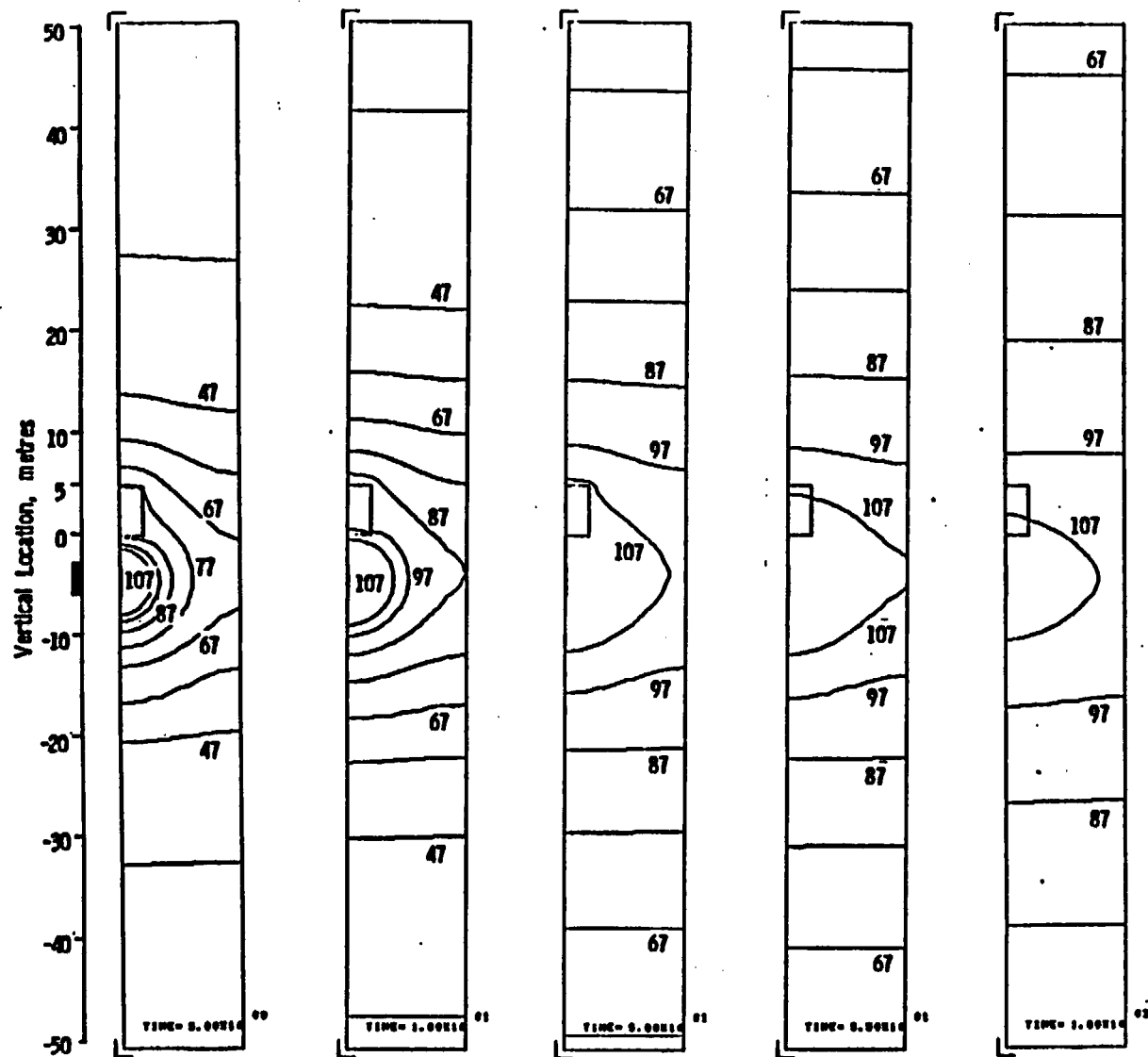


Figure 6 - Isotherms for Various Times
 ER = .20, GTL = 150 KW / ACRE
 $T_b = 100\text{ C}$, Saturated Backfill

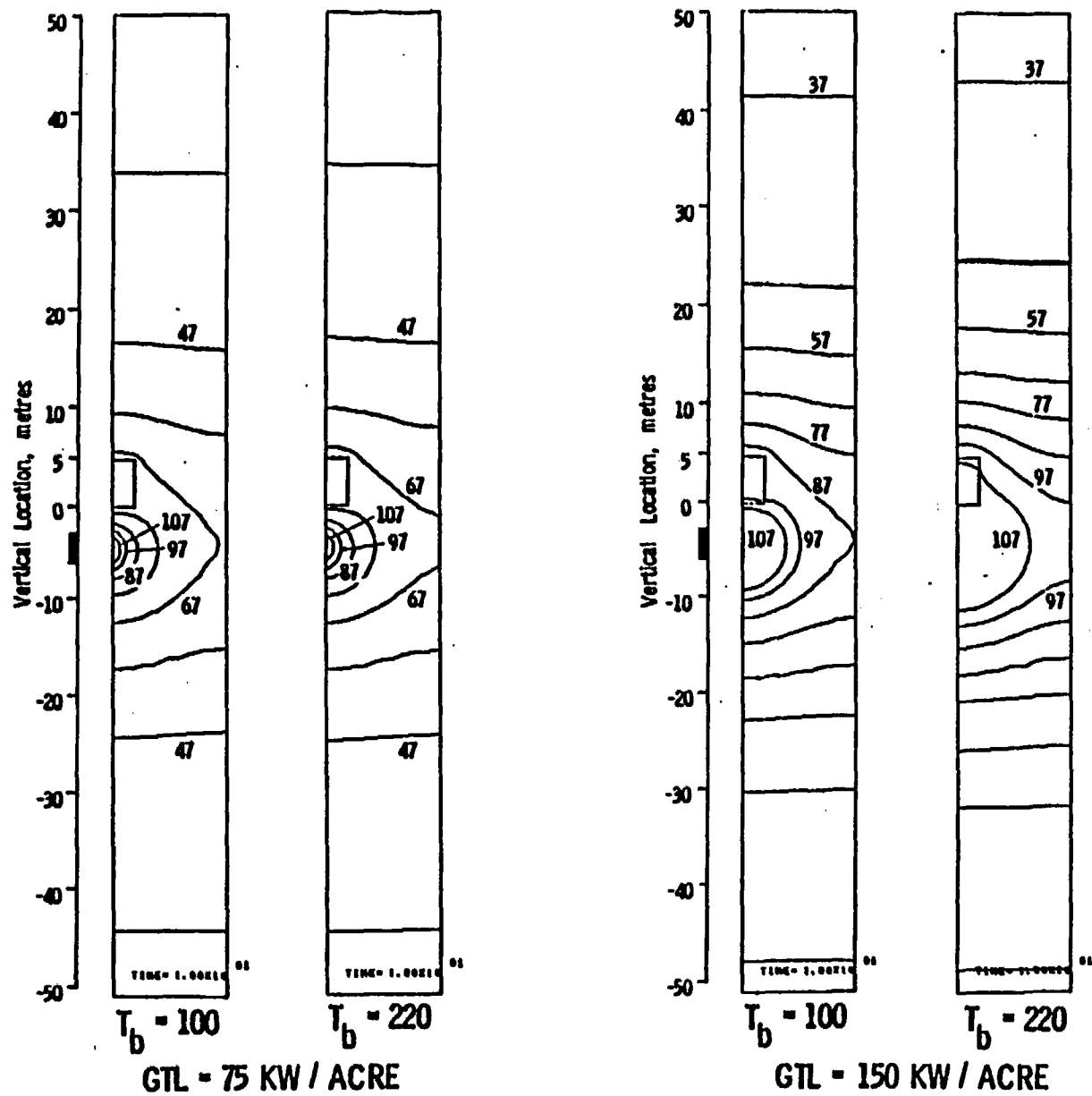


Figure 7 - Effect of Boiling Point, $ER = .20$

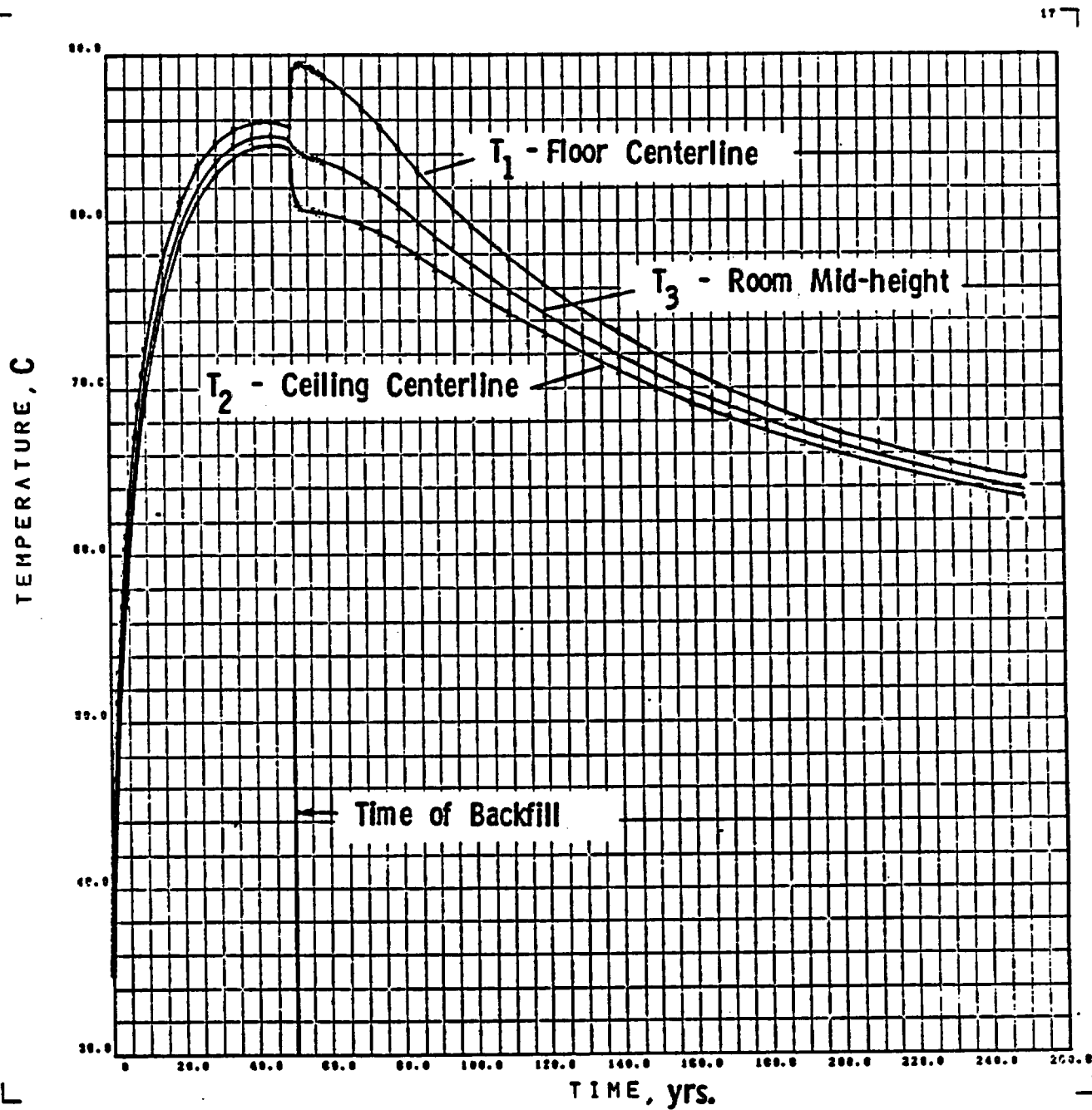


Figure 8 - Temperature Histories for Points on Room Boundary

ER = .20, GTL = 75 KW / ACRE

T_b = 100 C, Saturated Backfill

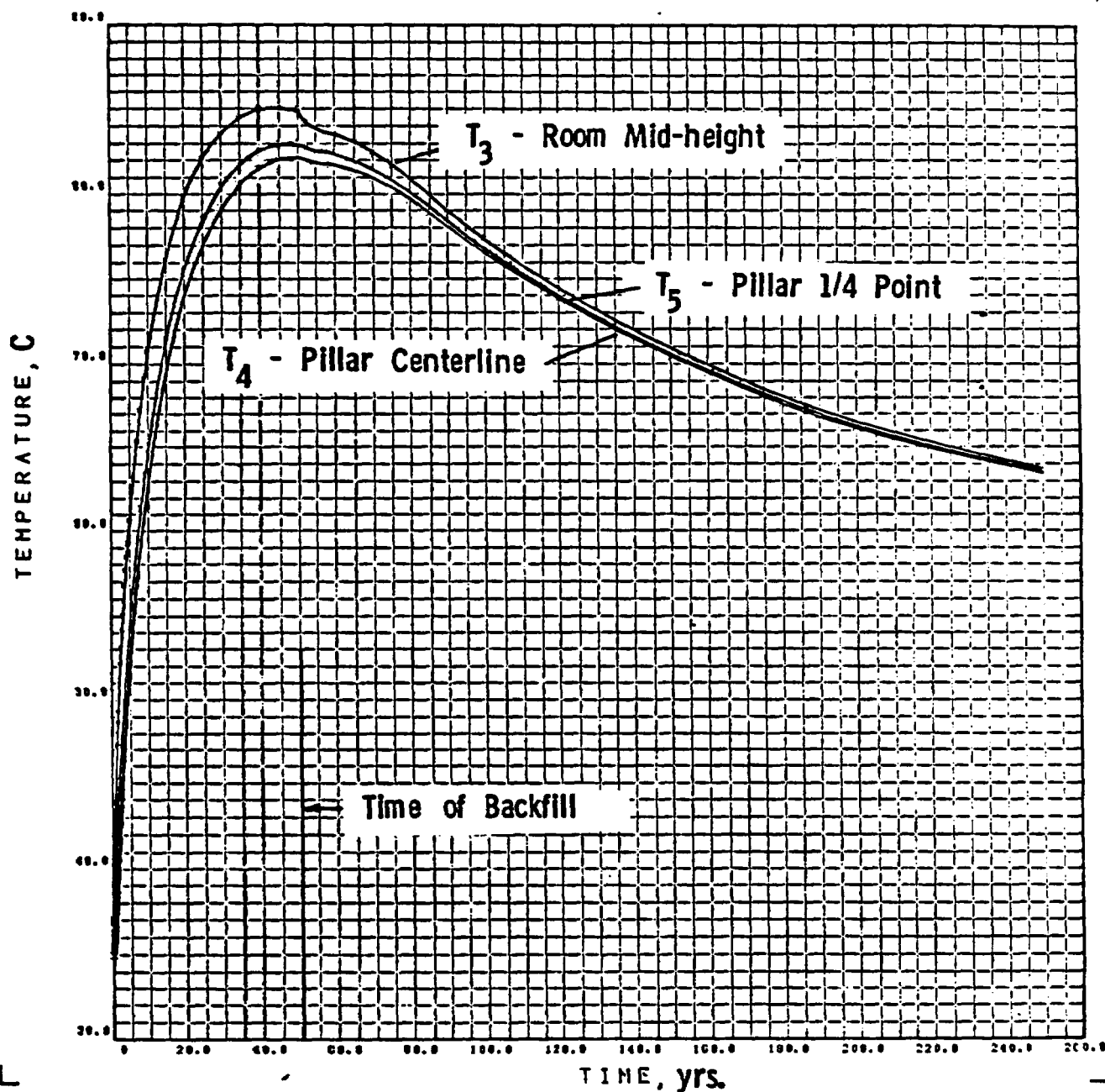


Figure 9 - Temperature Histories for Points Through the Pillar

ER = .20, GTL = 75 KW / ACRE

T_b = 100 C, Saturated Backfill

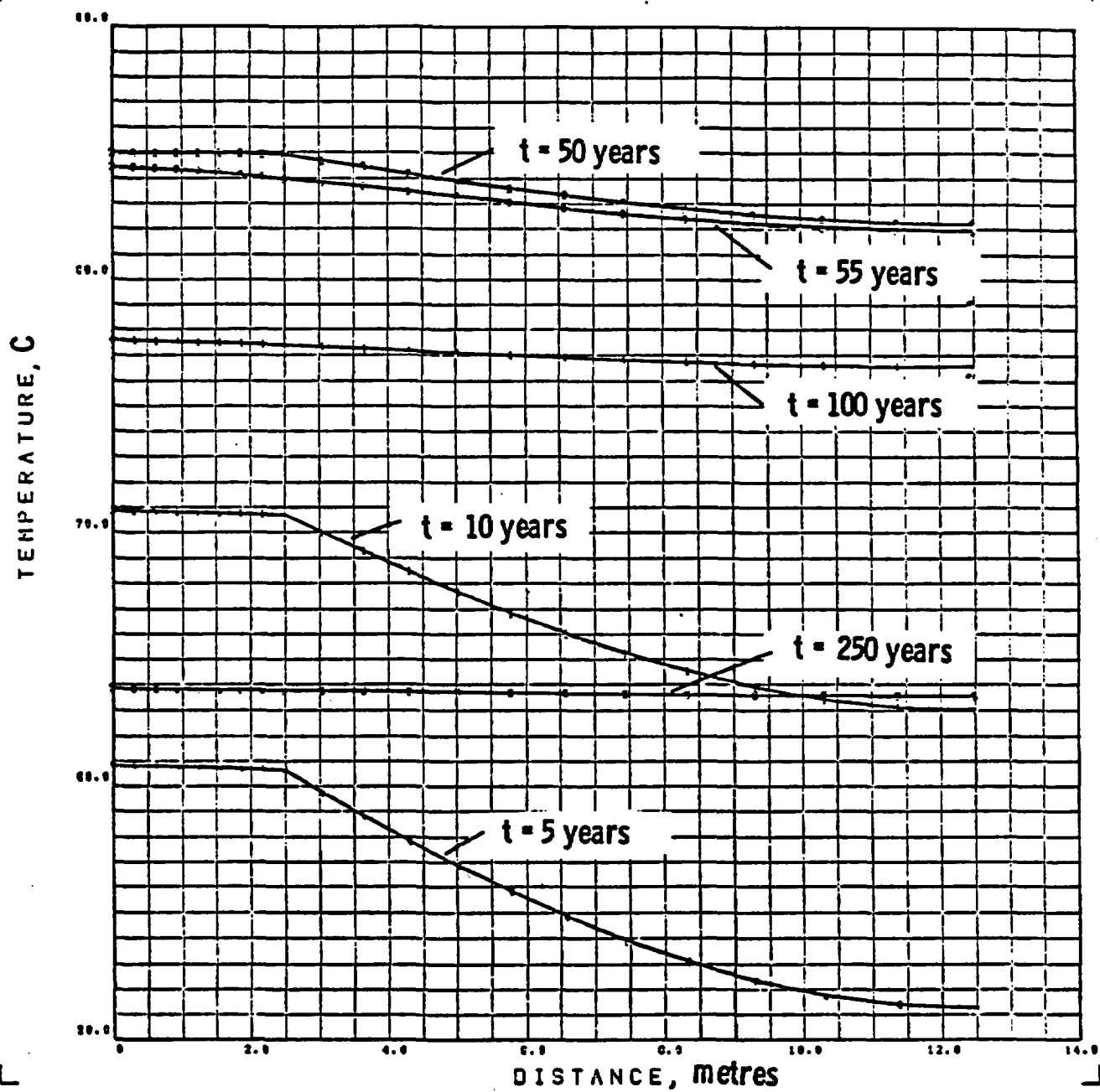


Figure 10 - Temperature Profiles Through the Pillar (Section A - A)
 ER = .20, GTL = 75 KW / ACRE
 T_b = 100 C , Saturated Backfill

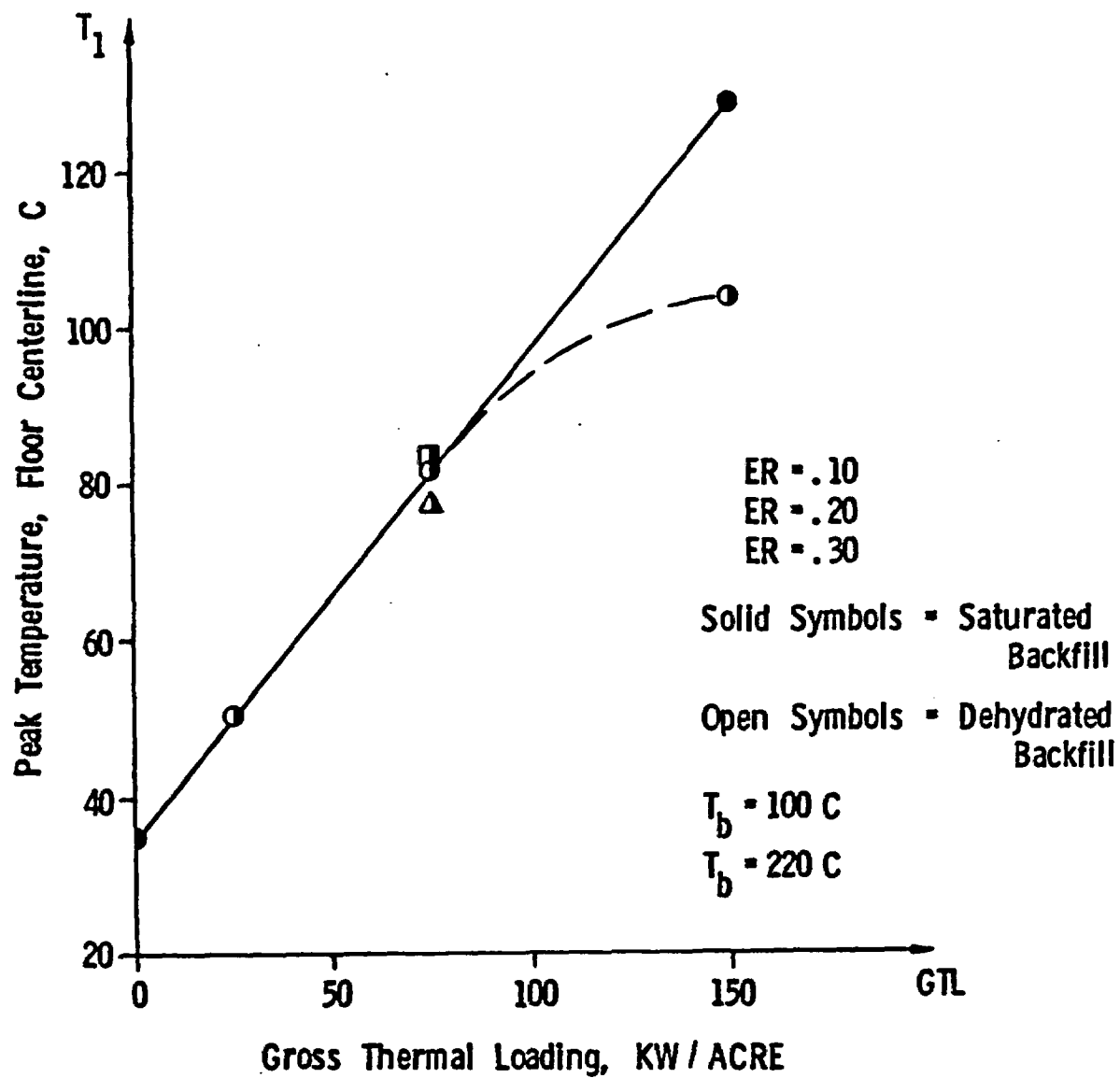


Figure 11 - Peak Floor Temperature versus GTL

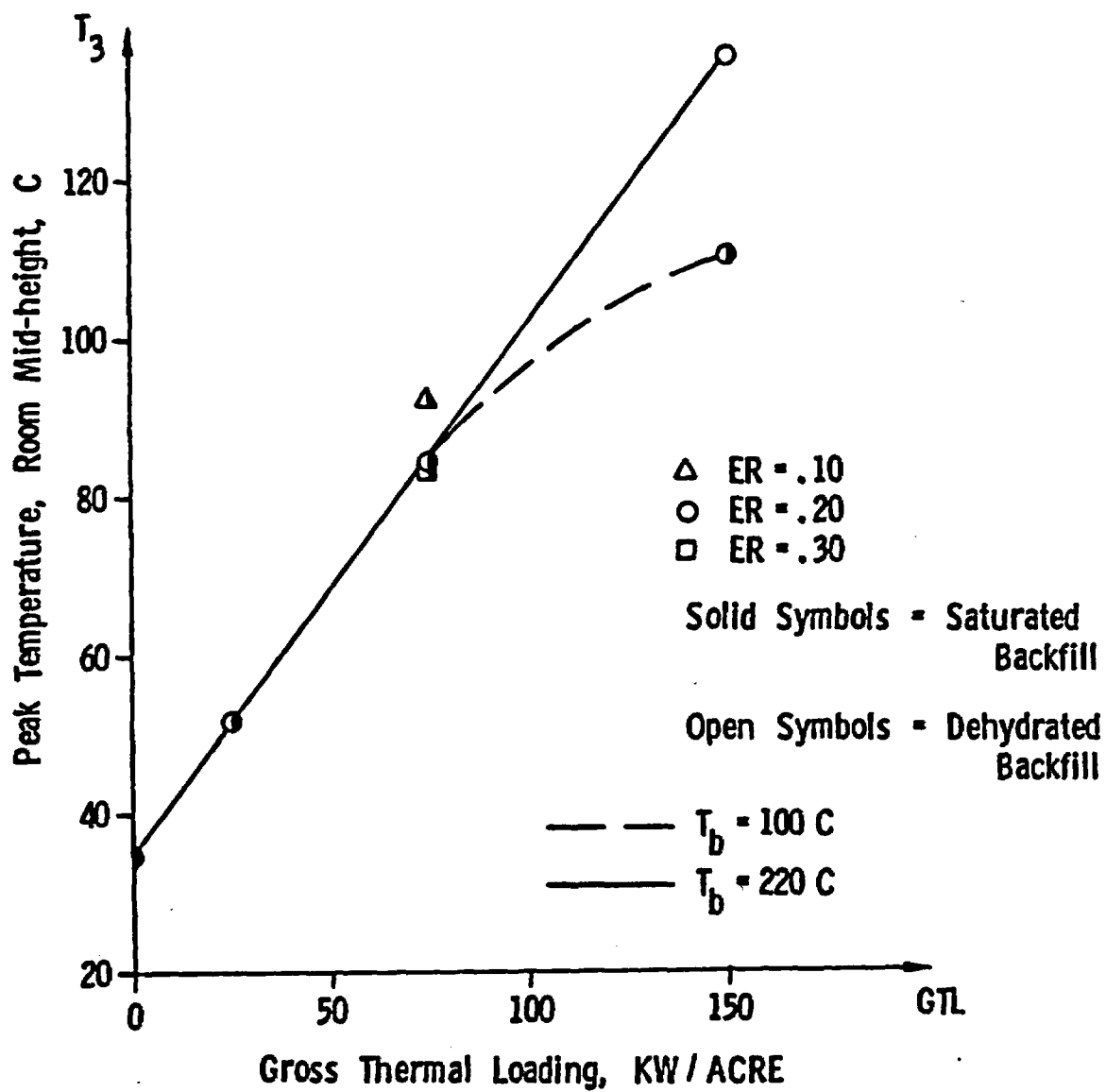


Figure 12 - Peak Room Mid-height Temperature versus GTL

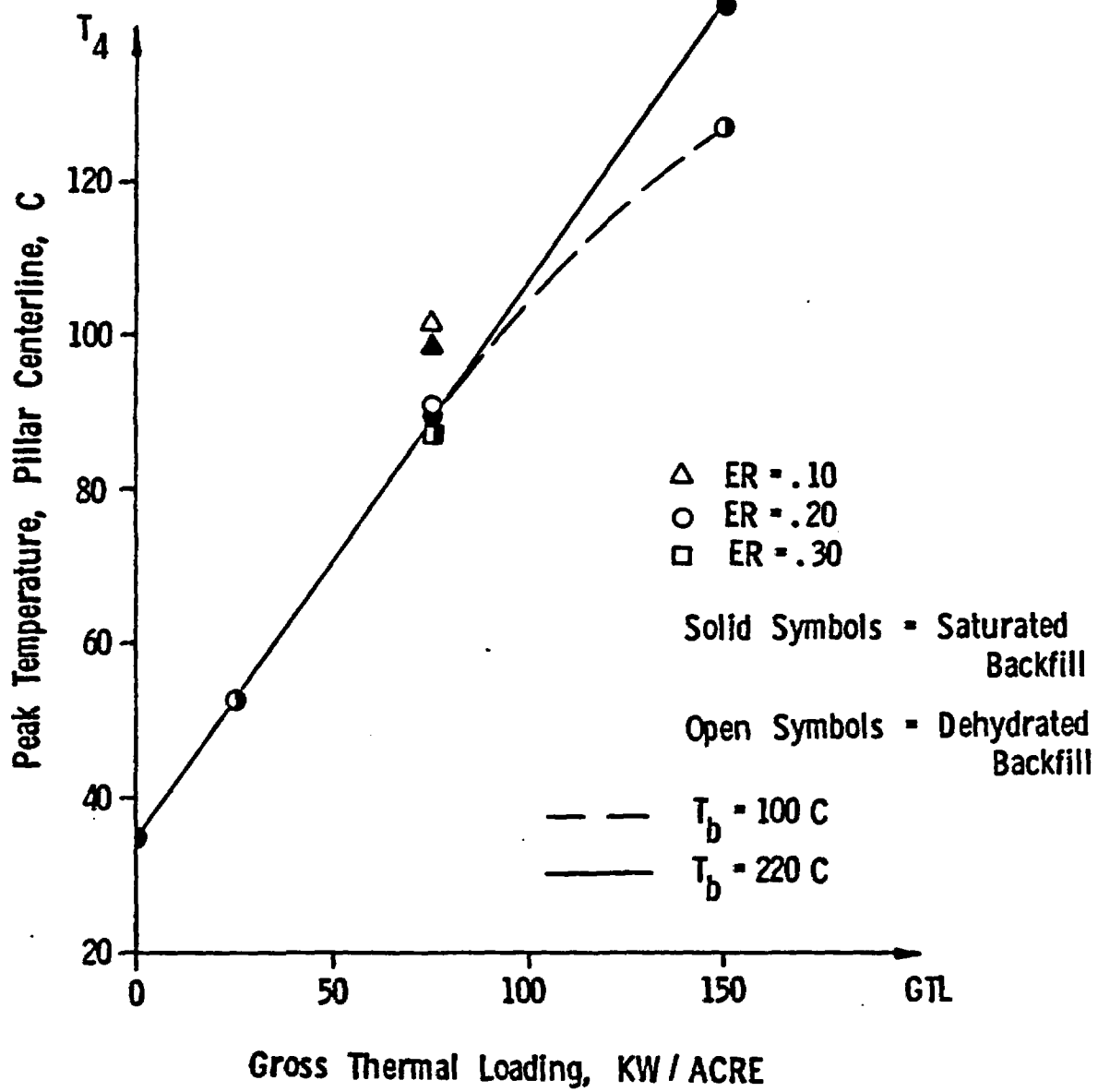


Figure 13 - Peak Pillar Centerline Temperature versus GTL

Sandia Laboratories

Albuquerque, New Mexico
Livermore, California

date: February 19, 1980

to: Distribution

D. K. Gartling

from: D. K. Gartling - 5511

subject: Further Results for Tuff Mine Design Thermal Analysis --
High Level Waste

Ref.: Memo, D. K. Gartling, 5511, to Distribution,
dtd 2/4/80, subject: Tuff Mine Design Thermal
Analysis -- High Level Waste

The thermal analysis reported in the referenced memo was carried out using the assumption that the initial temperature at the mine horizon was a uniform 35°C. This particular initial condition was specified as part of the problem description in the work packages issued by the mine design working group. As a result of more recent data, the initial temperature at the mine horizon is now felt to be ~55°C. The nonlinearity of the heat conduction process in the tuff (due to the assumed model for pore fluid boiling) precludes the scaling of the previously computed results to account for the change in initial condition. Therefore, several of the thermal analyses previously reported were re-computed to allow an assessment to be made of the influence of the assumed initial temperature.

The repository model, waste form, and material properties for the high level waste mine design were previously described in the referenced memo. For the present analyses, the extraction ratio (ER) was fixed at 20%; the gross thermal loading (GTL) for the repository was varied between 25, 75, and 150 kW/acre. Backfilling of the mine drift was assumed to occur 50 years after emplacement of the waste canister; the backfill material was assumed to be saturated tuff. The assumed boiling point for the pore fluid was varied between 100°C and 220°C. The initial temperature distribution in the thermal model was computed from an assumed geothermal heat flux of 1.6 HFU (1.6 $\mu\text{cal}/\text{cm}^2\text{s}$) and a temperature at the earth's surface of 20°C. With these values, the initial temperature in the vicinity of the room and pillar was ~53°C.

Six cases were analyzed for the high level waste configuration with the revised initial temperature distribution. In each case, the qualitative behavior of the thermal response was the same as reported in the previous memo. Of particular interest in this study were the peak room and pillar temperatures and their variation with GTL. Shown in Figures 1 through 3 are plots (re-plotted from the referenced memo) of peak temperature for the mine floor (T_1), room mid-height (T_3), and pillar centerline (T_4). The data shown in black are for cases with an initial temperature of 35°C; the data in red corresponds to an initial temperature based on the geothermal heat flux.

As observed in the analyses reported previously, the peak room and pillar temperatures are seen to vary linearly with GTL when a 220°C boiling point is assumed (solid red line). The uniform increase in the peak temperatures for this case is a direct reflection of the increase (~18°C) in the assumed initial room and pillar temperature. For the case of a 100°C boiling point, the temperature variation is linear with GTL up to 25 kW/acre (broken red line); the departure from linearity at higher GTL's is a result of the significant loss of energy from the system due to dryout. Note that as the initial temperature of the formation is increased (black data @ 35°C to red data @ 53°C) the GTL, at which boiling influences the peak temperature, is reduced.

DKG:5511:ljg

Distribution:

Mine Design Working Group Members

4530 R. W. Lynch
4537 J. K. Johnstone
4537 A. R. Lappin
5500 O. E. Jones
5510 D. B. Hayes
5511 J. W. Nunziato
5511 R. R. Eaton
5520 T. B. Lane
5521 R. K. Thomas
5530 W. Herrmann

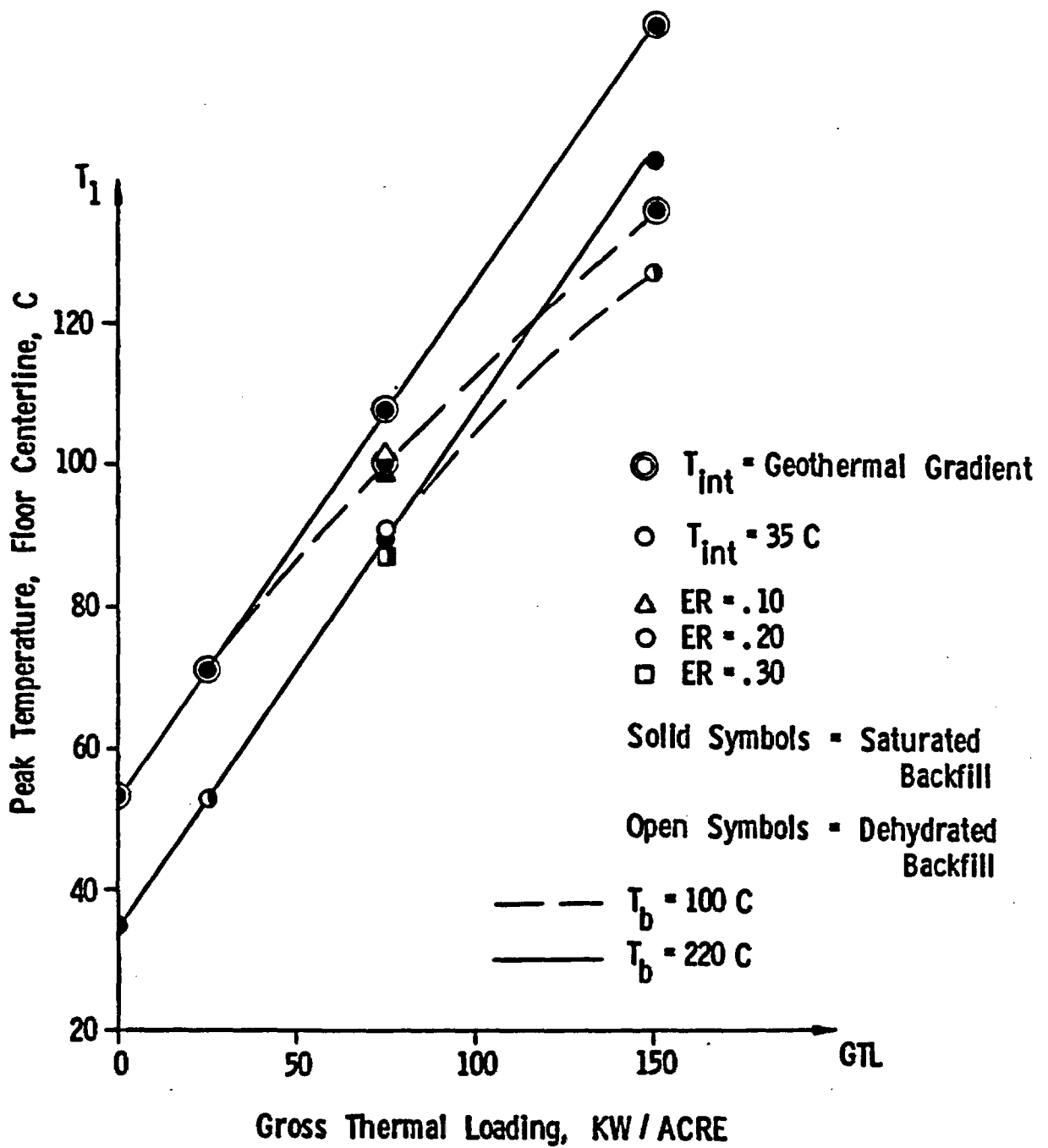


Figure 1 - Peak Floor Temperature versus GTL

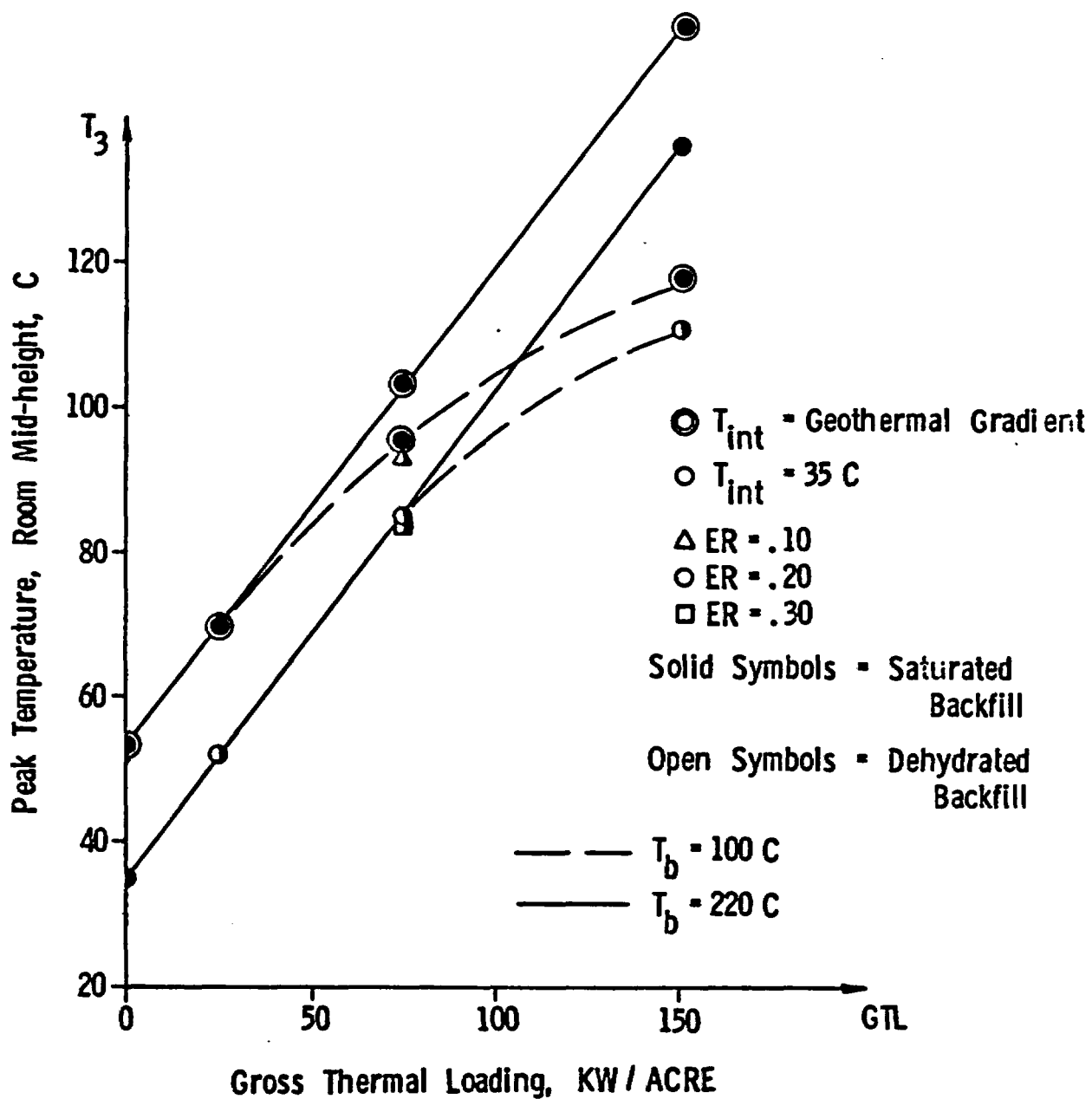


Figure 2 - Peak Room Mid-height Temperature versus GTL

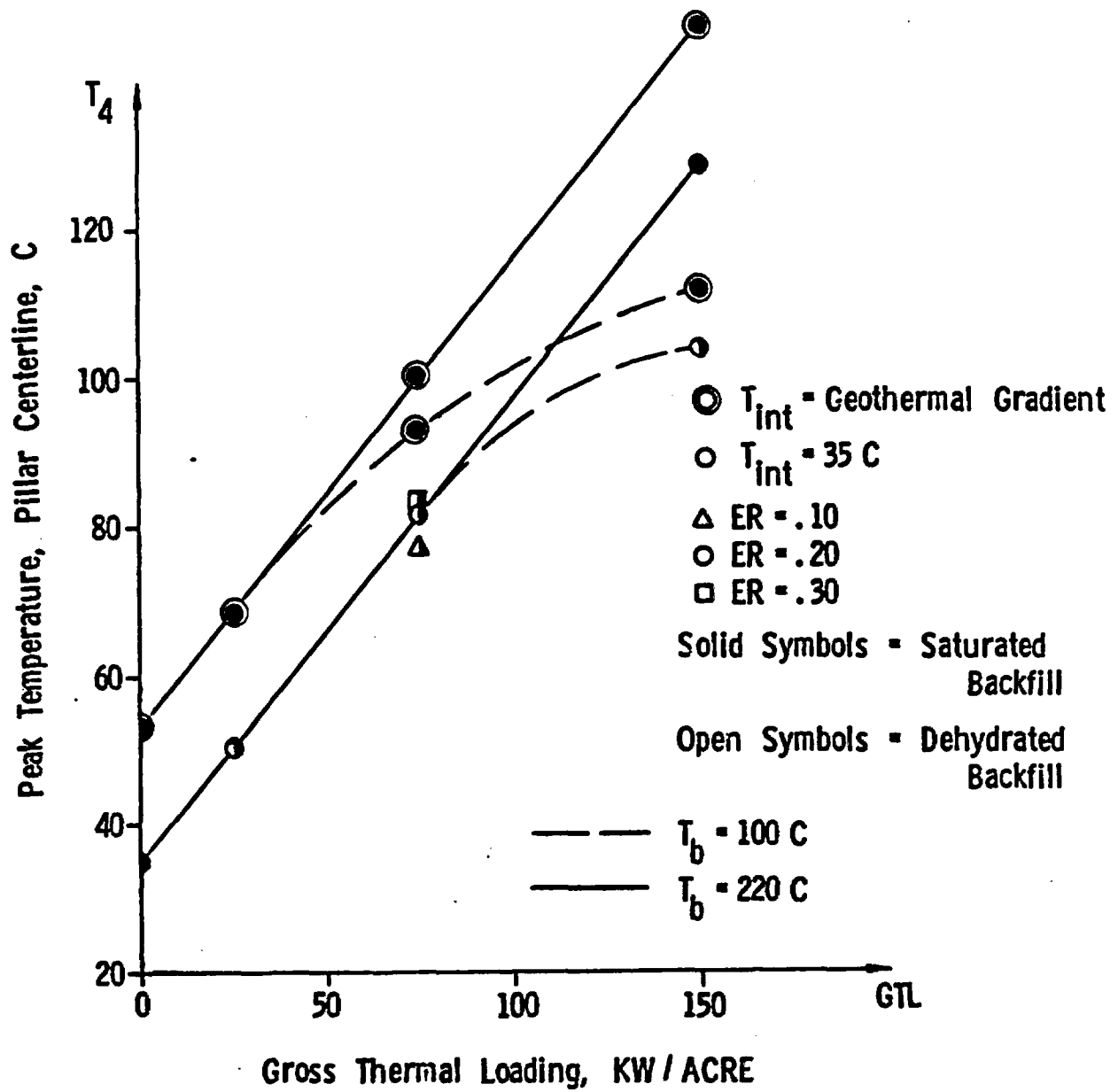


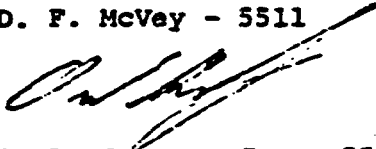
Figure 3 - Peak Pillar Centerline Temperature versus GTL

Sandia Laboratories

Albuquerque, New Mexico
Livermore, California

date: January 4, 1980

to: D. F. McVey - 5511



from: O. L. George, Jr. - 5511

subject: The Effect of Thermal Radiation in the Disposal of High Level Waste (HLW) in Tuff

In response to your request, a CINDA thermal model was created to determine the effect of thermal radiation on the interior drift temperatures for the case of HLW buried in tuff.

The model was two-dimensional, with the 75 kW/acre (initial emplacement density) heat source assumed to be uniformly distributed longitudinally beneath an infinitely long drift floor. This source was 3 m tall, with its top residing 3.05 m beneath the drift floor. The drift cross-section was 5 m x 5 m, and the extraction ratio was 30%. An initial temperature of 35°C was assumed. In the interest of expediency (short computer run times, resulting in quicker answers), the tuff thermal properties were assumed invariant with the following values: $\rho = 2280 \text{ kg/m}^3$, $c_p = 3.725 \times 10^{-5} \text{ watt-yr/kg-}^\circ\text{C}$, and $k = 2.0 \text{ watt/m-}^\circ\text{C}$.

Two computer runs were made; one assumed the drift surfaces to be adiabatic, while the other allowed radiation heat transfer to occur within the drift. The tuff emissivity was assumed to be 1.0 for the radiation run. Each run covered a period of 50 years from the time of emplacement. Figure 1 shows the mesh arrangement in close proximity to the drift. The heating was applied in the three cross-hatched nodes. The unit cell which was analyzed was 8.34 m wide, 1 m thick and 330 m high.

The graph in Figure 2 shows an elevation view of the drift with numbers indicating the locations for which temperature data are plotted. Arrows indicate the temperature/time curves for these locations when radiation was neglected. The temperature/time curves for all five locations fell within the shaded region on the graph when the effect of radiation was included. For the radiation case, all five temperatures remained within 2°C of one another (for times greater than two years).

D. F. McVey - 5511

-2-

It is apparent that radiation plays a significant role in this problem.

OLG:5511:ljg

Copy to:

4512 T. O. Hunter
4537 L. D. Tyler
4537 J. K. Johnstone
4537 A. R. Lappin
5500 O. E. Jones
5510 D. B. Hayes
5511 R. R. Eaton
5511 D. K. Gartling
5520 T. B. Lane
5521 S. W. Key
5521 R. D. Krieg
5521 C. M. Stone
5521 R. K. Thomas
5530 W. Herrmann



Figure 1. Noding Arrangement Near Drift and Heat Source

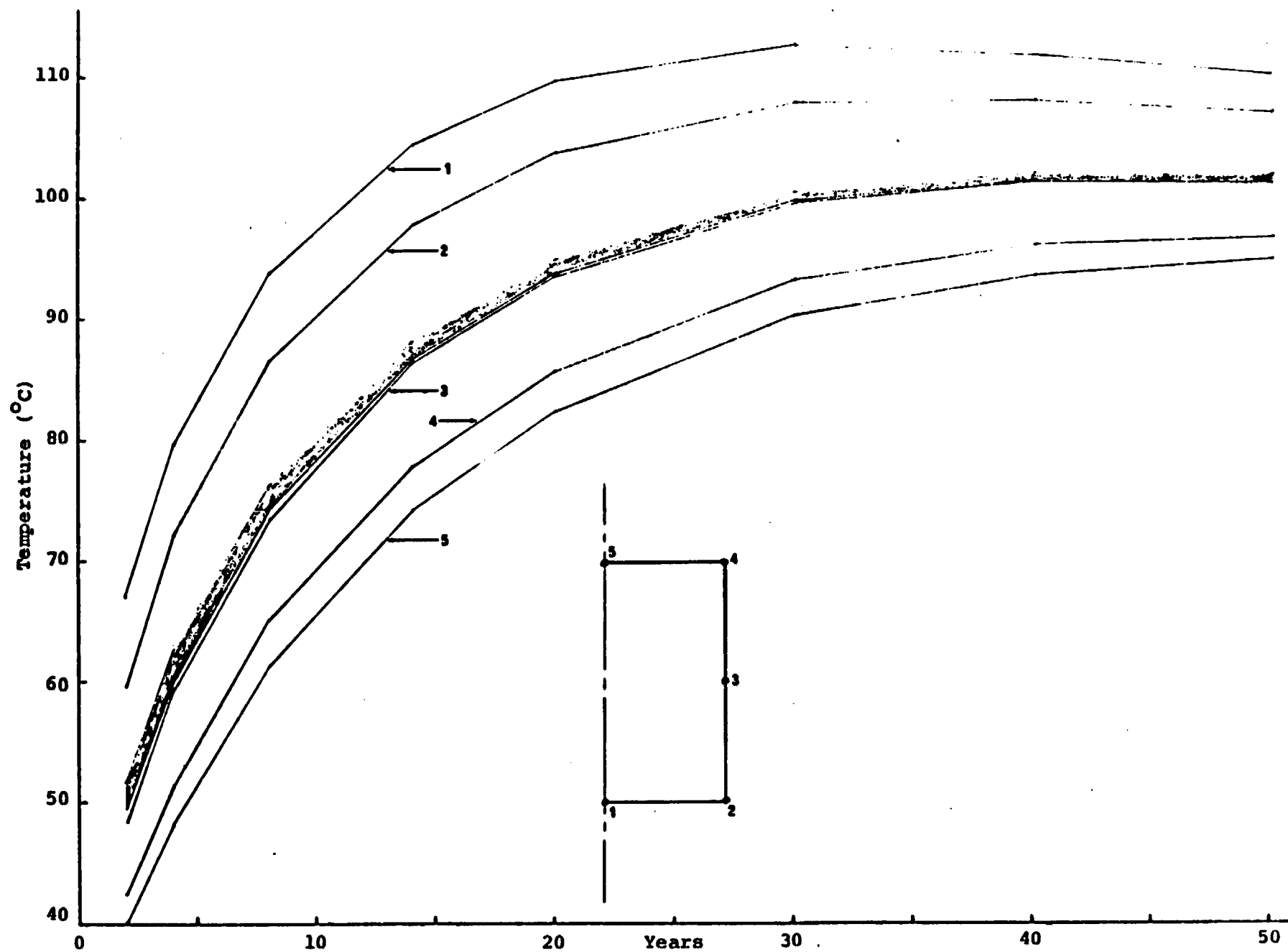


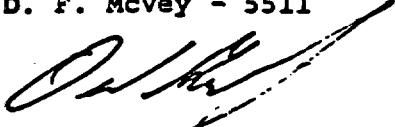
Figure 2. Temperature Histories With and Without Radiation

Sandia Laboratories

Albuquerque, New Mexico
Livermore, California

date: January 22, 1980

to: D. F. McVey - 5511



from: O. L. George, Jr. - 5511

subject: Further Results Concerning the Effects of Thermal Radiation and Free Convection in the Drift of a High Level Waste (HLW) Repository in Tuff

Ref.: Memo, O. L. George, Jr., 5511, to D. F. McVey, 5511, dtd 1/4/80, subject: The Effect of Thermal Radiation in the Disposal of High Level Waste (HLW) in Tuff

The referenced memo created considerable interest in pursuing the drift heat transfer problem further. Requests were received to (1) create a purely conductive CINDA model which would duplicate the radiation/conduction model results, and (2) investigate the effect of free convection in the drift.

The reason for the first request was that several codes which lack a radiation capability are being used to solve various aspects of the HLW/tuff problem. The most effective way for these codes to accommodate the effects of radiation would be to simulate radiation as a conduction phenomenon. The desire to evaluate convective effects was an extension of the question concerning the transfer of energy within the drift.

A CINDA model which included the presence of a fictitious conductive medium within the drift was created. This model was run strictly as a conduction model. It was found that if the fictitious medium had a thermal conductivity of 25 watts/m-°C, this model duplicated the results of the previous conduction/radiation model to within 1.2°C at all points throughout the model over the entire 50-year span of the run.

Hand-calculations were made to evaluate the effect of free convection vis-a-vis radiation. Input drift temperatures for the calculations were taken from the conduction/radiation results of Reference 1. The computed heat fluxes from the drift floor for both convection and radiation at 2-years and 50-years after emplacement are shown below.

D. F. McVey - 5511

-2-

At t = 2-years:

Convective flux = 1.6 watts/m²
Radiative flux = 12.5 watts/m²

At t = 50-years:

Convective flux = 0.3 watts/m²
Radiative flux = 5.1 watts/m²

Radiation is seen to be an order of magnitude more significant than convection.

OLG:5511:ljg

Copy to:

4512 T. O. Hunter
4537 L. D. Tyler
4537 J. K. Johnstone
4537 A. R. Lappin
5500 O. E. Jones
5510 D. B. Hayes
5511 R. R. Eaton
5511 D. K. Gartling
5520 T. B. Lane
5521 S. W. Key
5521 R. D. Krieg
5521 C. M. Stone
5521 R. K. Thomas
5530 W. Herrmann

APPENDIX B

Room and Pillar Analysis for SF

- Part I: MIDES Working Group - Work Package
- Part II: Tuff Room and Pillar Thermal Analysis - Spent Fuel
(Memo, R. K. Thomas, 5521, to Distribution, dtd. 2/4/80)
- Part III: Mine Design Working Group: Further Results for Room and Pillar
Thermal Analysis - Spent Fuel
(Memo, R. K. Thomas, 5521, to Distribution, dtd. 4/7/80)

TUFF MINE DESIGN WORKING GROUP

ACTIVITY WORK PACKAGE

TITLE: Room-and-Pillar Thermal Analysis - Spent Fuel

INVESTIGATOR: Bob Thomas (SLA, Division 5521)

PHONE NUMBER: (505) 264-1457

DESCRIPTION:

1. Model Geometry - 2-D planar
2. Room Initial Conditions - see specification (5)
3. Room and Canister Dimensions, Hole Geometry, Initial Canister Power - see specifications (7 & 8)
4. Waste - HLW, instantaneous emplacement; for waste thermal output history see specification (9); for waste material and thermal properties see (10)
5. Backfill - assume room open 50 years, with radiative heat transfer, but no active cooling; for backfill properties, see specifications (4)
6. Temperature-Dependent Rock Properties (K, ρC_p , etc.) - use properties for tuff layer at greater than 71¹ m depth, see specifications (2 & 3)

PARAMETERS:

1. Extraction Ratio and Power Densities
 - a. 10% extraction ratio - 75 kW/acre
 - b. 20% extraction ratio - 25, 75, 150 kW/acre
 - c. 30% extraction ratio - 75 kW/acre
2. Boiling Temperature
 - Case I - 100°C
 - Case II - hydrostatic-head - potential boiling (223°C)
see specification (2)
(Case II run at discretion of modeler)

DUE DATE: February 5, 1980

REPORTING: 1. Technical Memo (letter form) to Working Group Members
2. Presentation of Results

Sandia Laboratories

Albuquerque, New Mexico
Livermore, California

date: February 4, 1980

to: Distribution

R. K. Thomas

from: R. K. Thomas, 5521

subject: Tuff Room and Pillar Thermal Analysis - Spent Fuel

References:

1. Mine Design Working Group - Activity Work Package, December 4-5, 1979.
2. R. J. Bathe, "ADINAT - A Finite Element Program for Automatic Dynamic Incremental Nonlinear Analysis of Temperatures," MIT Report 82448-5, May, 1977 (Revised December 1978).
3. Memo, O. L. George, 5511, to D. F. McVey, 5511, "The Effect of Thermal Radiation in the Disposal of High Level Waste (HLW) in Tuff," January 4, 1980.
4. Memo, O. L. George, 5511, to D. F. McVey, 5511, "Further Results Concerning the Effects of Thermal Radiation and Free Convection in the Drift of a High Level Waste (HLW) Repository in Tuff," January 22, 1980.

Introduction

This memo summarizes the results of a thermal analysis of the room and pillar region for a nuclear spent fuel (SF) waste heat source. The analysis was performed as part of the NTS tuff repository study presently being conducted by the mine Design Working Group. These results are to be presented at the next meeting of the working group to be held on February 5-6, 1980.

The problem description for this analysis is fully documented in Ref. [1]. A summary of the work package taken from Ref. [1] is shown in Fig. 1. The design parameters specific to spent fuel, and the location of points where calculated temperatures are reported, are given in Fig. 2. A listing of the cases run is given in Fig. 3, and the temperature-dependent thermal properties of the tuff and backfill material used in this analysis are shown in Figs. 4 and 5, respectively.

Thermal Model

The numerical calculations were made using the ADINAT [2] finite element computer code. Four-node isoparametric quadrilateral elements were used exclusively. The heat capacity was modeled in a consistent manner and an implicit time integration scheme was employed. The finite element grid for 10% extraction ratio, shown in Fig. 6, was composed of 800 node points. The model for 20% extraction had 600 node points, and the model for 30% extraction had 500 node points.

Initially at zero time the entire region modeled was assumed to be a uniform 35°C. Calculations were carried to 250 years in 167 variable time steps, at which time the temperatures in the room and pillar vicinity had peaked and were declining in a monotonic fashion. The vertical boundaries of the model extended 250 m above and below the drift floor and were assumed to be adiabatic. At 250 years, the temperature at these boundaries had increased only 2°C in the worst case.

Calculations by George [3, 4] have shown the importance of thermal radiation in determining the temperatures around the perimeter of the drift, and that this mechanism could be satisfactorily approximated by a thermal conduction model with an appropriately large diffusivity. Using his recommended conduction properties,

$$K = 788 \times 10^6 \text{ J/yr} - \text{m} - ^\circ\text{C}$$

$$\rho c_p = 0.001 \times 10^6 \text{ J/ m}^3 - ^\circ\text{C},$$

the drift in this study was modeled as solid material for the first 50 years before backfilling.

Results and Conclusions

Since the nature of the thermal response was essentially the same for all cases considered, only one typical data set is shown in this memo (Figs. 7-16). Contour plots for Case 8 (identified in Fig. 3) are shown in Fig. 7. They extend horizontally 18.75 m to the centerline of the model, and vertically 50 m above and below the floor centerline. It is significant to note that the material heated above 100°C, the fluid boiling temperature in this case, is confined to a small region surrounding the heater. Contour plots for three different power levels (Cases 5, 8, and 11), are shown in Fig. 8. The increasingly larger volume of material heated above 100°C for the higher power levels is clearly evident.

Temperature-time history plots are shown for Case 8 in Figs. 9-10 at locations defined in Fig. 2. At 50 years in Fig. 9, when the drift is backfilled, the floor temperature rises

abruptly because the backfill material acts as a thermal barrier to conduction. For the same reason, the ceiling temperature decreases. Note that just prior to backfilling all three room temperatures are nearly equal, this being due to thermal radiation in the drift. As seen in Fig. 10, the temperature gradient through the pillar is greatest at early times yet does not appear to be severe. Temperature gradients through the pillar are best illustrated by the profile plots in Figs. 11-16. At 250 years, the gradient is insignificant.

Results for all cases examined are summarized in Figs. (17-19) where the peak temperatures at the T_1 , T_3 , T_4 locations defined in Fig. 2 are plotted as a function of the gross thermal loading for selected extraction ratios. Results are not shown comparing saturated and dehydrated backfill material because the predicted temperatures are nearly equal for the two situations. This must be due, in part, to inserting the backfill at the same temperature as the pseudo-radiative material in the drift. If the drift temperature is above boiling (high power loadings) at 50 years, then the backfill is inserted at the same temperature and there is no difference between saturated and dehydrated conditions. Below the boiling temperature (low power loadings) it appears that the baseline thermal conductivities of saturated and dehydrated backfill, although different, are both small in comparison to the conductivity of the pseudo-radiative material in the drift, and thus no significant difference is observed. Based on these assumptions, therefore, it can be concluded that prior knowledge of the water content of the backfill material is not necessary for room and pillar thermal predictions.

The primary design variables in room and pillar maximum temperatures are extraction ratio and gross thermal loading. As expected, all temperatures in the room and pillar region increase with power level, but at locations far removed from the waste heat source (pillar centerline in Fig. 19) the temperatures are approximately independent of extraction ratio. It should be remembered that the plotted values are peak temperatures and do not in general occur at the same time. The highest temperatures, and largest variation with extraction ratio, occur at the drift floor (Fig. 17). Because this location is nearest the waste source, the lower extraction ratios yield higher temperatures since they have larger volumetric power levels for the same gross thermal loading.

An equally important variable in the regime of high thermal loadings is the boiling criteria. The effect of the boiling temperature on the thermal field depends upon the volume of material that is heated to the boiling temperature and, as such, is difficult to ascertain without first performing the

calculations. Contour plots for 100°C and 220°C boiling are shown in Fig. 20. Note the larger volume of material contained within the 100°C isotherm for 220°C boiling. Based on these results, temperatures in the room and pillar region increase when the boiling criteria is increased from 100°C to 220°C because a smaller volume of material is heated to the boiling temperature. Less energy is extracted by vaporization and therefore more conduction takes place. It can be seen that the effect on room and pillar temperatures is marginal at lower power levels (<75 kw/acre), and hence, the boiling criteria is irrelevant for thermal calculations in these instances.

RKT:5521:njr:1951A

Distribution:

Mine Design Working Group Members

4530 R. W. Lynch
4537 J. K. Johnstone
4537 A. R. Lappin
5500 O. E. Jones
5510 D. B. Hayes
5511 J. W. Nunziato
5511 R. R. Eaton
5511 D. K. Gartling
5513 O. L. George
5520 T. B. Lane
5521 S. W. Key
5530 W. Herrmann
5521 R. K. Thomas

TUFF MINE DESIGN WORKING GROUP

ACTIVITY WORK PACKAGE

TITLE: Room-and-Pillar Thermal Analysis - Spent Fuel

INVESTIGATOR: Bob Thomas (SLA, Division 5521)

PHONE NUMBER: (505) 264-1457

DESCRIPTION:

1. Model Geometry - 2-D planar
2. Room Initial Conditions - see specification (5)
3. Room and Canister Dimensions, Hole Geometry, Initial Canister Power - see specifications (7 & 8)
4. Waste ~~SHW~~, instantaneous emplacement; for waste thermal output history see specification (9); for waste material and thermal properties see (10)
5. Backfill - assume room open 50 years, with radiative heat transfer, but no active cooling; for backfill properties, see specifications (4)
6. Temperature-Dependent Rock Properties (K, ρC_p , etc.) - use properties for tuff layer at greater than 711 m depth, see specifications (2 & 3)

PARAMETERS:

1. Extraction Ratio and Power Densities
 - a. 10% extraction ratio - 75 kW/acre
 - b. 20% extraction ratio - 25, 75, 150 kW/acre
 - c. 30% extraction ratio - 75 kW/acre
2. Boiling Temperature
 - Case I - 100°C
 - Case II - hydrostatic-head - potential boiling (223°C)
see specification (2)
(Case II run at discretion of modeler)

DUE DATE: February 5, 1980

REPORTING: 1. Technical Memo (letter form) to Working Group Members
2. Presentation of Results

FIGURE 1 Activity Work Package from Ref. [1]

$$s_1 = 3.75 \text{ m}$$

ER = Extraction Ratio = S_1/S_2

GTL = Gross Thermal Loading, kW/Acre

P = Cannister Pitch, m = 593.6 (ER/GTL)

$$Q_0 = \text{Initial Volumetric Power, J/YR-m}^3 = 0.2873/P$$

Temp-Time Plots at T_1, T_2, T_3, T_4, T_5

Temp Profile Plots At A-A

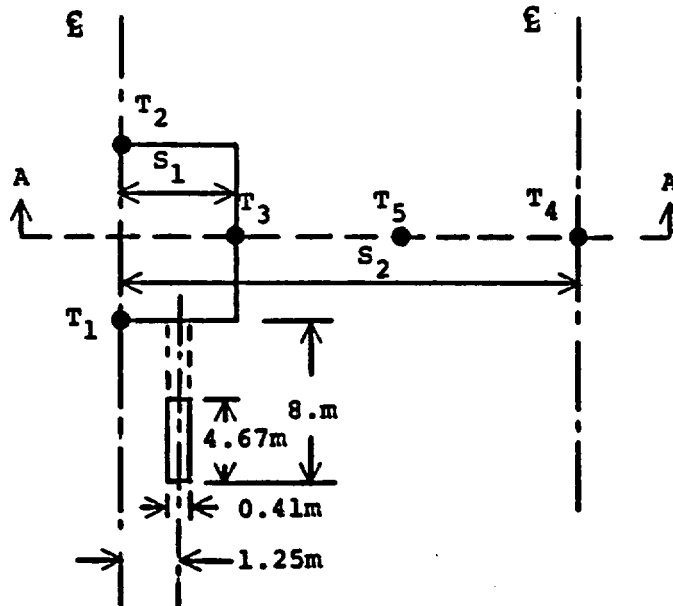


FIGURE 2 Room and Pillar Design Parameters
for Spent Fuel and Location of
Reported Temperatures

FIGURE 3 List of Cases Run and Design Parameters

Case Number	Extraction Ratio (ER)	Gross Thermal Loading (GTL) kW/Acre	Pitch (P) m	Initial Volumetric Power (Q_0) J/YR-m ³	Backfill Condition	H ₂ O Boiling Temp (T _{BOIL}) °C
1	0.1	25	2.374	3.815×10^9	SAT	100
2	0.1	75	0.7914	11.45×10^9	SAT	100
3	0.1	75	0.7914	11.45×10^9	DRY	100
4	0.1	75	0.7914	11.45×10^9	SAT	220
5	0.2	25	4.748	1.908×10^9	SAT	100
6	0.2	25	4.748	1.908×10^9	DRY	100
7	0.2	25	4.748	1.908×10^9	SAT	220
8	0.2	75	1.583	5.723×10^9	SAT	100
9	0.2	75	1.583	5.723×10^9	DRY	100
10	0.2	75	1.583	5.723×10^9	SAT	220
11	0.2	150	0.7914	11.45×10^9	SAT	100
12	0.2	150	0.7914	11.45×10^9	DRY	100
13	0.2	150	0.7914	11.45×10^9	SAT	220
14	0.3	75	2.374	3.815×10^9	SAT	100
15	0.3	75	2.374	3.815×10^9	DRY	100
16	0.3	75	2.374	3.815×10^9	SAT	220

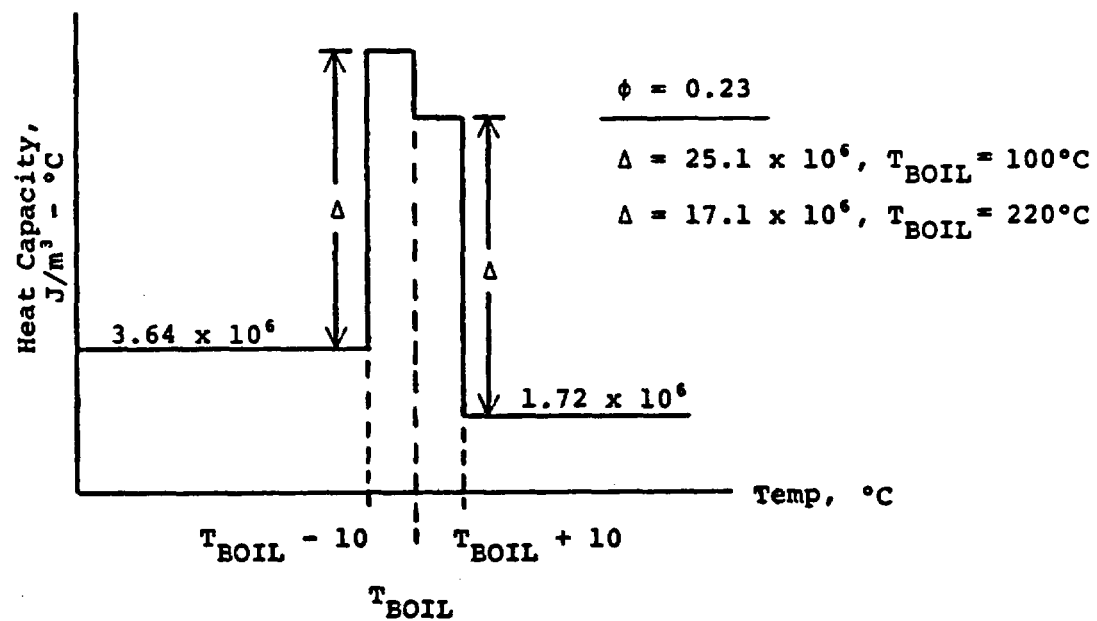
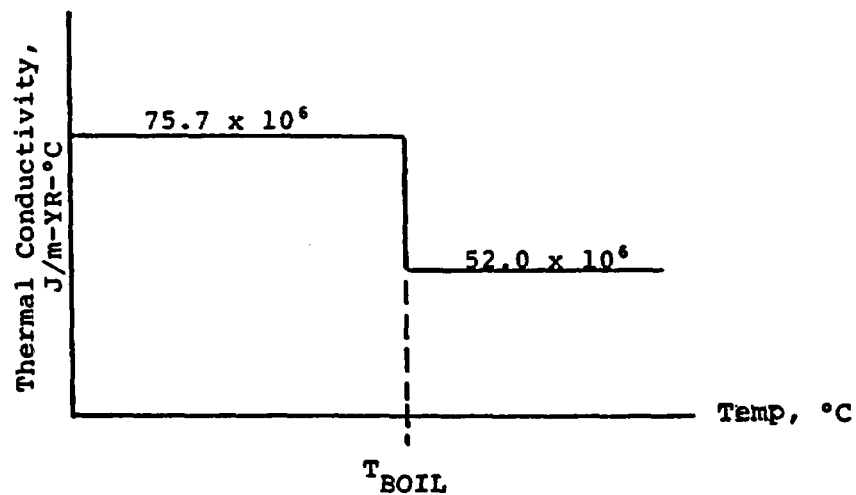


FIGURE 4 Thermal Properties Of Bullfrog
Member Of Crater Flats Tuff

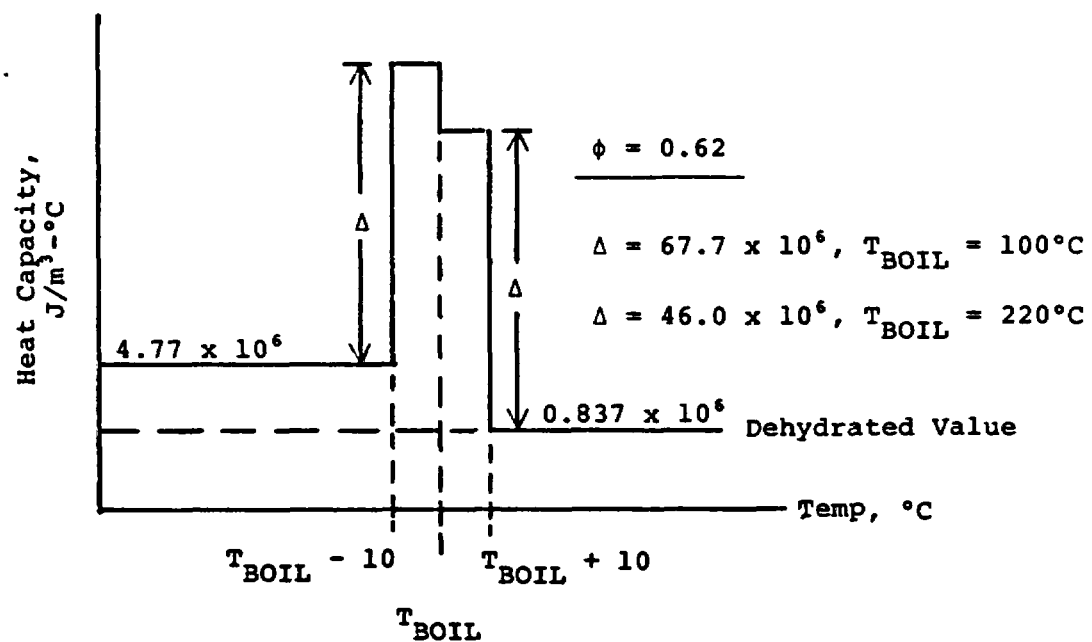
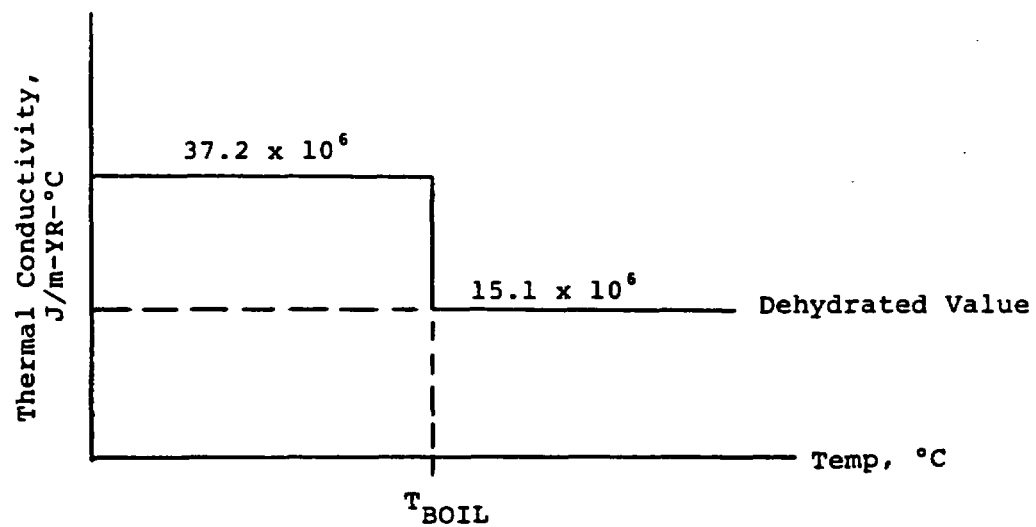


FIGURE 5 Thermal Properties Of
Backfill Material

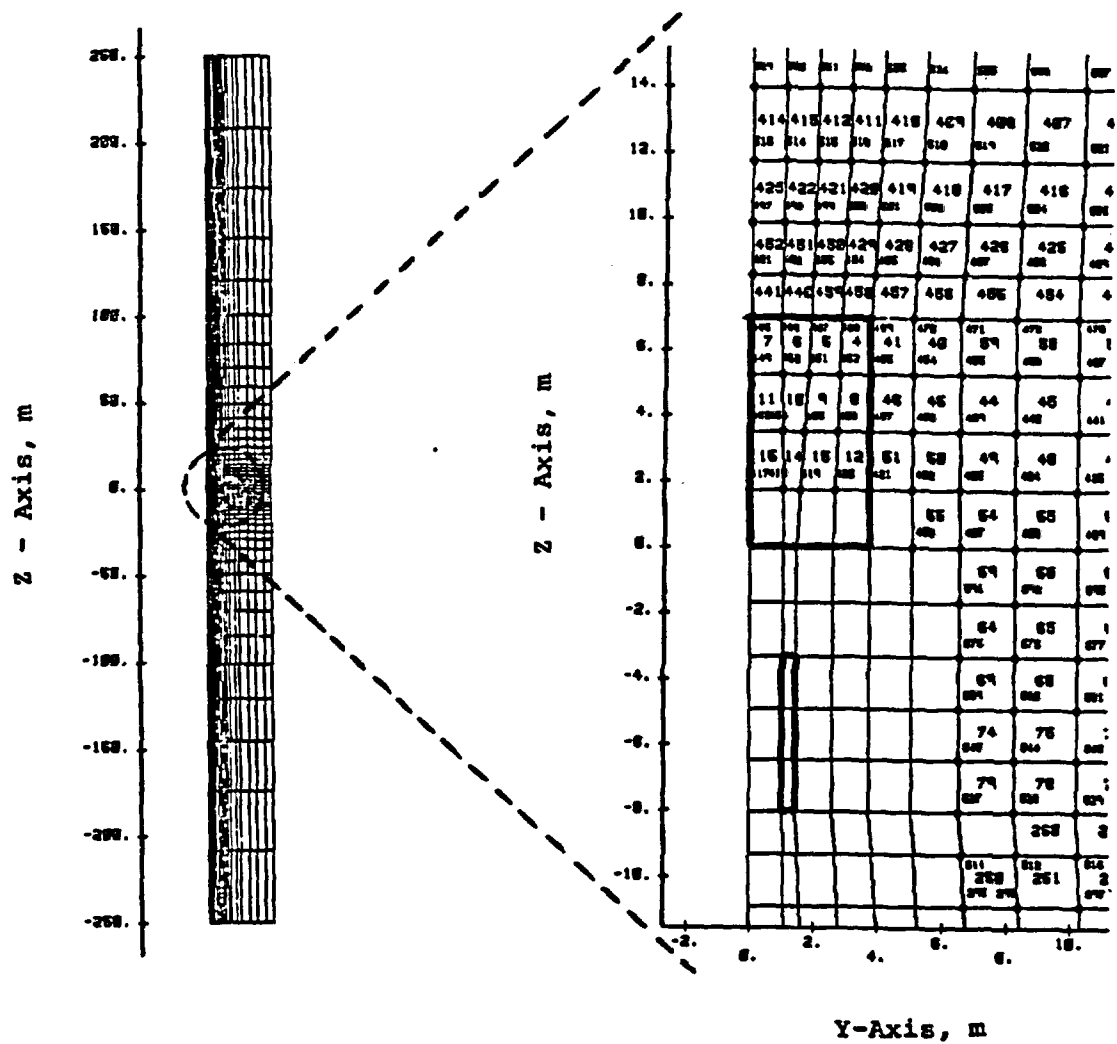


FIGURE 6 Finite Element Grid Of Room
And Pillar For 10% Extraction
Ratio

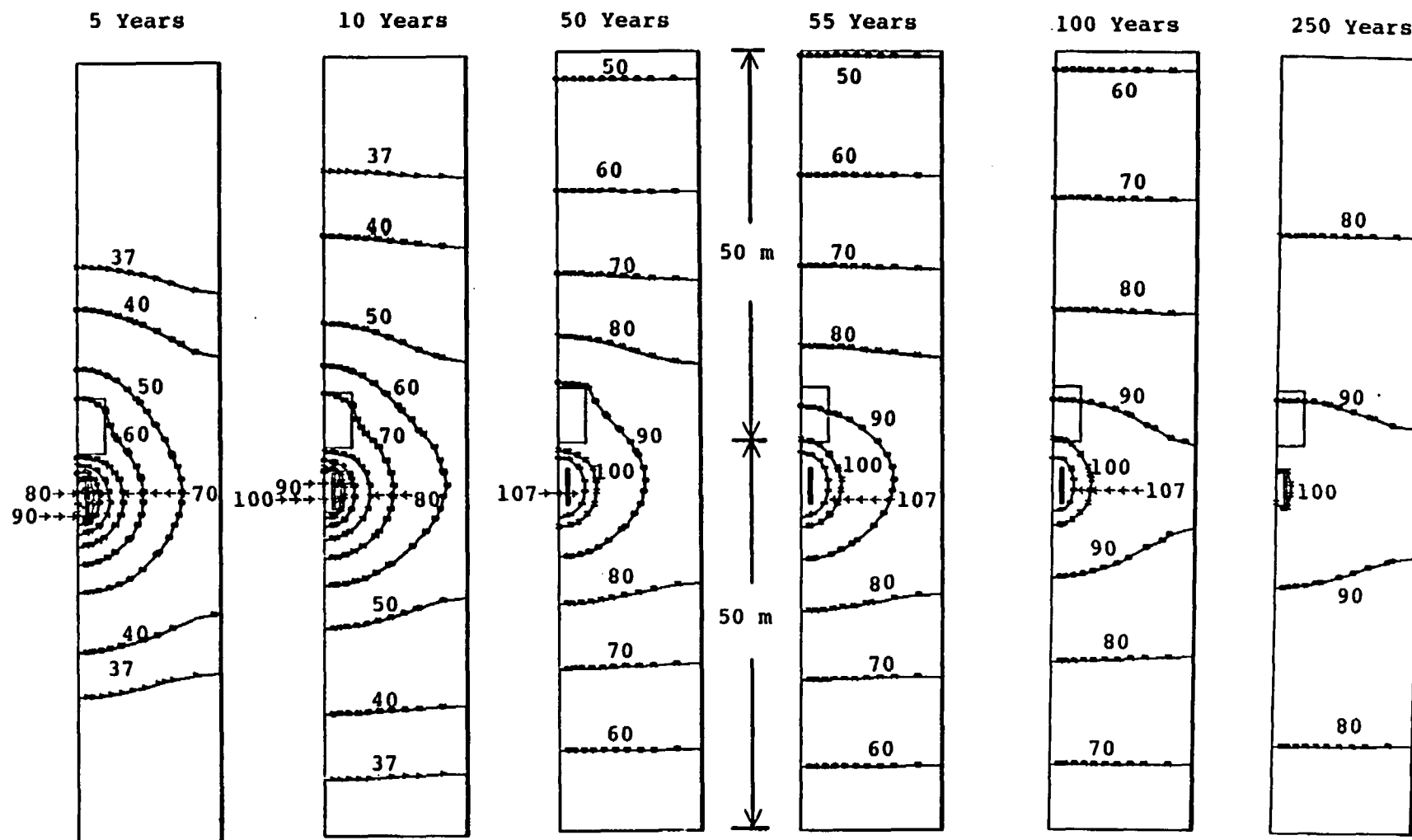


FIGURE 7 Temperature Isotherms at Various Times
for Case 8 (ER=0.2, GTL=75 kW/Acre,
100°C Boil, SAT Backfill)

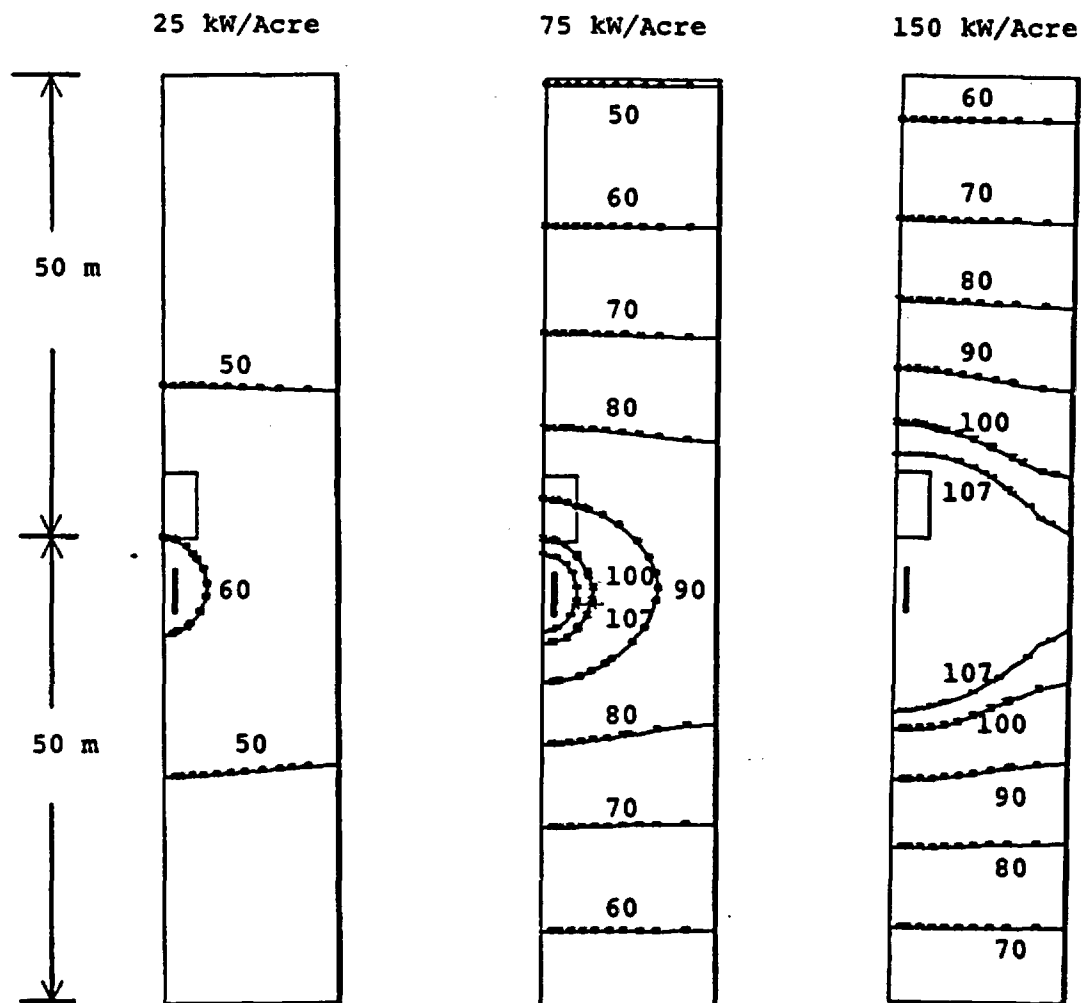


FIGURE 8 Temperature Isotherms For
Three Power Levels At 55 Years
(ER=0.2, 100°C Boil, SAT Backfill)

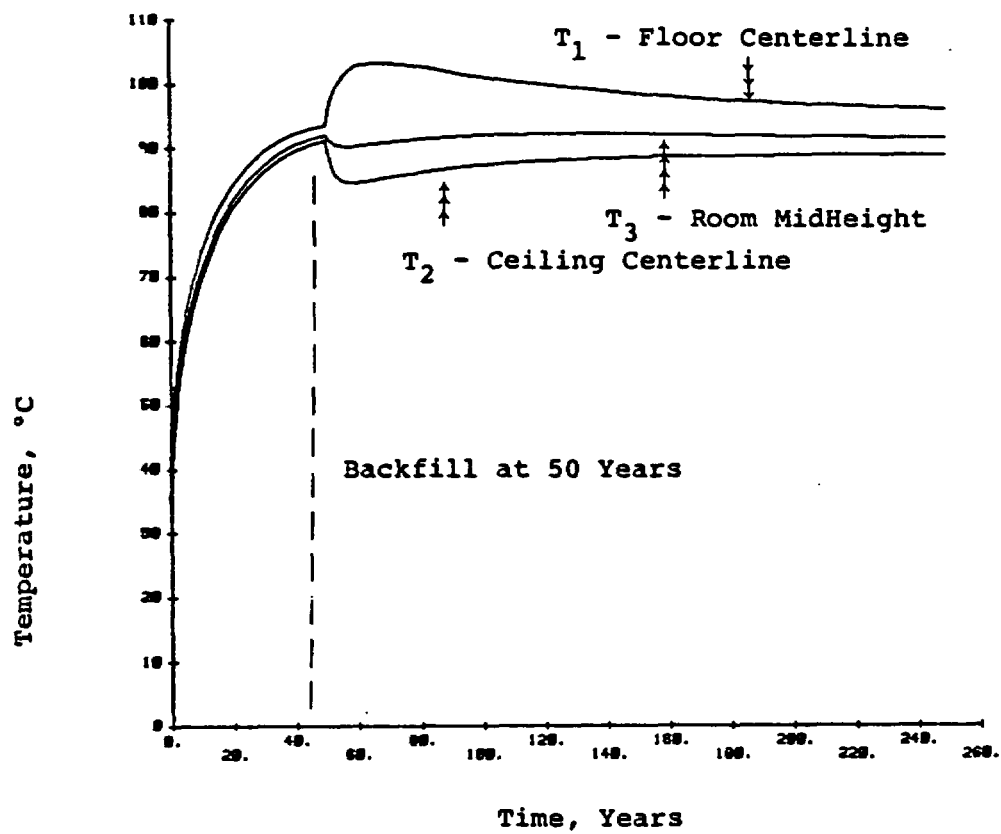


FIGURE 9 Temperature-Time History of Three Room Locations For Case 8 (ER=0.2, GTL=75 kW/acre, 100°C Boil, SAT Backfill)

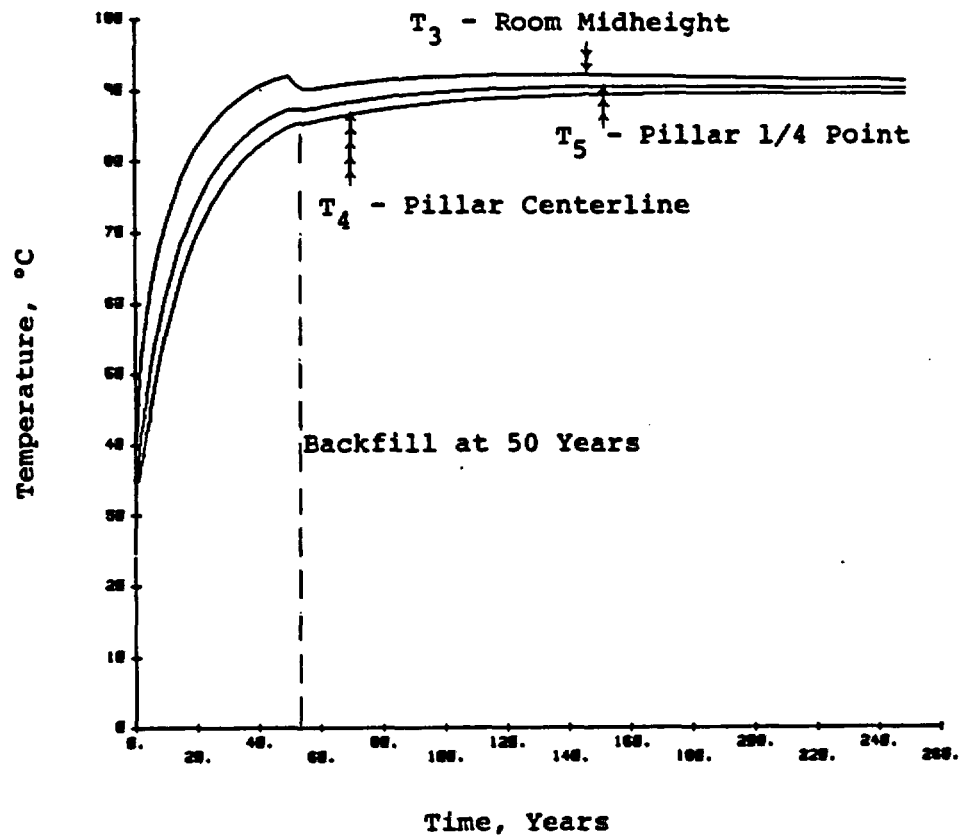


FIGURE 10 Temperature-Time History of Three Pillar Locations for Case 8 (ER=0.2, GTL=75 kW/Acre, 100°C Boil, SAT Backfill)

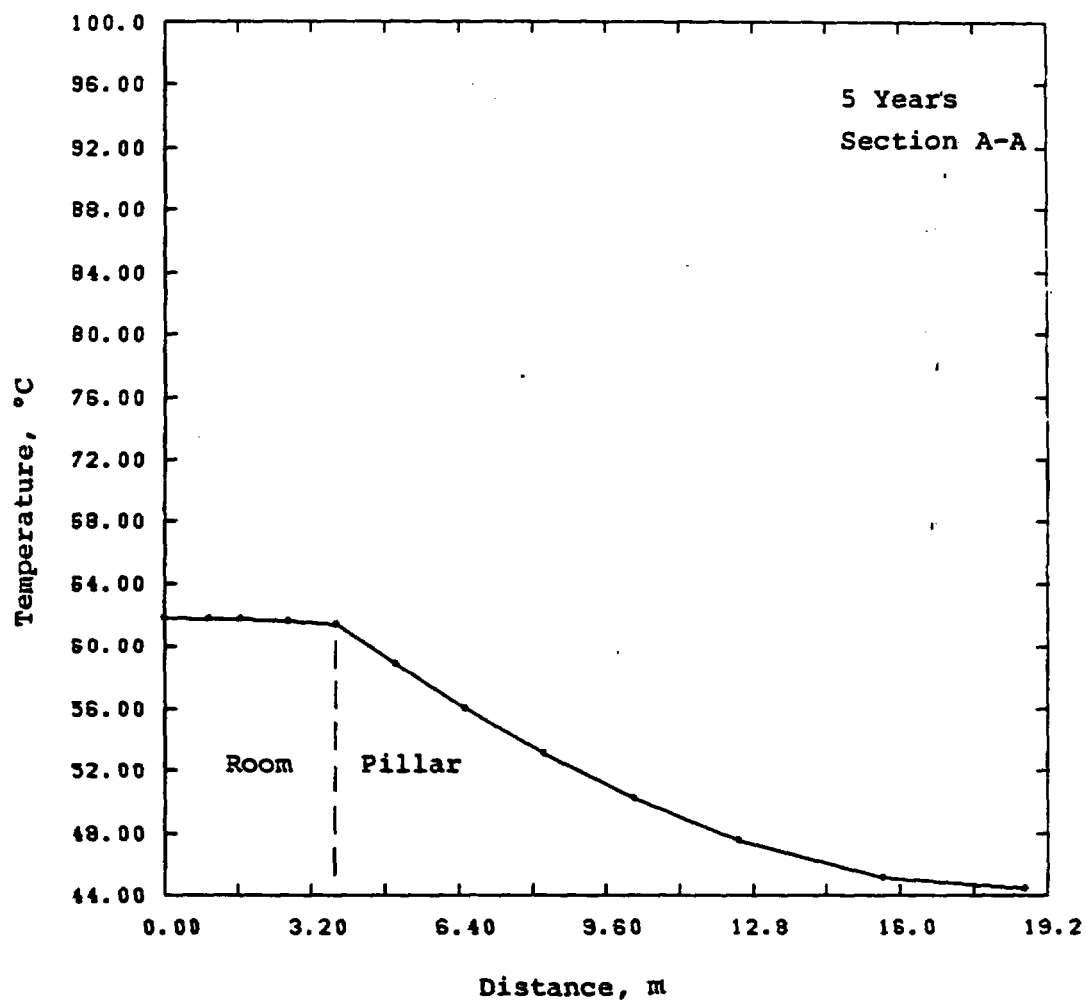


FIGURE 11 Temperature Profile Through Room and Pillar at 5 Years for Case 8 (ER=0.2, GTL=75 kW/Acre, 100°C Boil, SAT Backfill)

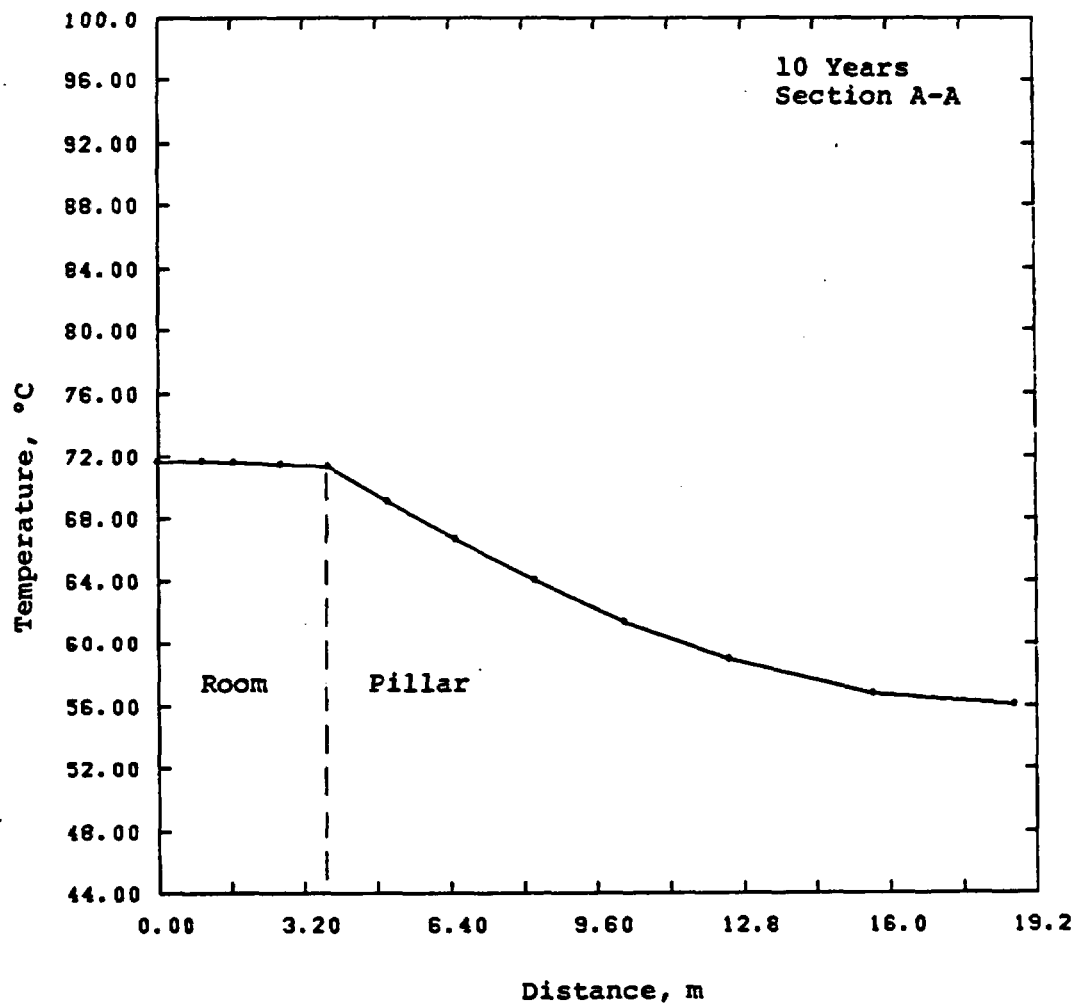


FIGURE 12 Temperature Profile Through Room and Pillar
at 10 Years for Case 8 (ER=0.2, GTL=75 kW/Acre,
100°C Boil, SAT Backfill)

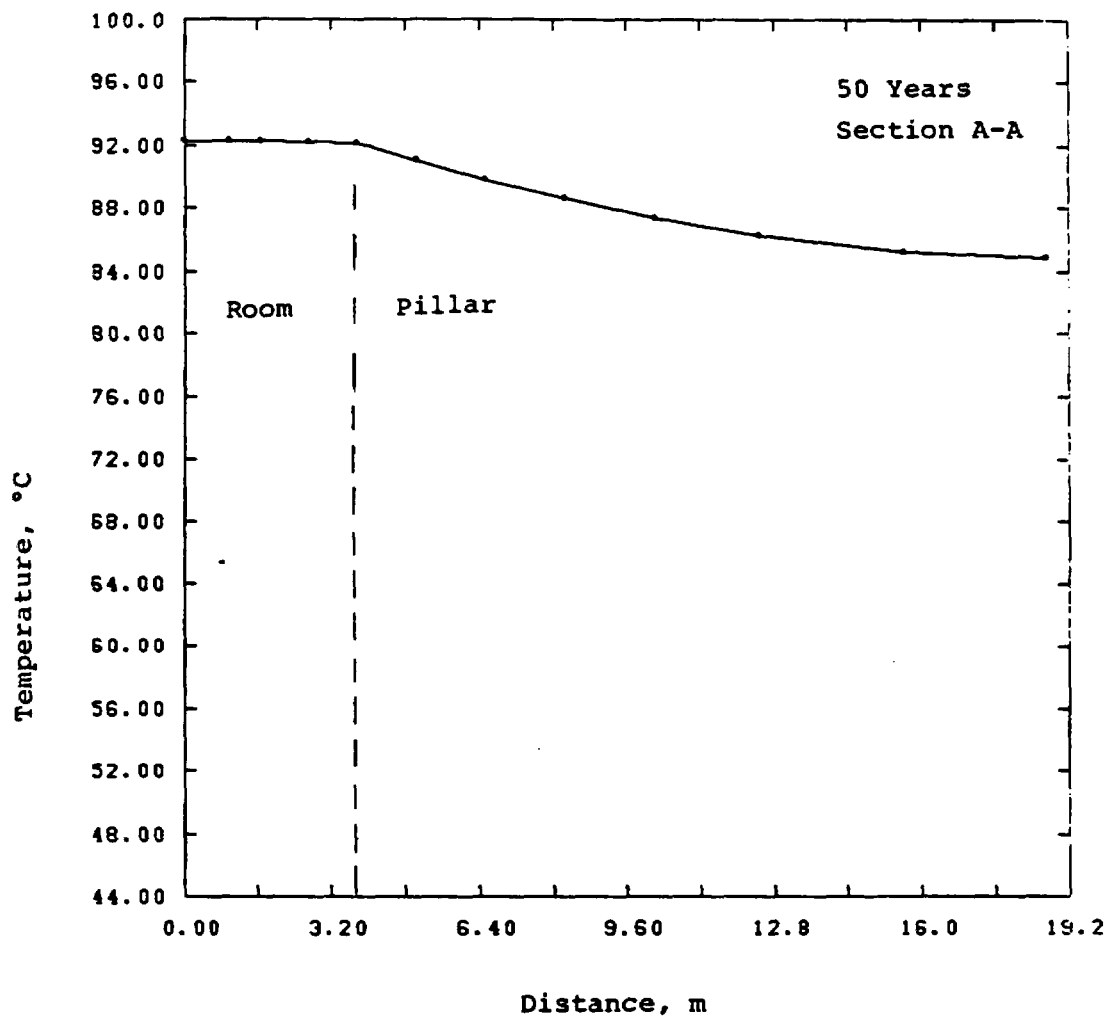


FIGURE 13 Temperature Profile Through Room and Pillar
at 50 Years for Case 8 (ER=0.2, GTL=75 kW/Acre,
100°C Boil, SAT Backfill)

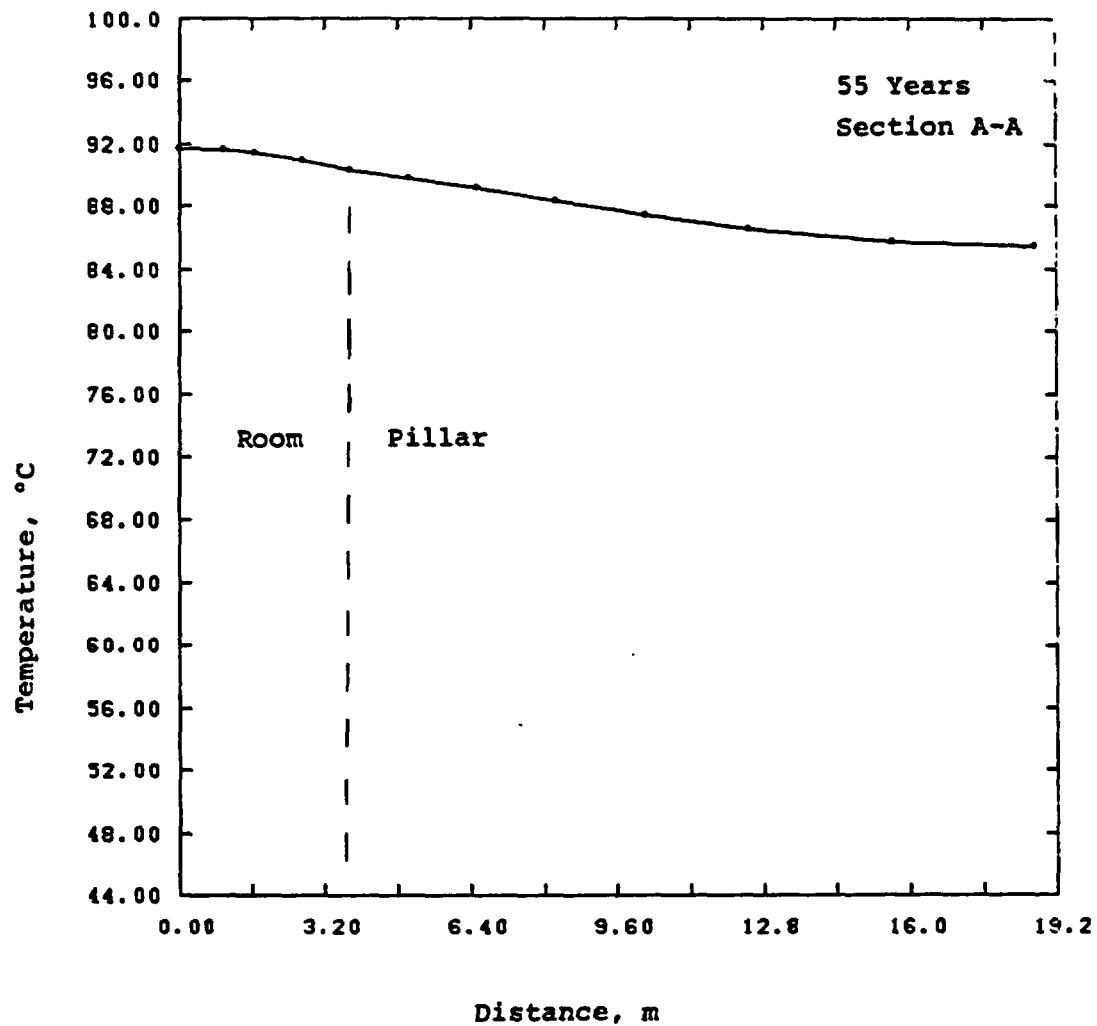


FIGURE 14 Temperature Profile Through Room and Pillar
at 55 Years for Case 8 (ER=0.2, GTL=75 kW/Acre,
100°C Boil, SAT Backfill)

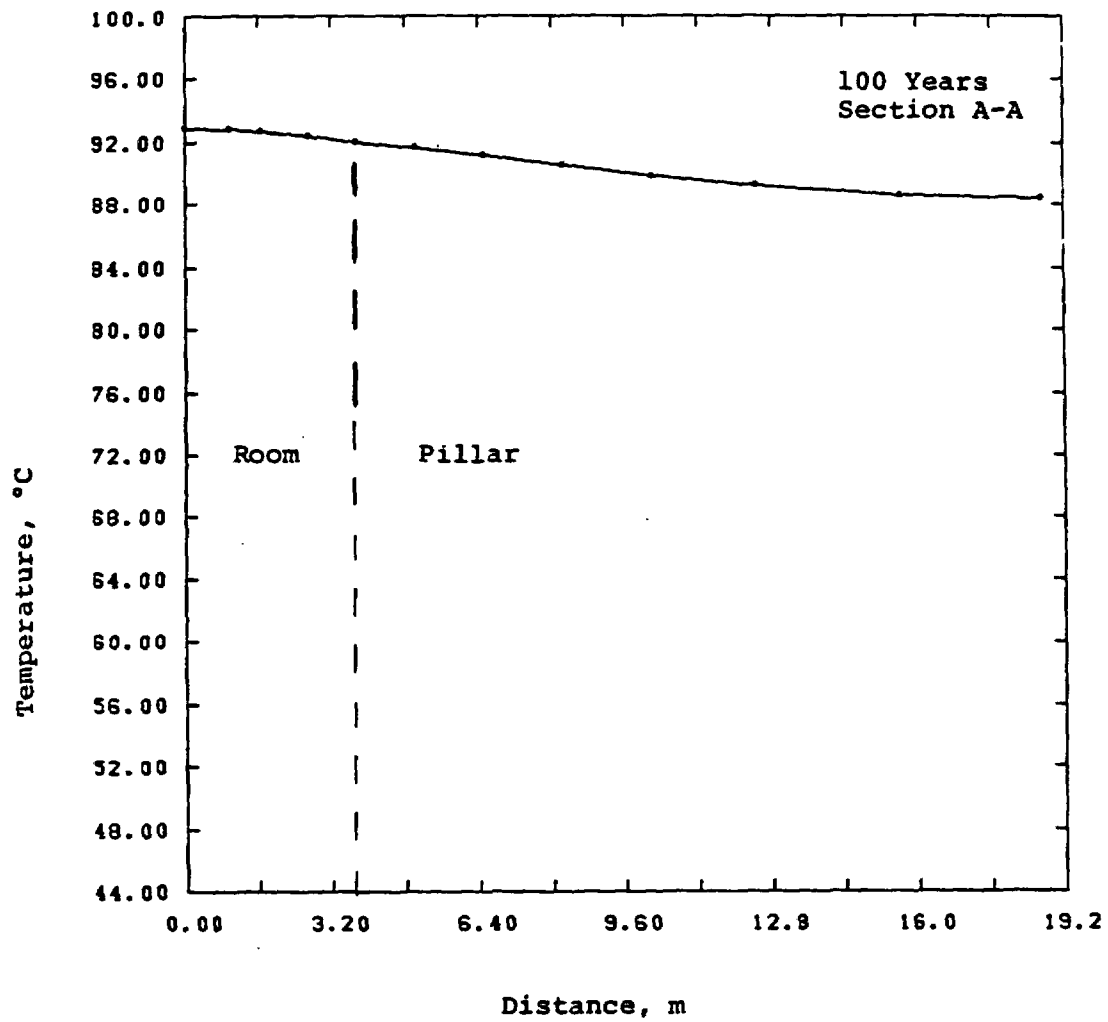


FIGURE 15 Temperature Profile through Room and Pillar
at 100 Years for Case 8 (ER=0.2, GTL=75 kW/Acre,
100°C Boil, SAT Backfill)

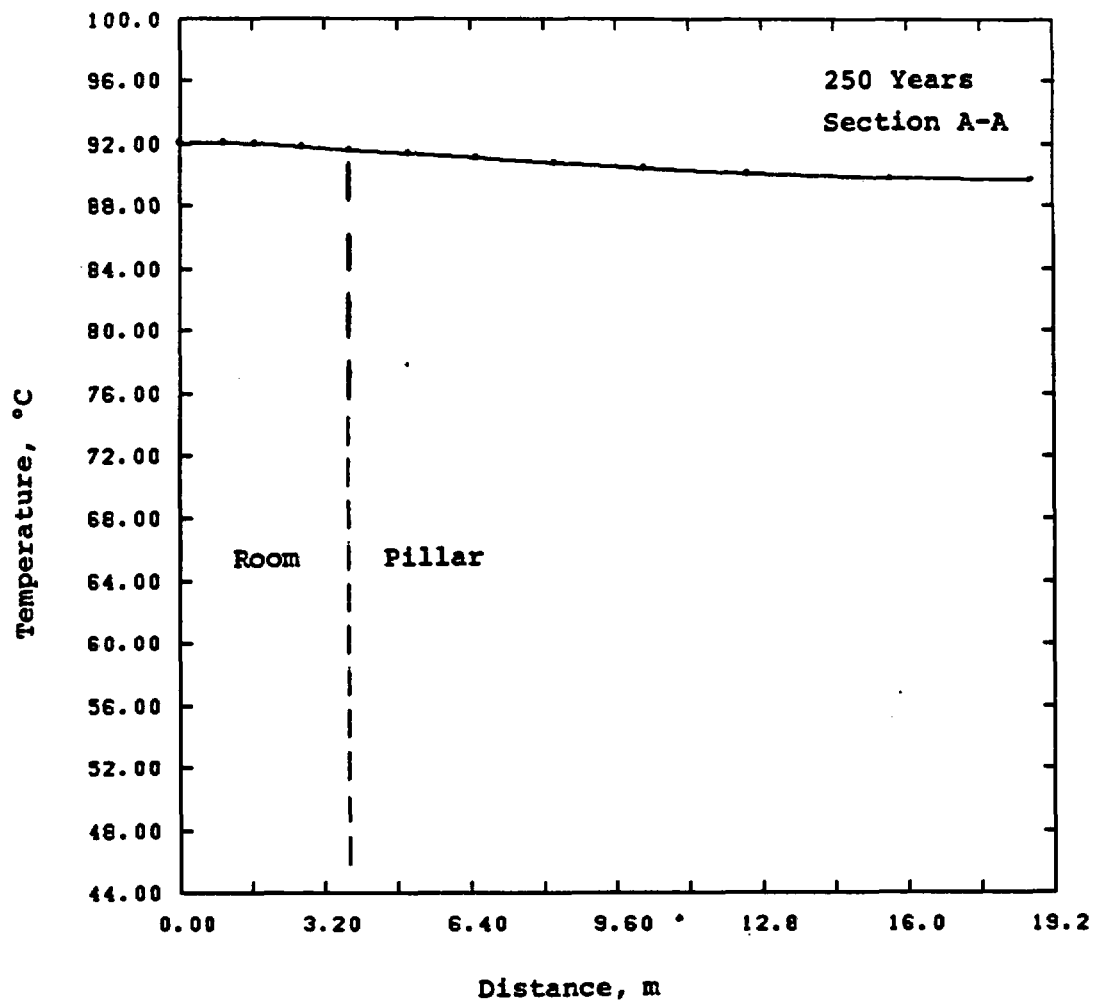


FIGURE 16 Temperature Profile Through Room and Pillar at 250 Years for Case 8 (ER=0.2, GTL=75 kW/Acre, 100°C Boil, SAT Backfill)

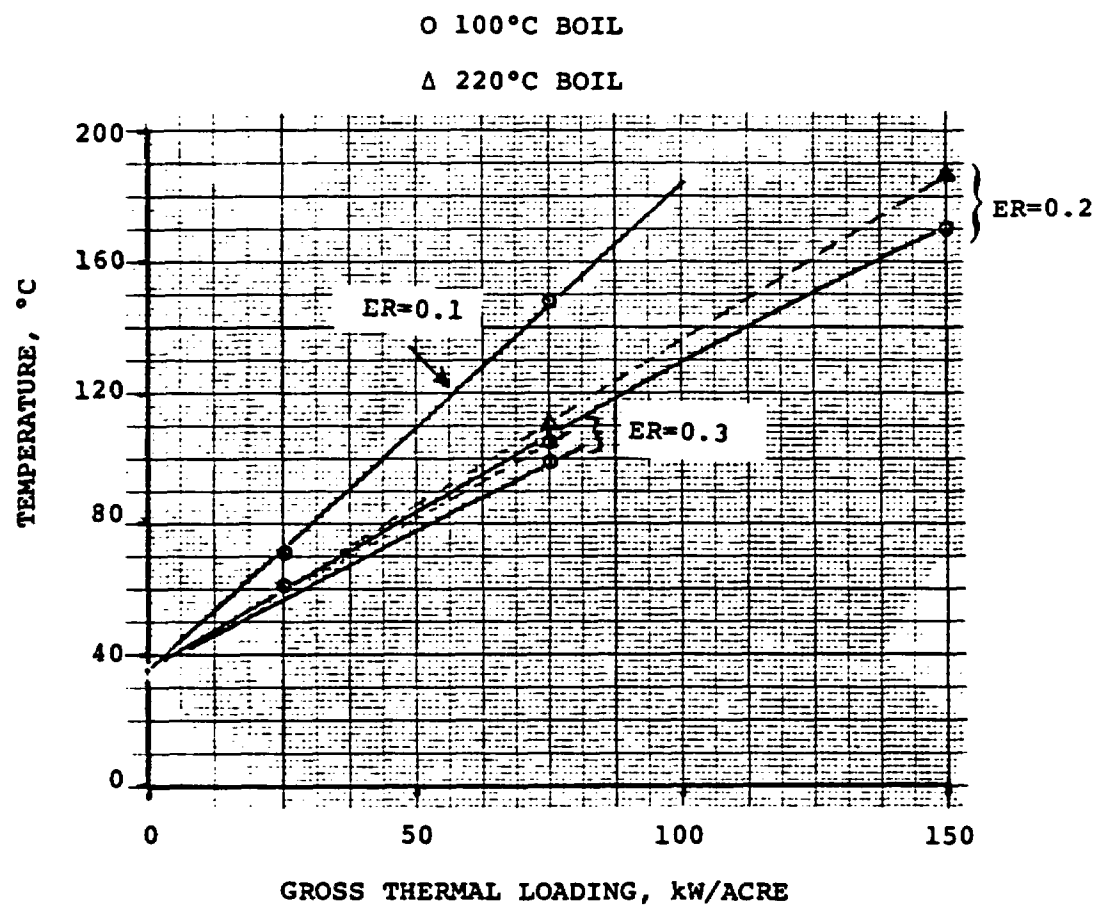


FIGURE 17 Peak Floor Centerline Temperature (T1) Versus GTL

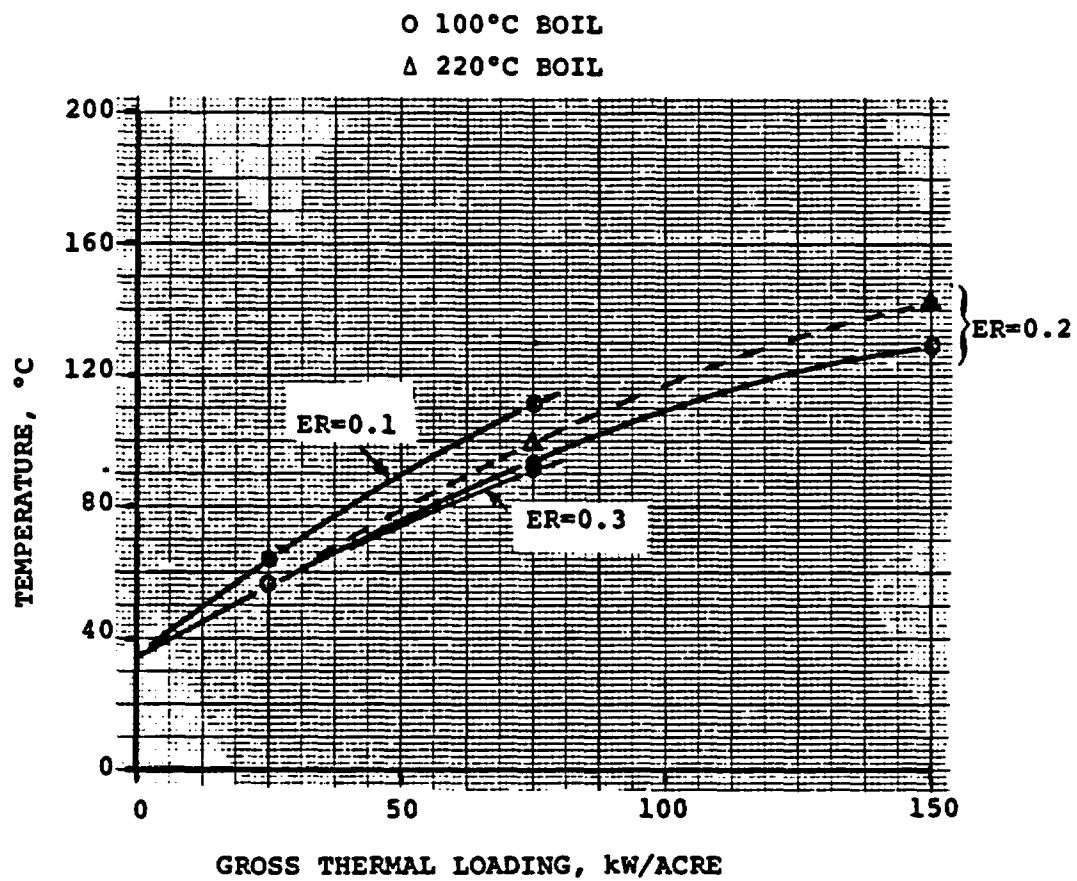


FIGURE 18 Peak Room Midheight
Temperature (T3) Versus GTL

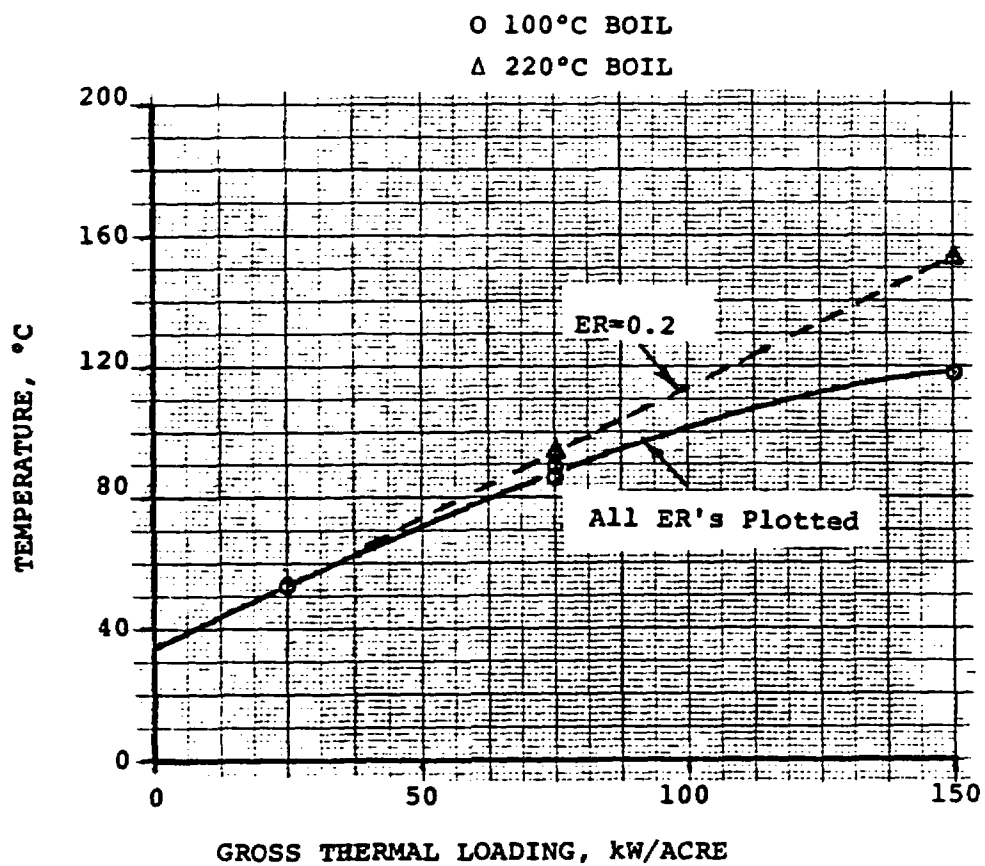
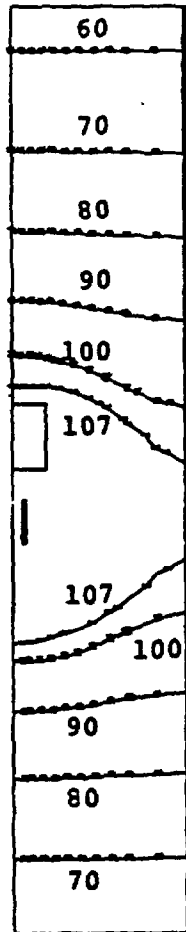


FIGURE 19 Peak Pillar Centerline
Temperature (T4) Versus GTL

100°C BOIL



220°C BOIL

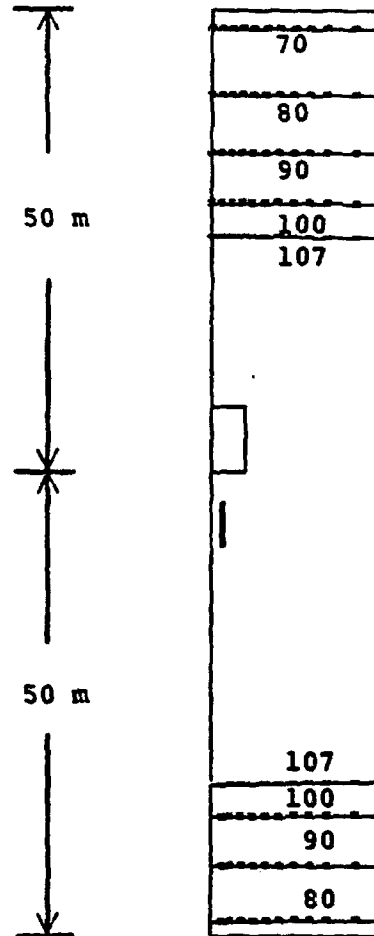


FIGURE 20

Temperature Isotherms at 55
Years for Two Boiling Conditions
(ER=0.2, 150 kW/Acre, SAT Backfill)

Sandia Laboratories

Albuquerque, New Mexico
Livermore, California

date: April 7, 1980

to: Distribution

R. K. Thomas

from: R. K. Thomas, 5521

subject: Mine Design Working Group: Further Results for Room and Pillar Thermal Analysis - Spent Fuel

Ref: Memo, R. K. Thomas, 5521, to Distribution, "Tuff Room and Pillar Thermal Analysis - Spent Fuel," Feb. 4, 1980.

At the request of B. Langkopf, 4537, several additional thermal scoping calculations were made with the 2-D room and pillar geometry for spent fuel. The only difference between these additional calculations and those presented at the Feb. 5-6 meeting of the Mine Design Working Group, and referenced above, is that the uniform initial temperature was taken to be 55°C, instead of 35°C.

Results of these calculations are summarized in Figs 1-7, the form of which is identical to plots presented in the above reference. Calculations were made for 75 and 150 kW/Acre, 100°C and 220°C boiling, with a fixed 20% extraction ratio and saturated backfill after 50 years. The nature of the thermal response was found to be the same as that reported previously, except that the magnitude of response in the room and pillar region is approximately 20°C higher. Temperatures above the boiling criteria were found in all cases, except for 75 kW/Acre and 220°C boiling.

Incidentally, in Fig 3 in the above reference, the exponent of numbers in the column labeled "Initial Volumetric Power" should read $\times 10^9$, not $\times 10^6$ as shown.

RKT:5521:njr

Distribution:
Mine Design Working Group Members

4530 R. W. Lynch
4537 J. K. Johnstone
4537 A. R. Lappin
5500 O. E. Jones
5510 D. B. Hayes
5511 J. W. Nunziato
5511 R. R. Eaton
5511 D. K. Gartling
5513 O. L. George
5520 T. B. Lane
5521 S. W. Key
5530 W. Herrmann
5521 R. K. Thomas

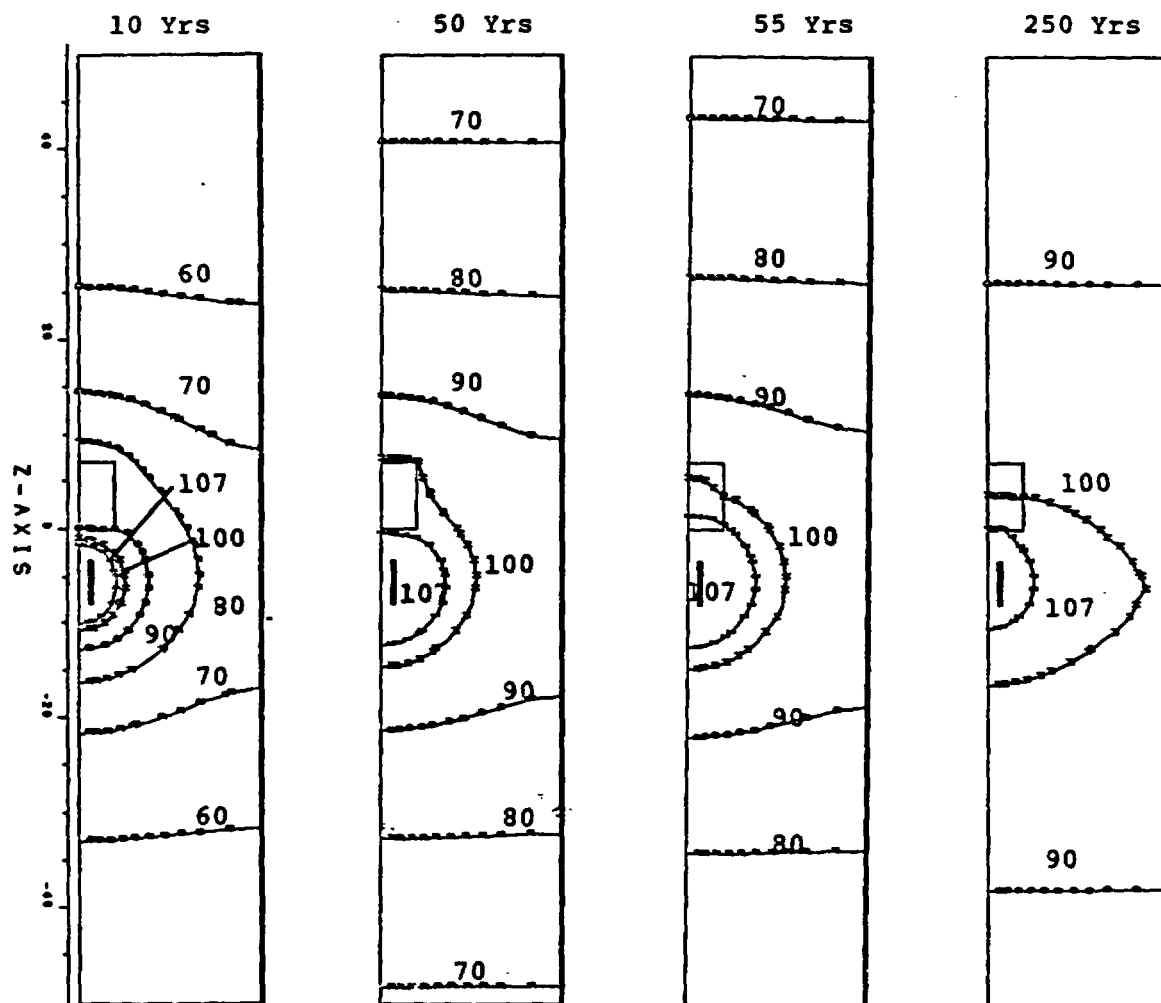


Fig. 1 Temperature Isotherms at Various Times for 20% Extraction Ratio, 75 kW/Acre, 100°C Boiling, and Saturated Backfill After 50 Yrs.

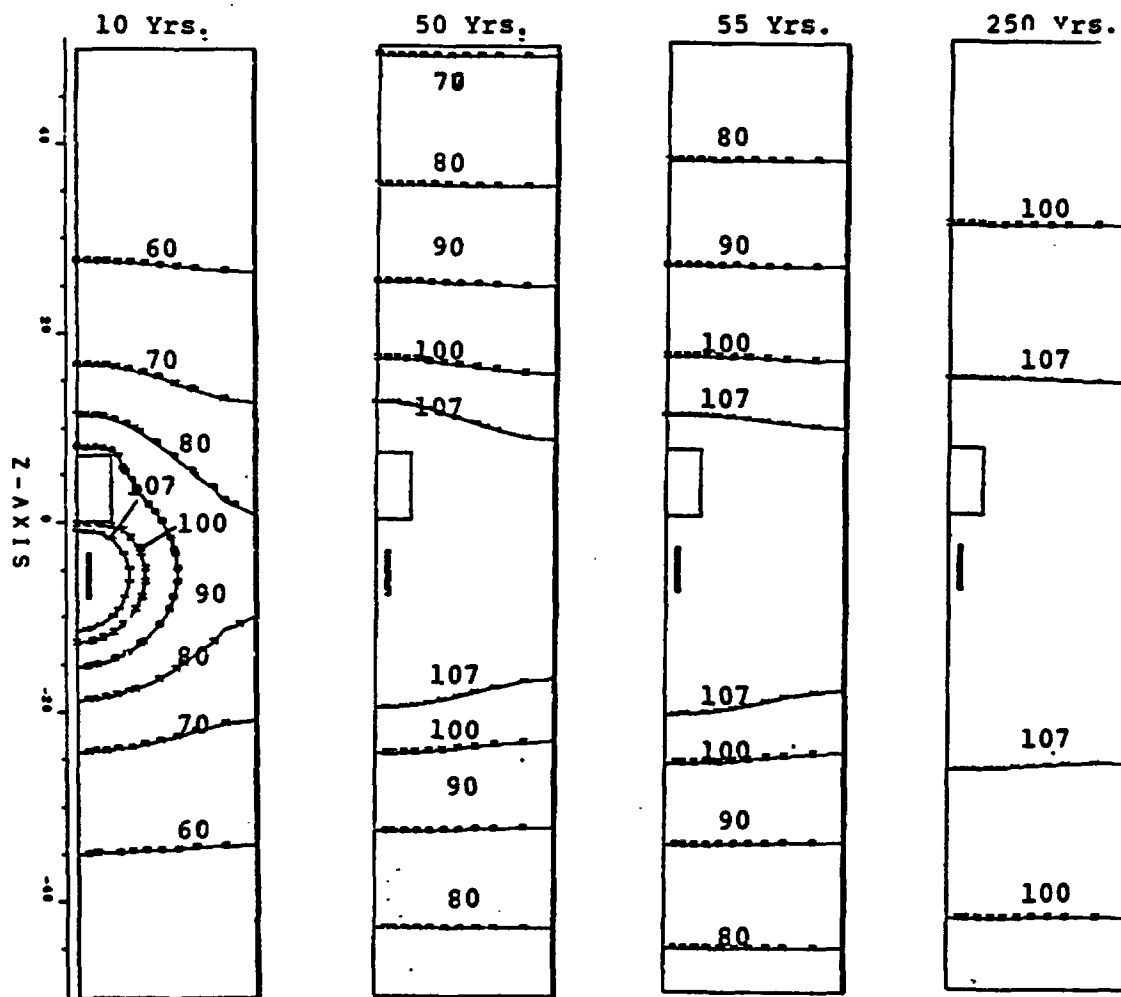


Fig. 2 Temperature Isotherms at Various Times for
20% Extraction Ratio, 75 kW/Acre, 220°C
Boiling, and Saturated Backfill After
50 Yrs.

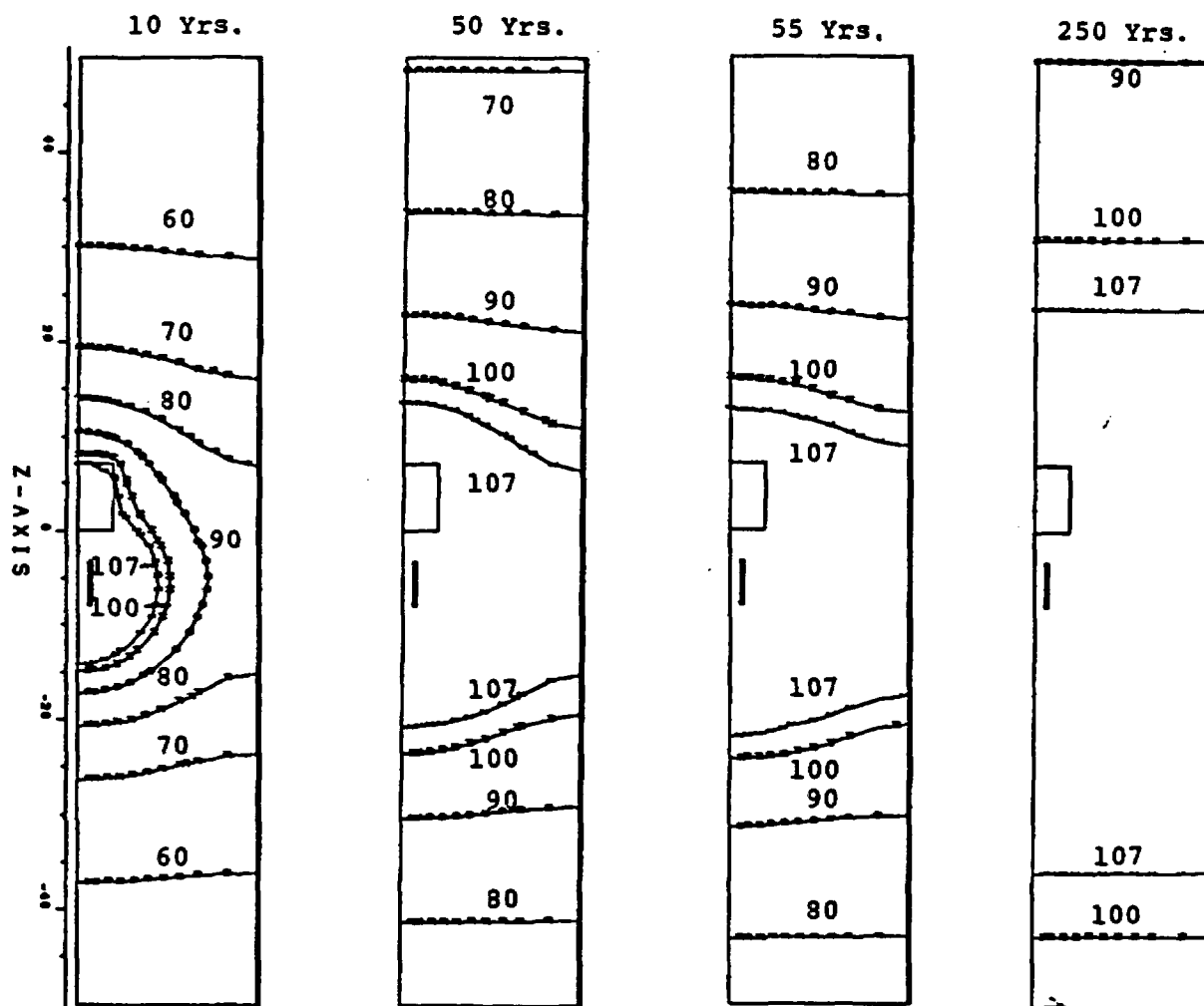


Fig. 3 Temperature Isotherms at Various Times For 20% Extraction Ratio, 150 kW/Acre, 100°C Boiling, and Saturated Backfill After 50 Years.

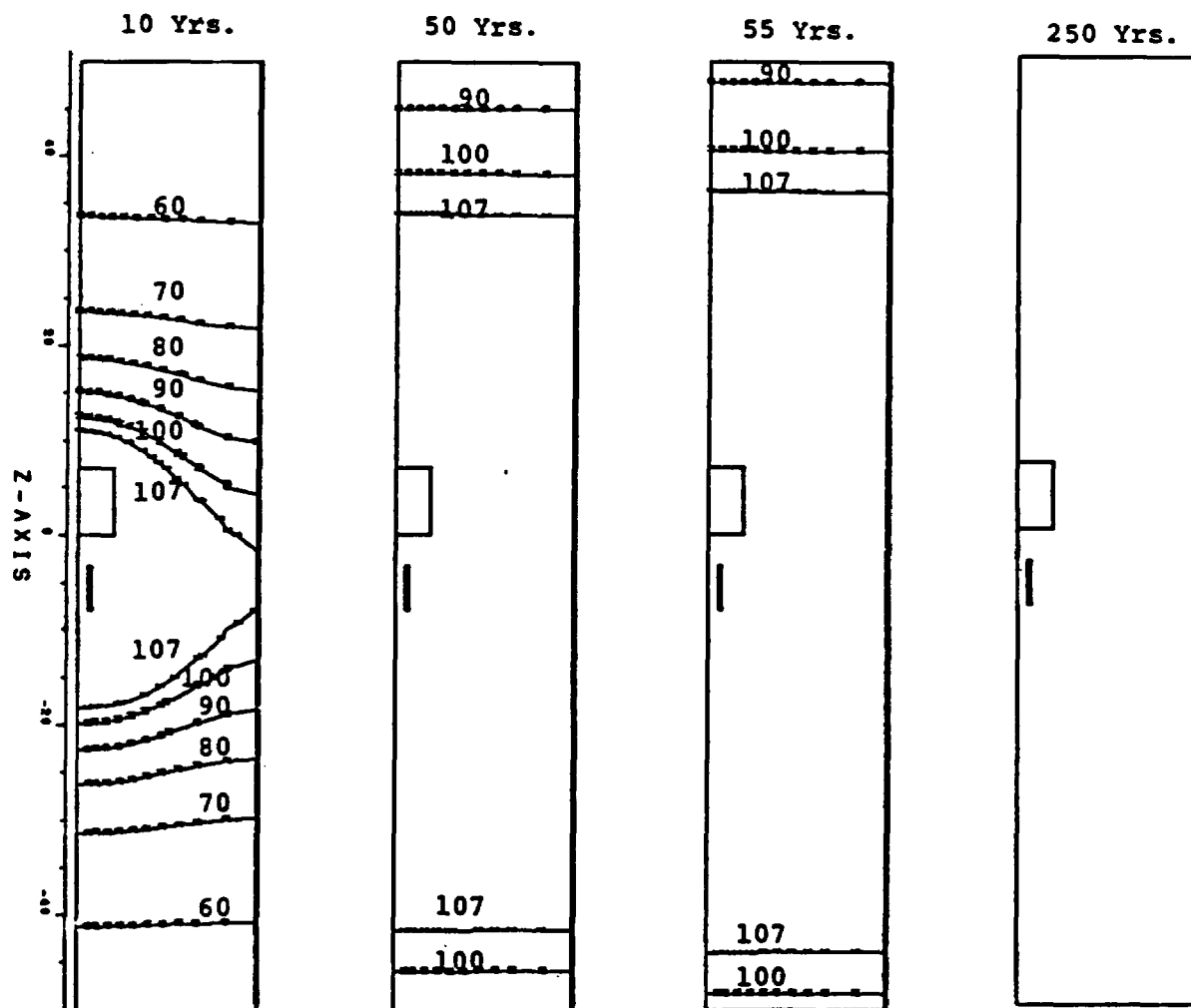


Fig. 4 Temperature Isotherms at Various Times
For 20% Extraction Ratio, 150 kW/Acre,
220°C Boiling, and Saturated Backfill
After 50 Years.

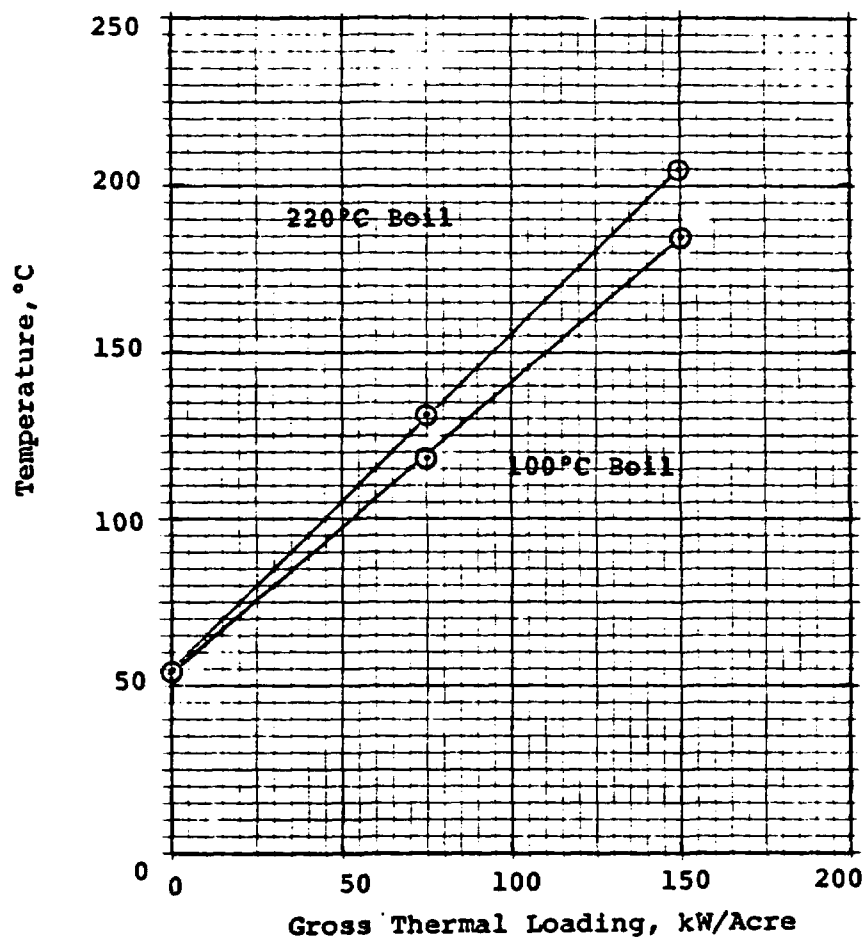


Fig. 5 Peak Floor Centerline Temp(T1)
for 20% Extraction Ratio, Sat.
Backfill, and 55°C Initial Temp

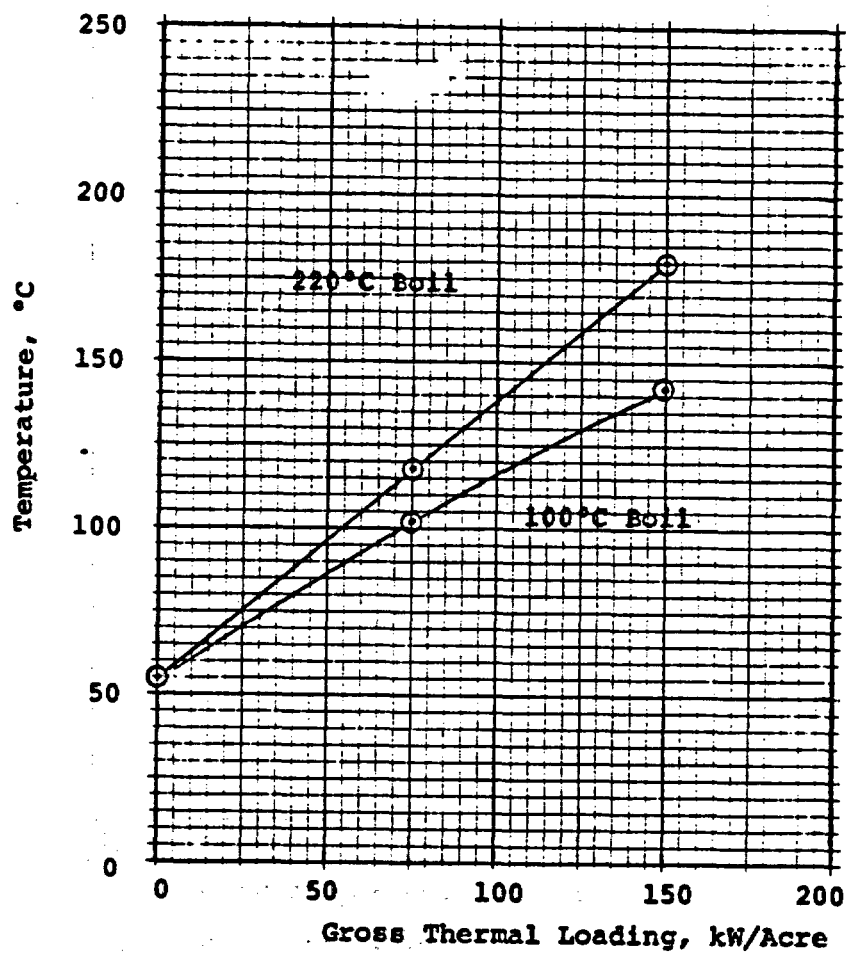


Fig. 6 Peak Room Midheight Temp(T3)
for 20% Extraction Ratio, Sat.
Backfill, and 55°C Initial Temp

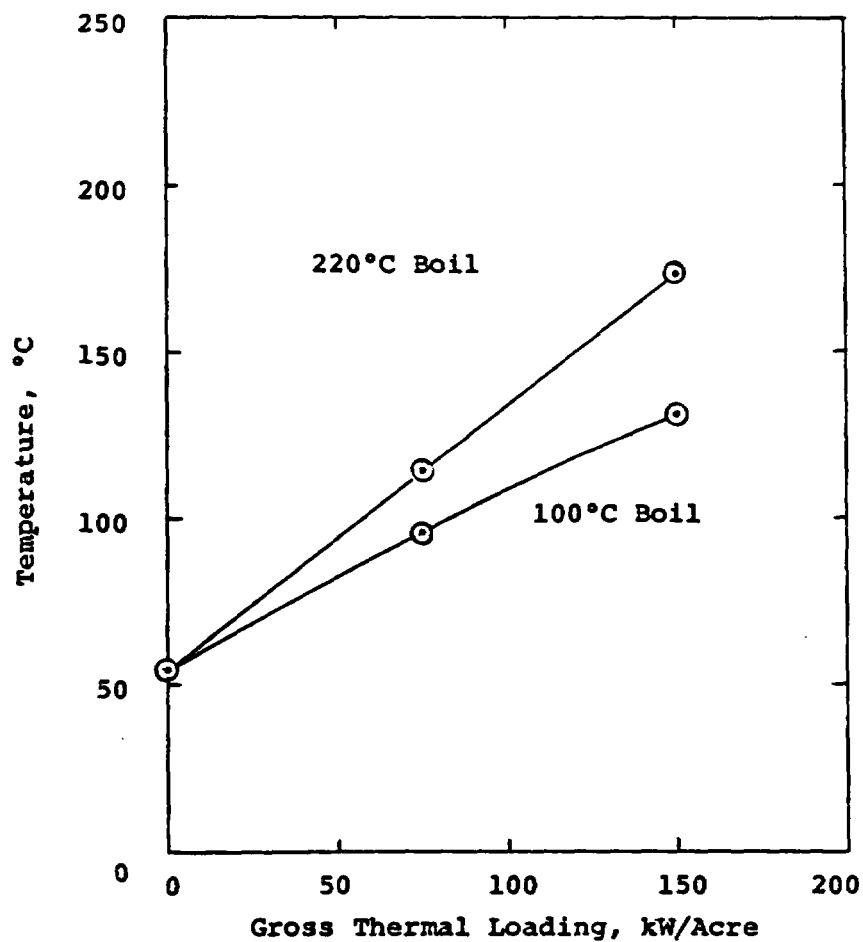


Fig. 7 Peak Pillar Centerline Temp(T4)
for 20% Extraction Ratio, Sat.
Backfill, and 55°C Initial Temp

APPENDIX C

Near Field Analysis for HLW

- Part I: MIDES Working Group - Work Package
- Part II: Single Canister Thermal Calculations to Estimate Canister and Very Near-Field Temperatures Resulting from Emplacement of High Level Waste in Welded Tuff
(Memo, R. R. Eaton, 5511, to A. R. Lappin, 4537, dtd. 1/31/80)
- Part III: Single Canister Thermal Calculations to Estimate Canister and Very Near-Field Temperatures Resulting from Emplacement of High Level Waste in Welded Tuff for an Initial Tuff Temperature of 55°C
(Memo, R. R. Eaton, 5511, to Distribution, dtd. 3/7/80)
- Part IV: Single Canister Thermal Calculations to Estimate Canister and Very Near-Field Temperatures Resulting from Emplacement of High Level Waste in Welded and Non-Welded Tuff
(Memo, R. R. Eaton, 5511, to Distribution, dtd. 5/12/80)
- Part V: Single Canister Thermal Calculations in Welded Tuff for an Initial Tuff Temperature of 35°C
(Memo, R. R. Eaton and C. M. Korbin, 5511, to Distribution, dtd. 7/3/80)
- Part VI: Comparison of Effective Radius 2-Dimensional Thermal Simulation with Full 3-Dimensional Results
(Memo, R. R. Eaton, 5511, and R. K. Thomas, 5521, to Distribution, dtd. 11/12/80)

TUFF MINE DESIGN WORKING GROUP

ACTIVITY WORK PACKAGE

TITLE: Very Near-Field Thermal Analysis - High Level Waste

INVESTIGATOR: D. F. McVey (SLA, Div. 5511)

PHONE NUMBER: (505) 264-4949

OBJECTIVE: To perform single-canister thermal calculations to estimate canister and very near-field temperatures resulting from emplacement of HLW.

DESCRIPTION:

1. Model Geometry - 2-D axisymmetric
2. Initial Conditions - see specification list (5)
3. Canister and Hole Geometry, Baseline Canister Initial Power - see specifications list (8)
4. Waste - HLW; for thermal output history and waste material and thermal properties, see specifications list (9 & 10)
5. Baseline Temperature-Dependent Rock Properties - use values for Bullfrog Member of Crater Flat Tuff (> 711 m depth), see specifications list (2 & 3)
6. Boiling Temperature - 100°C.

PARAMETERS:

1. Initial Canister Power (Cases, I, II, III) - 3.5 kW (base-line case) plus 2 lower levels (picked at modeler's discretion)
2. Temperature-Dependent Rock Properties (Cases IV-VII, 3.5 kW)

Case	K ($T < T_{\text{boil}}$)	K ($T > T_{\text{boil}}$)
I, II, III	2.40	1.65 (W/mK)
IV	2.88	1.98
V	2.88	1.32
VI	1.92	1.98
VII	1.92	1.32

DUE DATE: February 5, 1980

REPORTING: 1. Technical Memo (letter form) to Working Group Members
2. Presentation of Results

Sandia Laboratories

Albuquerque, New Mexico
Livermore, California

date: January 31, 1980

to: A. R. Lappin - 4537



from: R. R. Eaton - 5511

subject: Single Canister Thermal Calculations to Estimate Canister and Very Near-Field Temperatures Resulting from Emplacement of High Level Waste (HLW) in Welded Tuff

A preliminary thermal analysis has been completed for the very near-field (radius ≤ 15 m) of a single canister containing HLW (3.5, 2.16, and 1.0 kW) emplaced in welded tuff. Specifications not given in this memo regarding canister geometry, canister output versus time, canister and tuff properties are given in, "Mine Design Working Group Activity Work Package," dtd 12/4-5/79 and authored by Division 4537.

The COYOTE finite element heat conduction code* was used to generate time-dependent, two-dimensional axisymmetric temperature solutions in the canister and tuff. A schematic of the nodalization used is given in Figure 1. A total of 273 elements were used to simulate the geometry. A total of 15 runs were made using three different canister output levels (3.5, 2.16, and 1.0 at time = 0) and 20% variations from the norm in thermal conductivity (see Table 1). The plus-minus symbolism designating variations in K will be used when referring to specific cases.

The drift above the canister was modeled by using the properties of air ($\rho = 1.2 \text{ kg/m}^3$, $c = 1.6 \times 10^3 \text{ J/m}^3\text{-}^\circ\text{C-kg}$), and an effective thermal conductivity of $K = 25 \text{ W/m-K}$ to simulate the effect of radiation.** In an attempt to determine the effect of the adiabatic conditions imposed at the boundaries of the finite region considered, three runs were repeated after increasing y_{max} from 15 m to 25 m, and r_{max} from 9 m to 14 m (see Figure 2). This change effects the maximum canister and tuff temperature by less than 2°C one year after canister emplacement. It was, therefore, concluded that the boundary conditions imposed were satisfactory

*D. K. Gartling, "COYOTE--A Finite Element Computer Program for Non-Linear Heat Conduction Problems," SAND77-1332, Sandia Laboratories, Albuquerque, NM, June 1978.

**Memo, O. L. George, Jr., 5511, to D. F. McVey, 5511, dtd 1/4/80, subject: The Effect of Thermal Radiation in the Disposal of High Level Waste (HLW) in Tuff.

for times up to one year. Figure 3 shows isotherms, at one year, for the nominal (0) case for an initial canister output of 3.5 kW. Figure 4 shows the radial distribution of temperature for the nominal case for three different initial canister output levels. It can be seen from Figure 5 that at one year the center point of the drift floor ranges from 1.5°C to 10.5°C above the initial temperature of 35°C. This implies that the simulated drift boundary condition must be made more realistic in order to obtain reliable calculated temperatures for run times longer than one year. It is anticipated that the drift will be convective cooled at early times ($t < 50$ yrs). No convection was considered in this model. Figures 6a and 6b show that at one year, the peak canister and tuff temperature have been adequately approached for this study. The temperature time slope (dT/dt) is less than 3°C/year. Because of this small slope and the boundary limitations discussed above, all calculations were terminated at one year.

Figure 7 shows the 100°C isotherm for the three canister outputs. The volume of the tuff which is above the 100°C (unsaturated or dried) is plotted on Figure 8. This volume was estimated assuming it to be equal to the volume of an ellipsoid. The major and minor axes are taken from Figure 7.

Figure 9 shows the influence of the thermal conductivity of the tuff on the 100°C isotherm for the 3.5 kW case. The volume of tuff above 100°C is given in Table 2. It is difficult, and slightly confusing, to attempt to decipher the significance of the conductivity magnitude. The data presented in Figures 10 and 11 are easier to interpret. They give the maximum canister temperature (centerline-centerplane) and maximum tuff temperature (centerplane, $r = 0.185$ m). From these two figures, it can be seen for the conductivities considered that for initial canister outputs above 3.0 kW the magnitude of the thermal conductivity used for tuff above 100°C is closely coupled to the maximum calculated temperatures for the canister and tuff. The smaller the conductivity, the larger the peak temperature. The maximum canister temperature of 358°C for the nominal case (3.5 kW) increases by 17% for the (-,-) case and decreases by 11% for the (+,+) case. For initial canister outputs of less than 2.0 kW, the tuff conductivities used below 100°C are the most strongly coupled to the maximum calculated temperatures. The maximum canister temperature for the 1.0 kW case of 113°C increases by 23% for the (-,-) case and decreases by 7% for the (+,+) case.

RRE:5511:ljg

Table 1

Thermal Conductivity (W/m-K)
for the Nominal Case and Four Parametric Cases

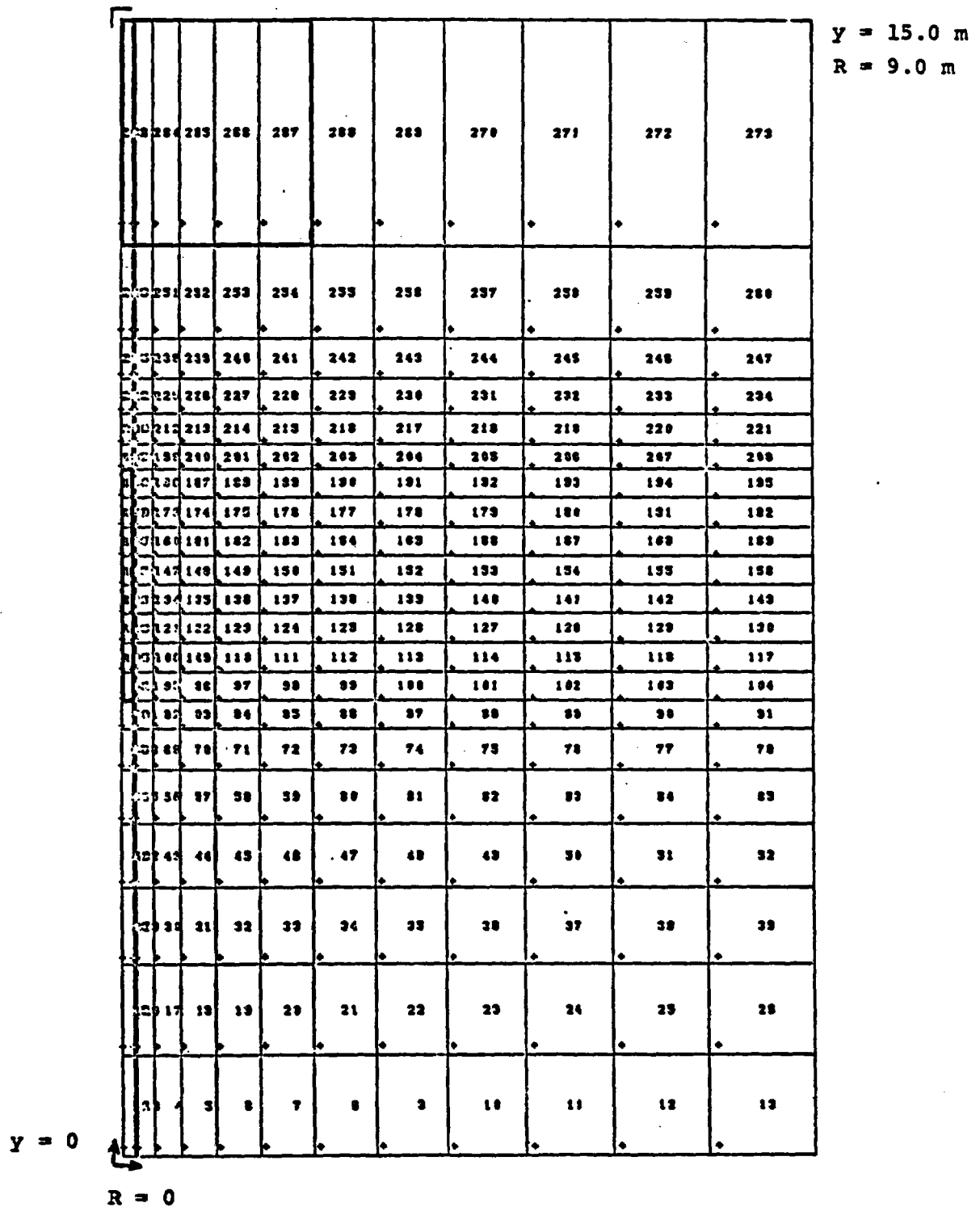
<u>Symbol</u>	<u>K (T < 100°C)</u>	<u>K (T > 100°C)</u>
--	1.92	1.32
+-	2.88	1.32
0	2.4	1.65 (nominal case)
-+	1.92	1.98
++	2.88	1.98

Note that each case varied by $\pm 20\%$.

Table 2

Effect of Thermal Conductivity on Volume of Tuff
Above 100°C at One Year for 3.5 kW Case

<u>Case</u>	<u>Volume of Tuff Inside the 100°C Isotherm (m³)</u>
--	18.17
+-	15.12
0	10.0 (nominal case)
-+	7.889
++	7.4

FIGURE 1. COYOTE Element Network, $y_{\max} = 15.0$ m, $R_{\max} = 9.0$ m

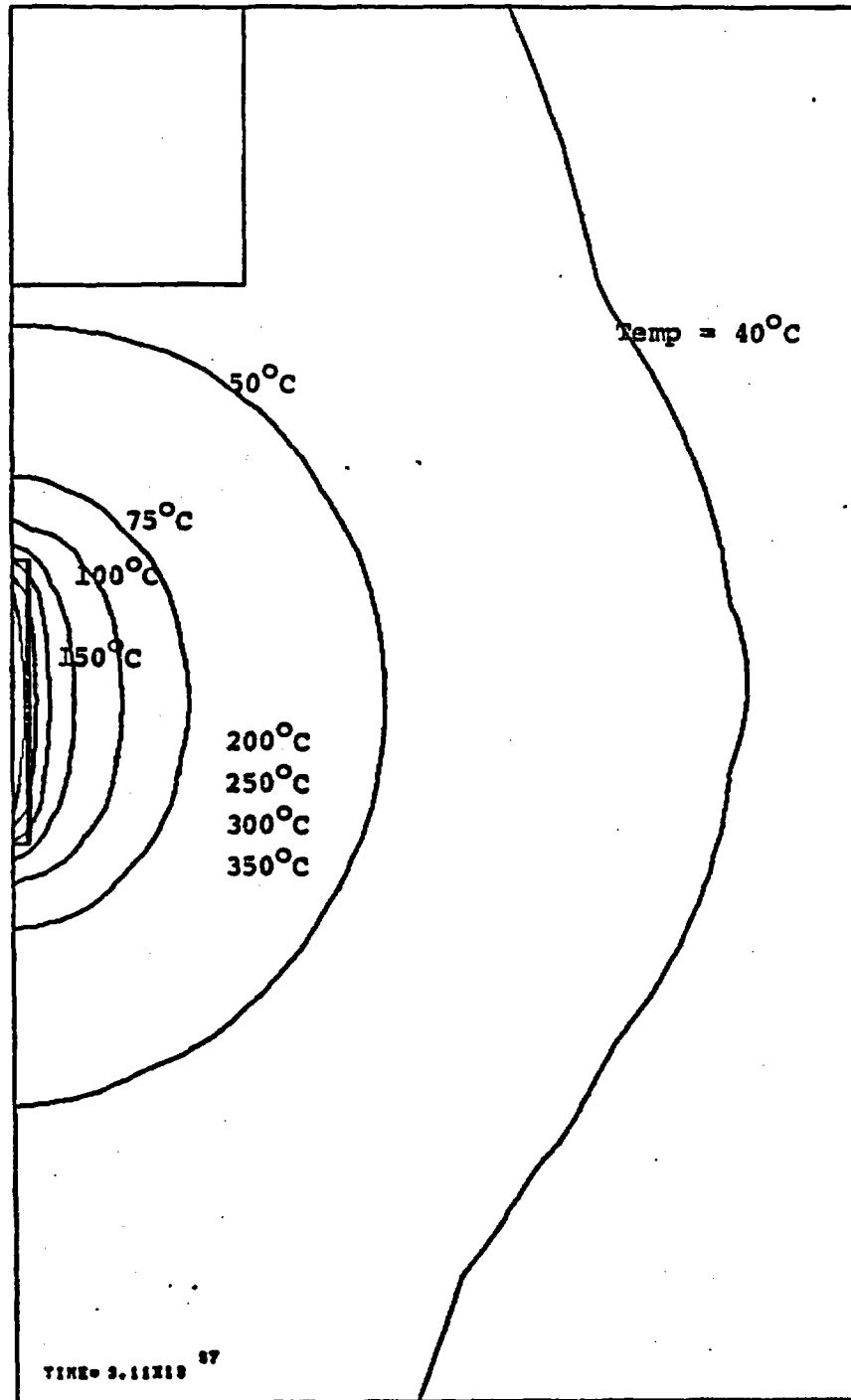


FIGURE 3. Isotherms at $t = 1$ yr, Power = 3.5 kW, Nominal Case

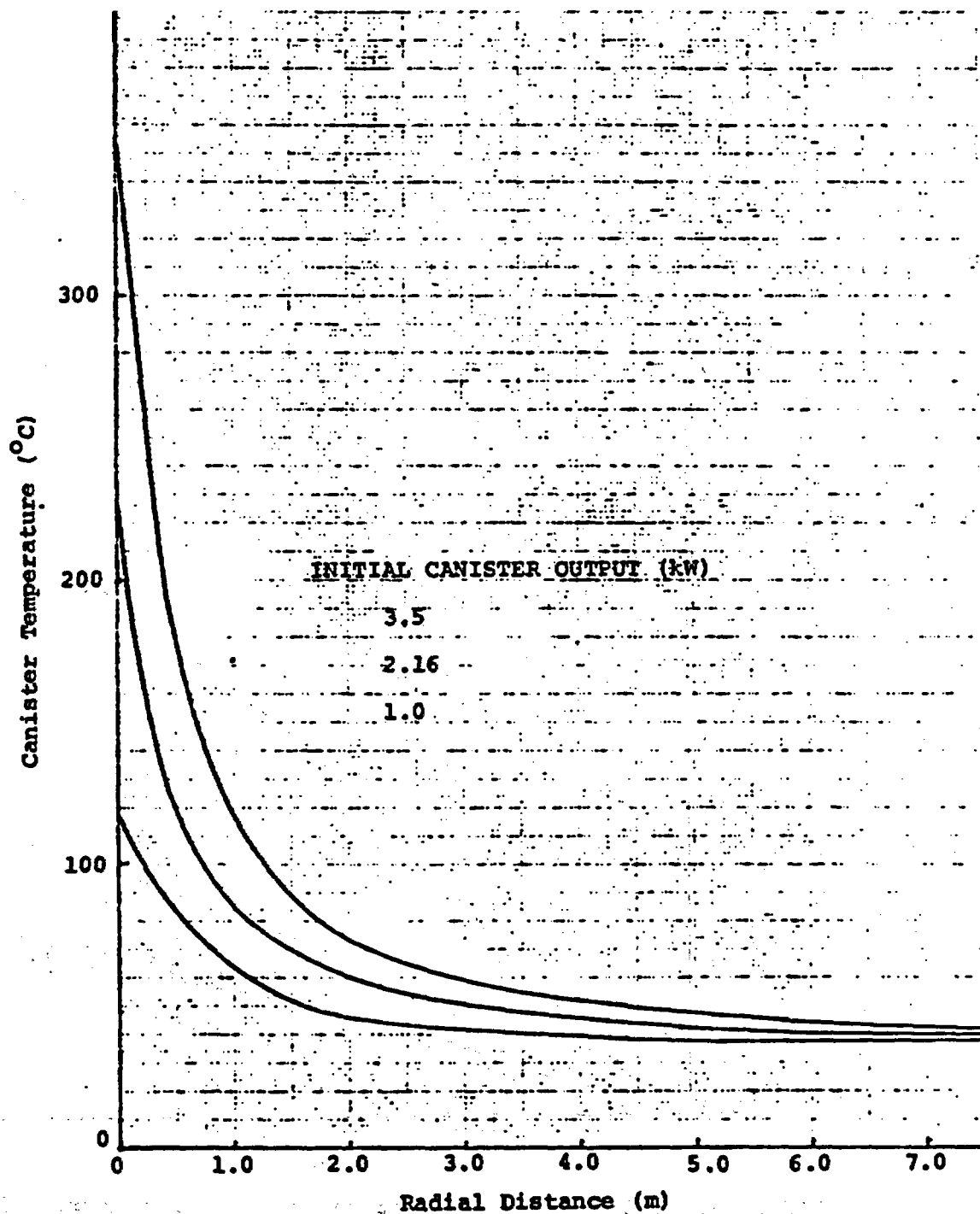


FIGURE 4. Radial Temperature Distribution Through Centerplane of Canister, Nominal Case, Time = 1 Year.

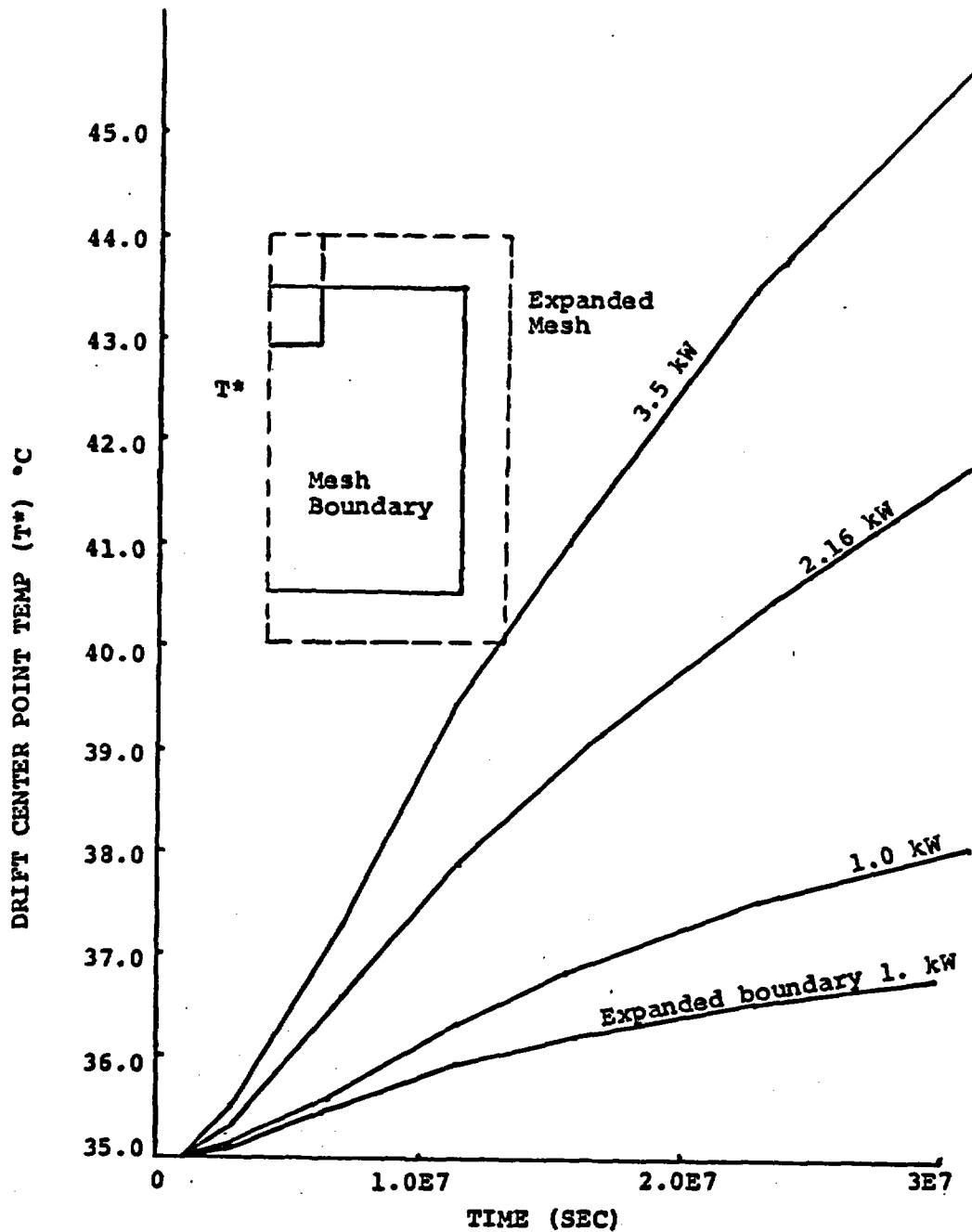


FIGURE 5. Drift Floor Temperature for Canister Output of 3.5, 2.16, and 1.0 kW, Time = 1 Year.

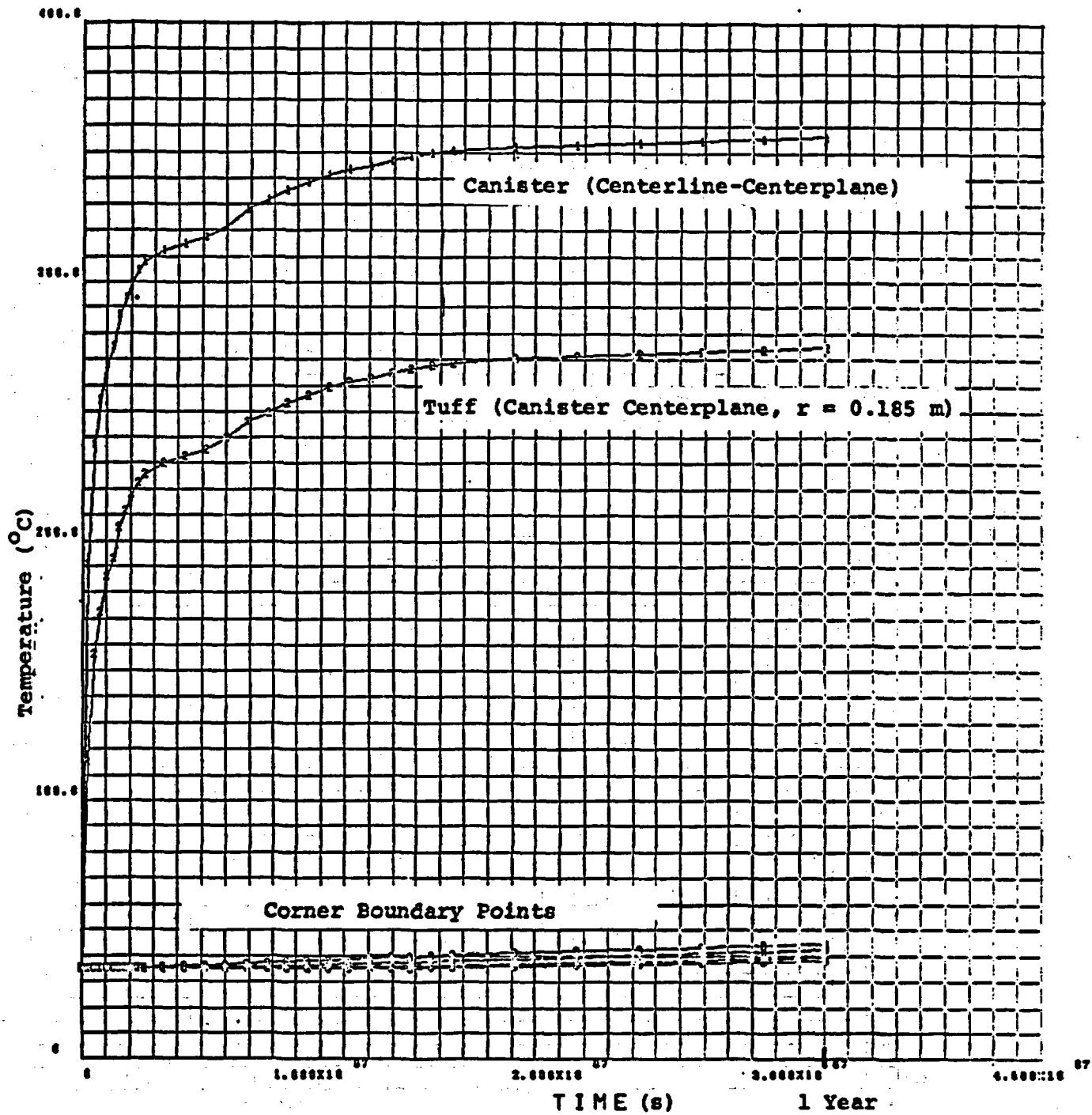


FIGURE 6a. Maximum Canister and Tuff Temperatures, Nominal Case, Canister Output = 3.5 kW.

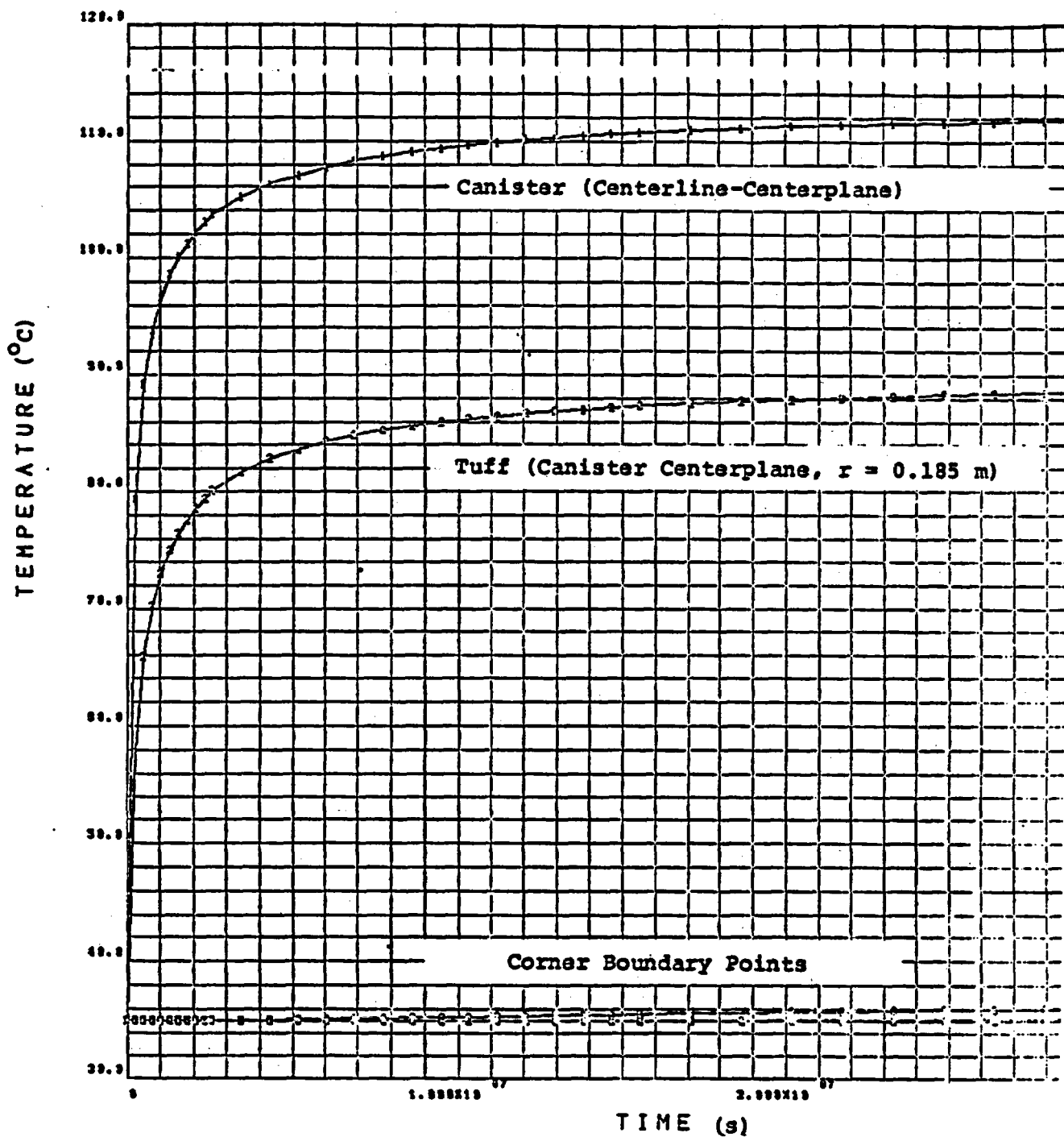


FIGURE 6b. Maximum Canister and Tuff Temperatures, Nominal Case, Canister Output = 1.0 kW.

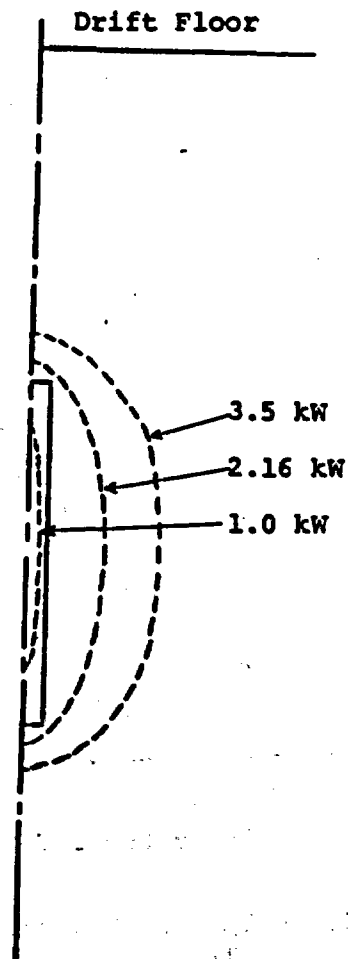


FIGURE 7. 100°C Isotherm for Nominal Case with Three Canister Outputs, Time = 1 Year.

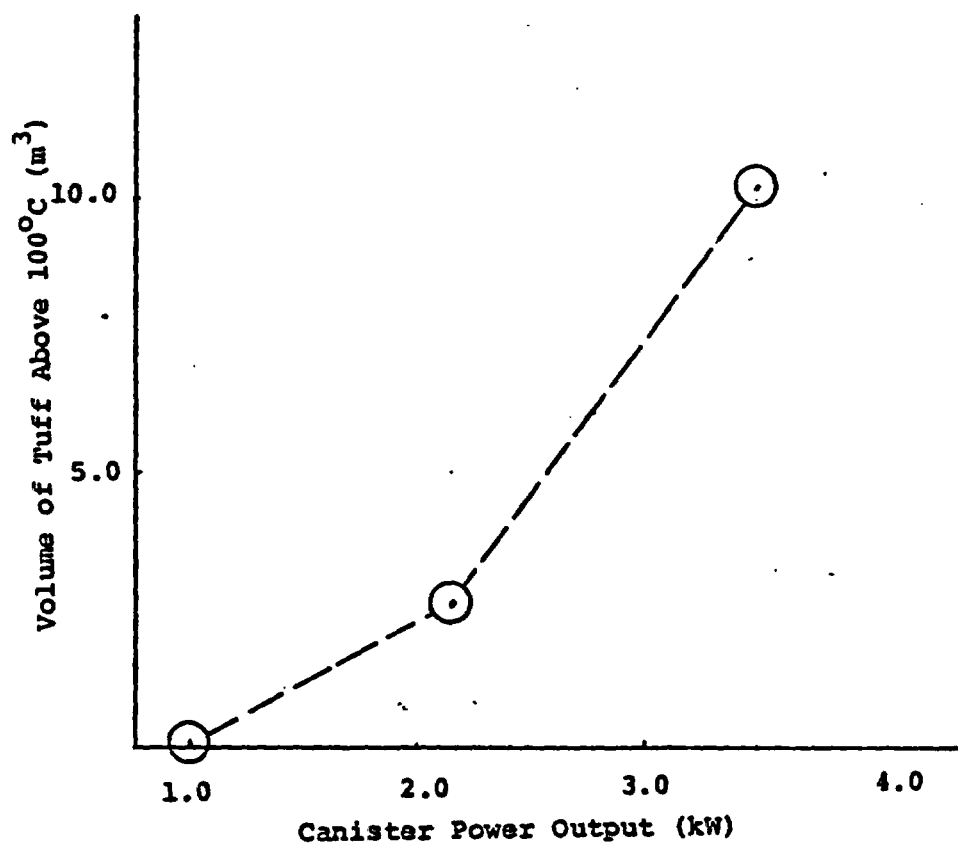


FIGURE 8. Volume of Unsaturated Tuff for Nominal Case.

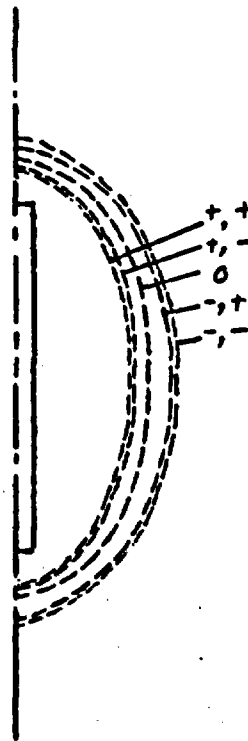


FIGURE 9. Effect of Tuff Conductivities on Location of 100°C Isotherm for Parametric Cases.

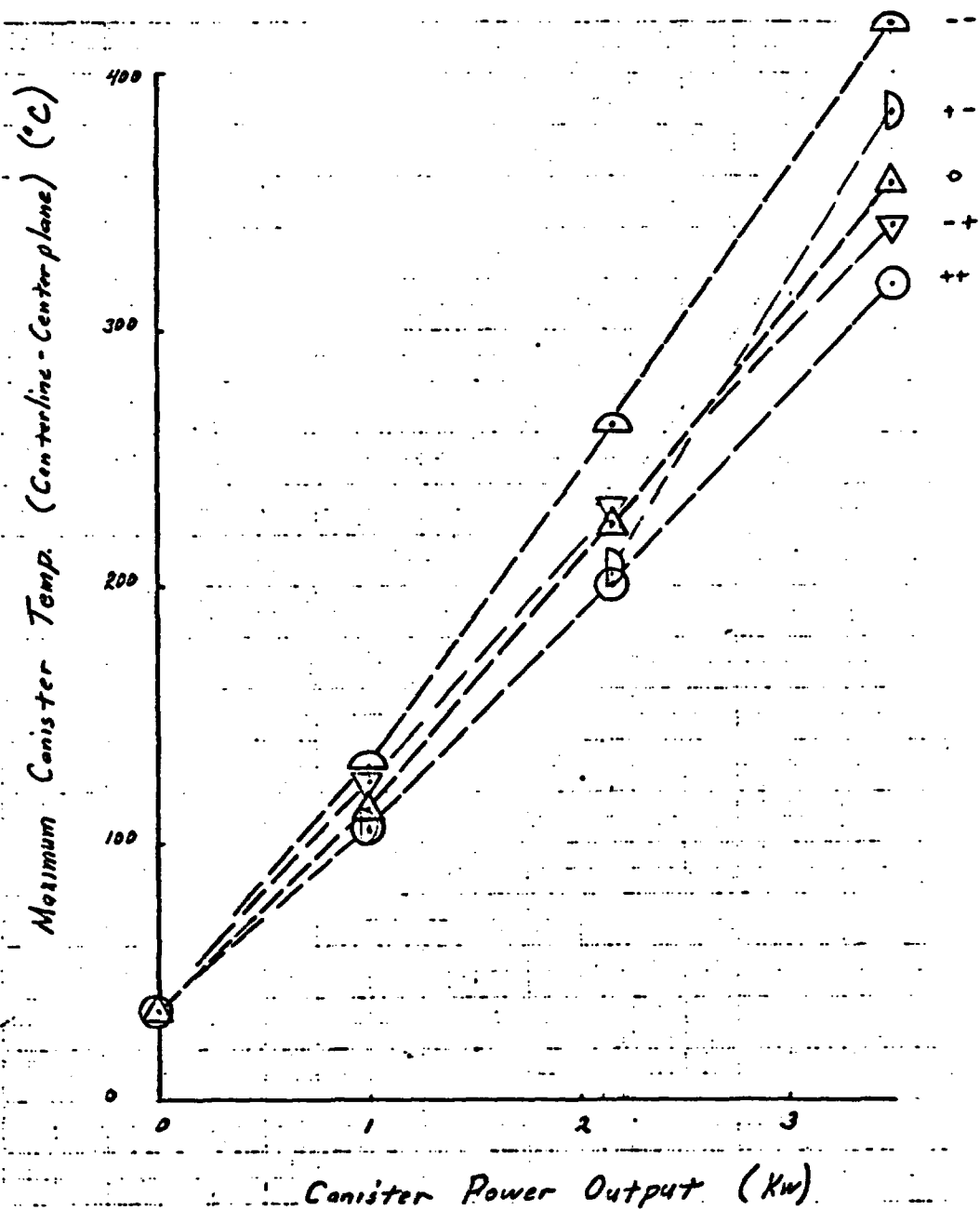


FIGURE 10. Effect of Tuff Conductivity on Maximum Canister Temperature, Time = 1 Year.

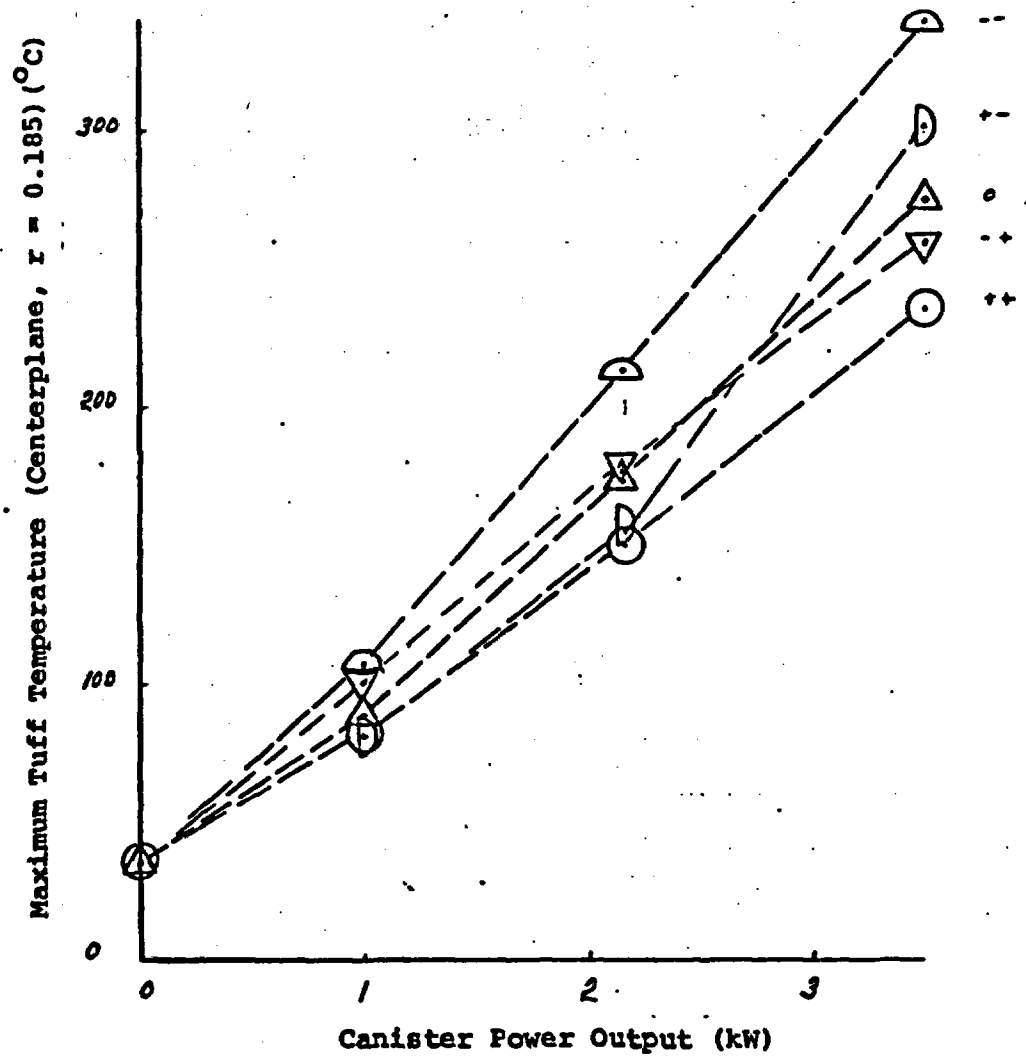


FIGURE 11. Effect of Tuff Conductivity on Maximum Tuff Temperature, Time = 1 Year.

A. R. Lappin

-16-

Copy to:

4530 R. W. Lynch
4537 L. D. Tyler
4537 J. K. Johnstone
5500 O. E. Jones
5510 D. B. Hayes
5511 J. W. Nunziato
5520 T. B. Lane
5530 W. Herrmann
5531 L. D. Berthoff

All members of Tuff Mine Design Working Group

Sandia Laboratories

Albuquerque, New Mexico
Livermore, California

date: March 7, 1980

to: Distribution

from: 
R. R. Eaton - 5511

subject: Single Canister Thermal Calculations to Estimate Canister and Very Near-Field Temperatures Resulting from Emplacement of High Level Waste (HLW) in Welded Tuff for an Initial Tuff Temperature of 55°C

Ref: Memo, R. R. Eaton, 5511, to A. R. Lappin, 4537, dtd 1/31/80, subject: Single Canister Thermal Calculations to Estimate Canister and Very Near-Field Temperatures Resulting from Emplacement of High Level Waste (HLW) in Welded Tuff

A preliminary thermal analysis has been completed for the very near-field of a single canister containing HLW (3.5, 2.16, and 1.0 kW) emplaced in welded tuff for ER = 20% and canister loading of 75 kW/acre. Specifications not given in this memo regarding canister geometry, canister output versus time, canister and tuff properties are given in, "Mine Design Working Group Activity Work Package," dtd 12/4-5/79 and authored by Division 4537.

The primary purpose of making these calculations was to supplement the calculations reported in the referenced memo where all initial temperatures were set to 35°C. All initial tuff and canister temperatures used in this study were equal to 55°C. Additionally, the size of the mesh grid used was determined using the size of unit cell (m^2) concept. The mesh grid maximum radius was determined such that the total material considered equal that of a unit cell for a single canister (see Table 1). Secondly, the calculation extended to +30 m in the vertical direction thus eliminating all end boundary effects. Finally, the maximum times considered were extended so the peak canister and tuff temperatures were calculated for the nominal cases.

The COYOTE finite element heat conduction code¹ was used to generate time-dependent, two-dimensional axisymmetric temperature solutions in the canister and tuff. A schematic of the nodalization used is given in Figure 1. A total of 338 elements were used to simulate the geometry. A total of 15 runs were made using three different canister output levels (3.5, 2.16, and 1.0 at time = 0) and 20% variations

from the norm in thermal conductivity (see Table 2). The plus-minus symbolism designating variations in K will be used when referring to specific cases.

The drift above the canister was modeled by using the properties of air ($\rho = 1.2 \text{ kg/m}^3$, $c_p = 1.6 \times 10^3 \text{ J/m}^3\text{-}^\circ\text{C}\text{-kg}$), and an effective thermal conductivity of $K = 25 \text{ W/m-K}$ to simulate the effect of radiation.² Figure 2 shows isotherms, at two years, for the nominal (0) case for an initial canister output of 3.5 kW. It shows that a considerable portion of the canister skin is above 400°C . Portions of the drift floor exceed 65°C . This implies that the simulated drift boundary condition must be made more realistic in order to obtain reliable calculated temperatures for run times longer than two years. It is anticipated that the drift will be convective cooled at early times ($t < 50$ years). No convection was considered in this model. Figures 3a, 3b, 3c and 3d show that the peak canister and tuff temperature have been calculated. The maximum canister temperatures occurred within one year for the 3.5 kW case and six years for the 1.0 kW case. The temperatures calculated at two years were within 8°C of the maximum temperatures.

Figure 4 shows the 100°C isotherm for the three canister outputs. The volume of the tuff which is above the 100°C (unsaturated or dried) is plotted on Figure 5. This volume was estimated assuming it to be equal to the volume of an ellipsoid. The major and minor axes are taken from Figure 4.

Figure 6 shows the influence of the thermal conductivity of the tuff on the 100°C isotherm for the 3.5 kW case. The volume of tuff above 100°C is given in Table 3. Figure 6 also shows the results of the $T_{\text{initial}} = 35^\circ\text{C}$ study. The temperatures for this study range from 20°C to 30°C higher. The maximum canister temperature (centerline-centerplane) and maximum tuff temperature (centerplane, $r = 0.185 \text{ m}$) is given in Figures 7 and 8. From these two figures, it can be seen for the conductivities considered that for initial canister outputs above 1.5 kW, the magnitude of the thermal conductivity used for tuff above 100°C is closely coupled to the maximum calculated temperatures for the canister and tuff. The smaller the conductivity, the larger the peak temperature. The maximum canister temperature of 384°C for the nominal case (3.5 kW) increases by 17% for the $(-, -)$ case and decreases by 11% for the $(+, +)$ case. These percentages are within 1% of the results obtained for the $T_{\text{initial}} = 35^\circ\text{C}$ study. For initial canister outputs of less than 1.0 kW, the tuff conductivities used below 100°C are the most strongly coupled to the maximum calculated temperatures. The two year canister temperature for the 1.0 kW (0) case of 148°C increases by 10% for the $(-, -)$ case and decreases by 5% for the $(+, +)$ case (as compared to 23% and 7% for the $T = 35^\circ\text{C}$ study).

Distribution

-3-

It is concluded that maximum canister and tuff temperatures are obtainable for the very near-field using unit cell, two-dimensional axisymmetric nodalization. R. K. Thomas, 5521, is currently running the nominal cases using a fully three-dimensional code. Comparisons will be made when these results become available.

RRE:5511:ljg

Distribution:

4537 L. D. Tyler
4537 A. R. Lappin
5500 O. E. Jones
5510 D. B. Hayes
5511 J. W. Nunziato
5512 D. F. McVey
5513 D. W. Larson
5520 T. B. Lane
5530 W. Herrmann

TABLE 1

Dimensions for Unit Cell Calculations
for 20% ER, 75 kW/acre

<u>Canister Output</u>	<u>Pitch (m)</u>	<u>Mesh Radius (m)</u>	<u>Drift Radius (m)</u>	<u>Drift Height (m)</u>
1.0	2.153	4.14	1.85	1.85
2.16	4.662	6.09	2.72	2.72
3.5	7.554	7.75	3.47	3.47

TABLE 2

Thermal Conductivity (W/m-K) for the
Nominal Case and Four Parametric Cases

<u>Symbol</u>	<u>K (T < 100°C)</u>	<u>K (T > 100°C)</u>
--	1.92	1.32
+-	2.88	1.32
0	2.4	1.65 (nominal case)
-+	1.92	1.98
++	2.88	1.98

Note that each case varied by +20%.

TABLE 3

Effect of Thermal Conductivity on Volume of
Tuff Above 100°C at Two Years for 3.5 kW Case

<u>Case</u>	<u>Volume of Tuff Inside the 100°C Isotherm (m³)</u>
--	59.00
+-	53.95
0	45.86 (nominal case)
-+	35.68
++	30.93

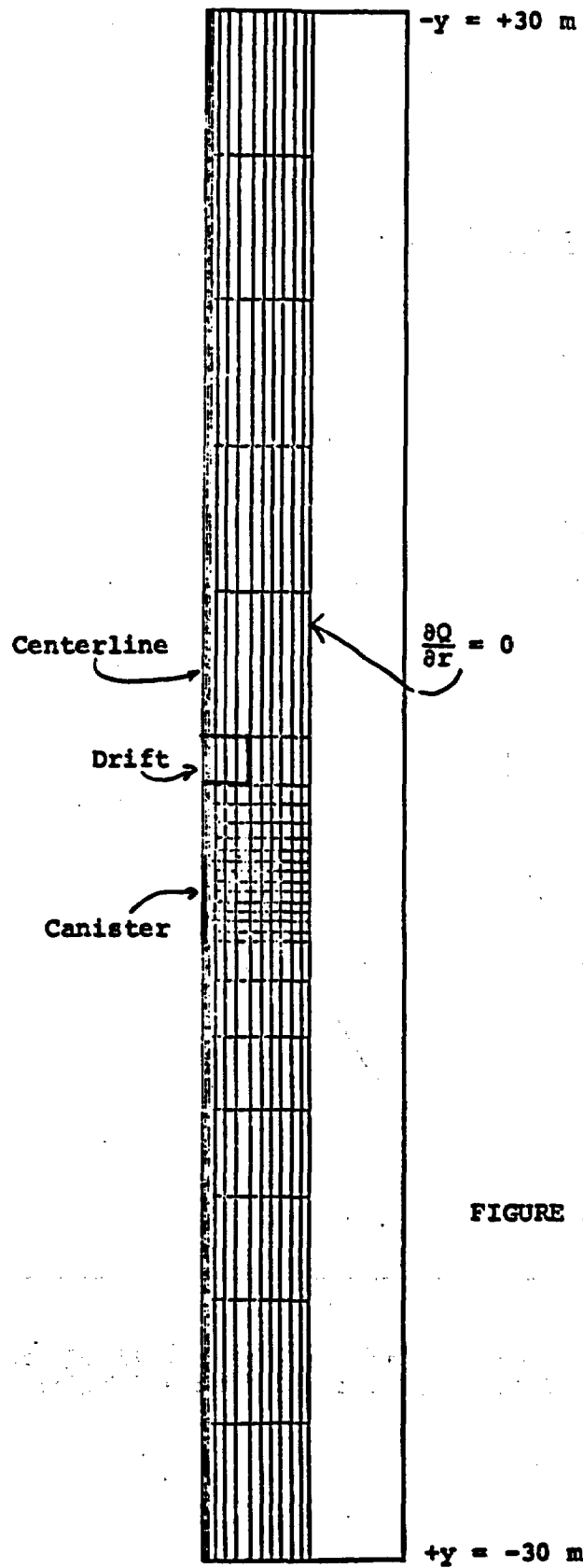


FIGURE 1. COYOTE
Element
Network

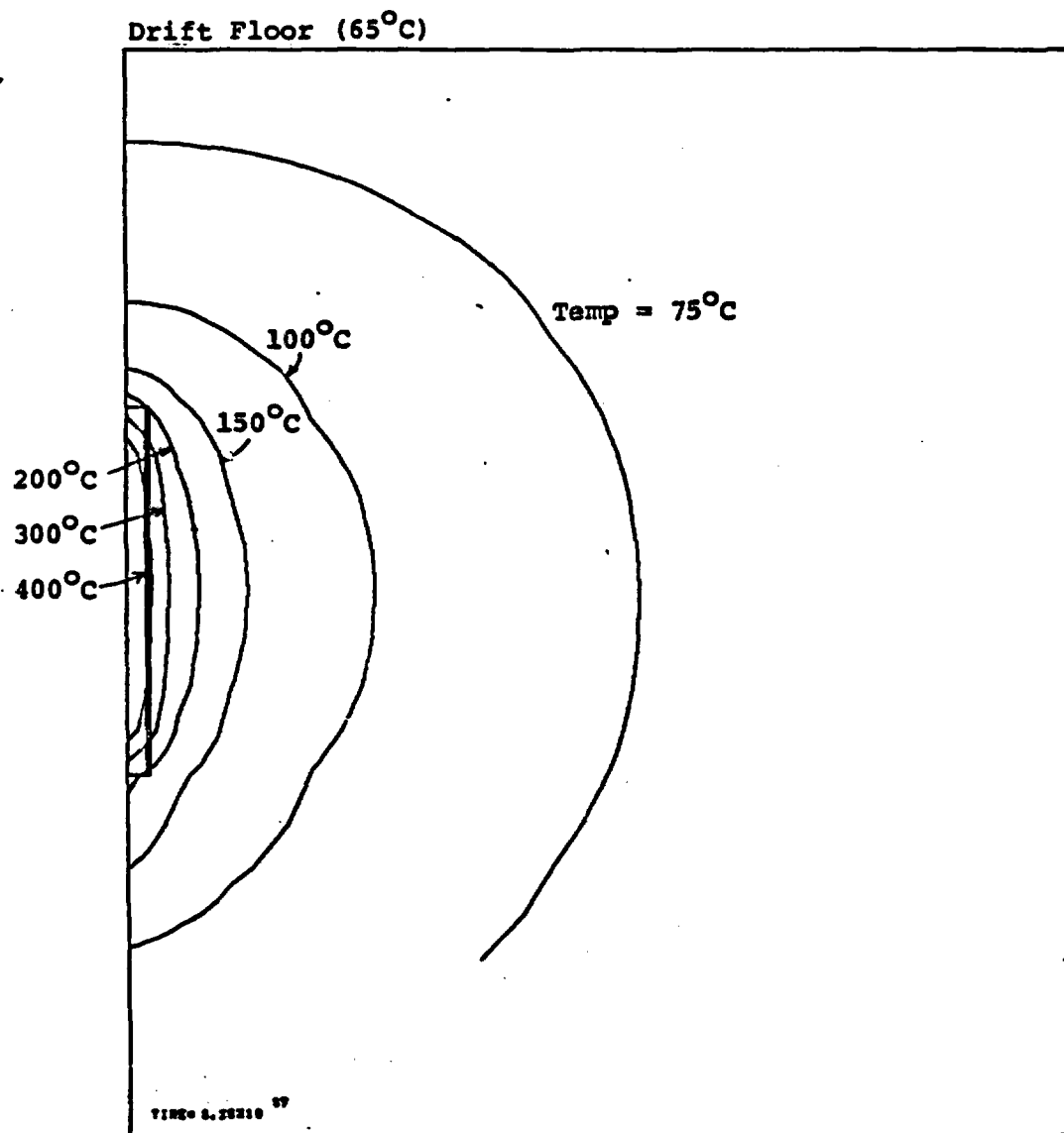


FIGURE 2. Isotherms at $t = 2$ years, 75 kW/acre, ER = 20%
Initial Canister Output 3.5 kW/can, Nominal Case

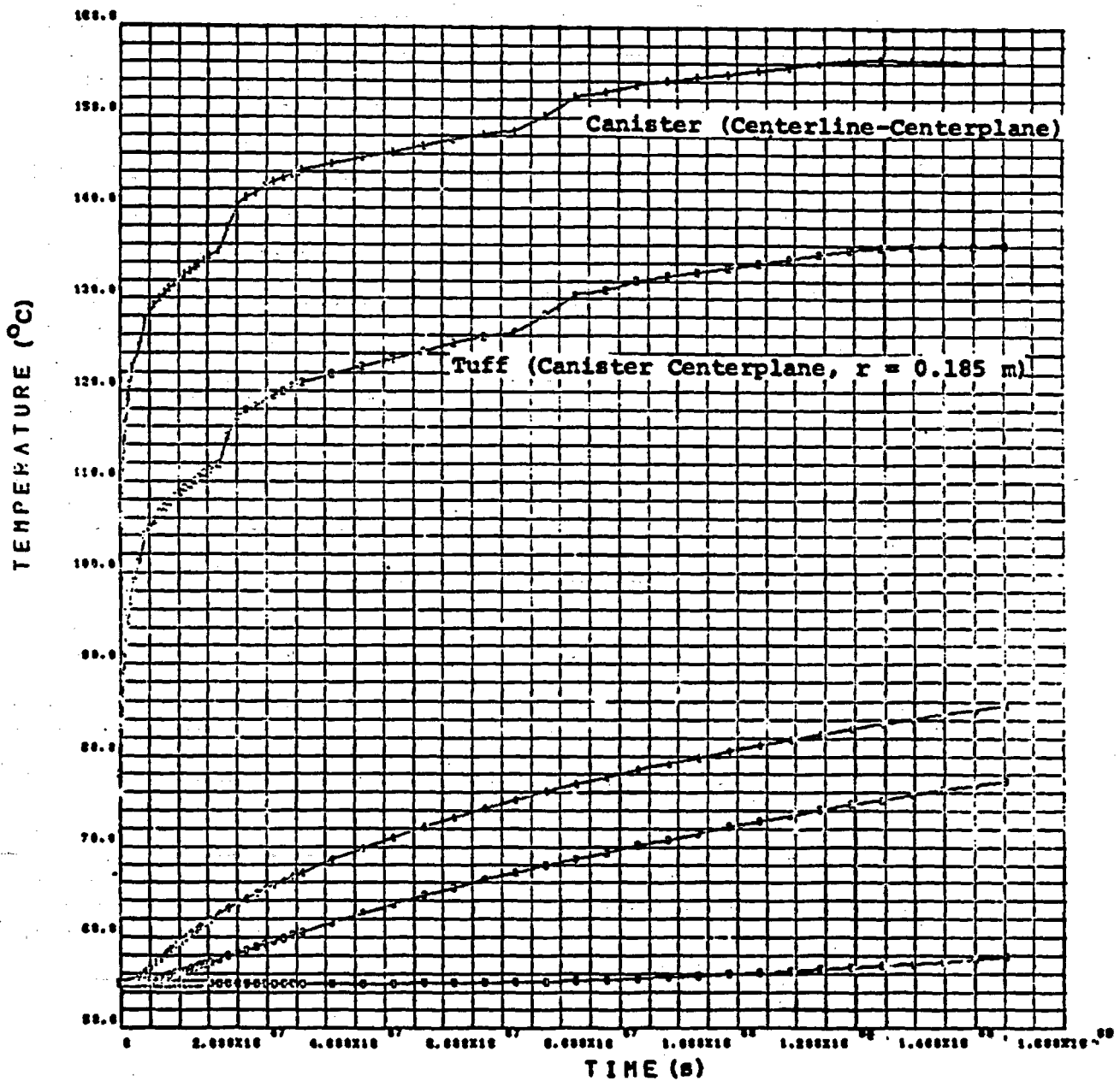


FIGURE 3b. Maximum Canister and Tuff Temperature, Nominal Case
Initial Canister Output = 1.0 kW, 75 kW/acre, ER = 20%

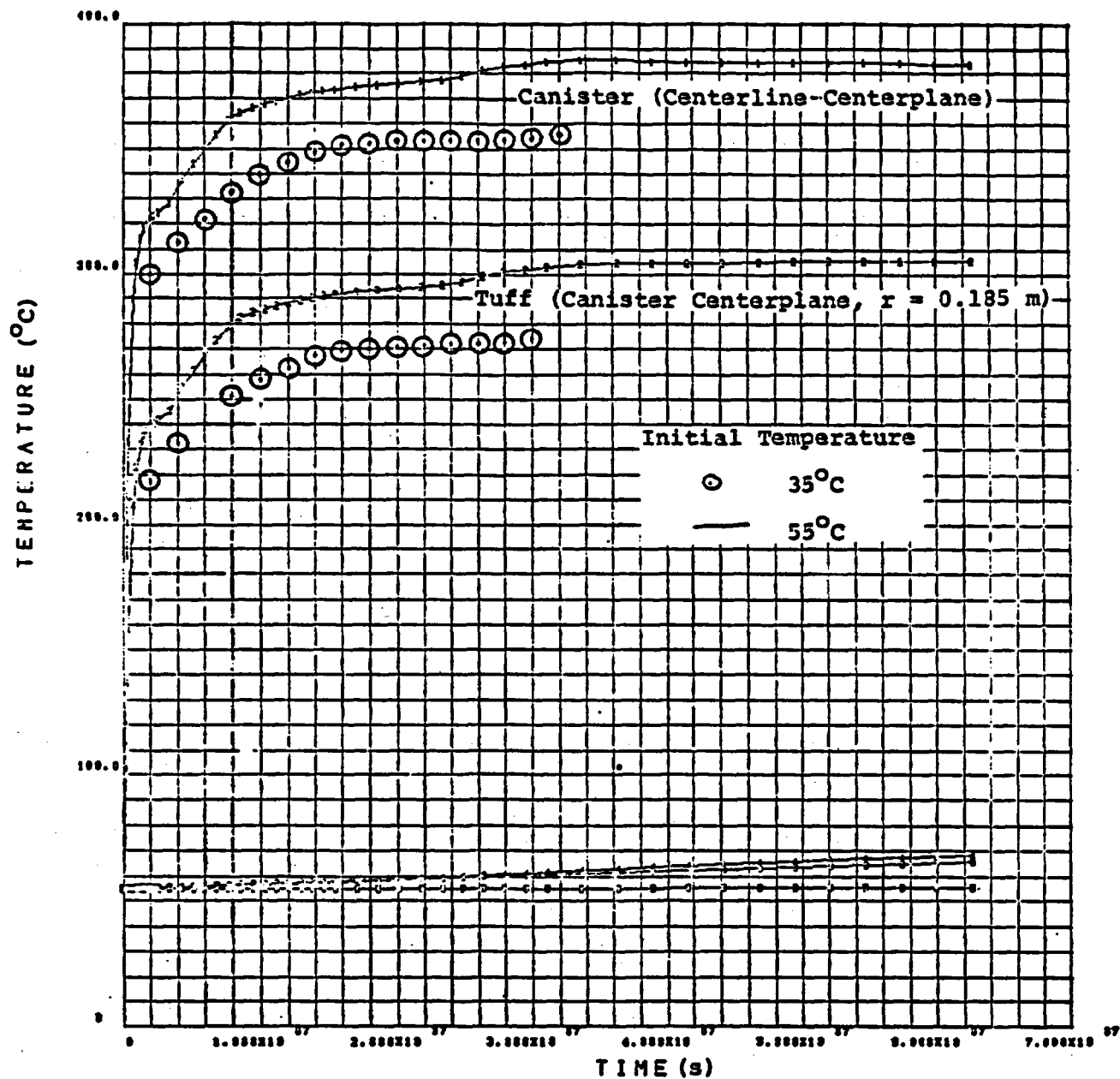


FIGURE 3a. Maximum Canister and Tuff Temperatures, Nominal Case
Initial Canister Output = 3.5 kW, 75 kW/acre, ER = 20%

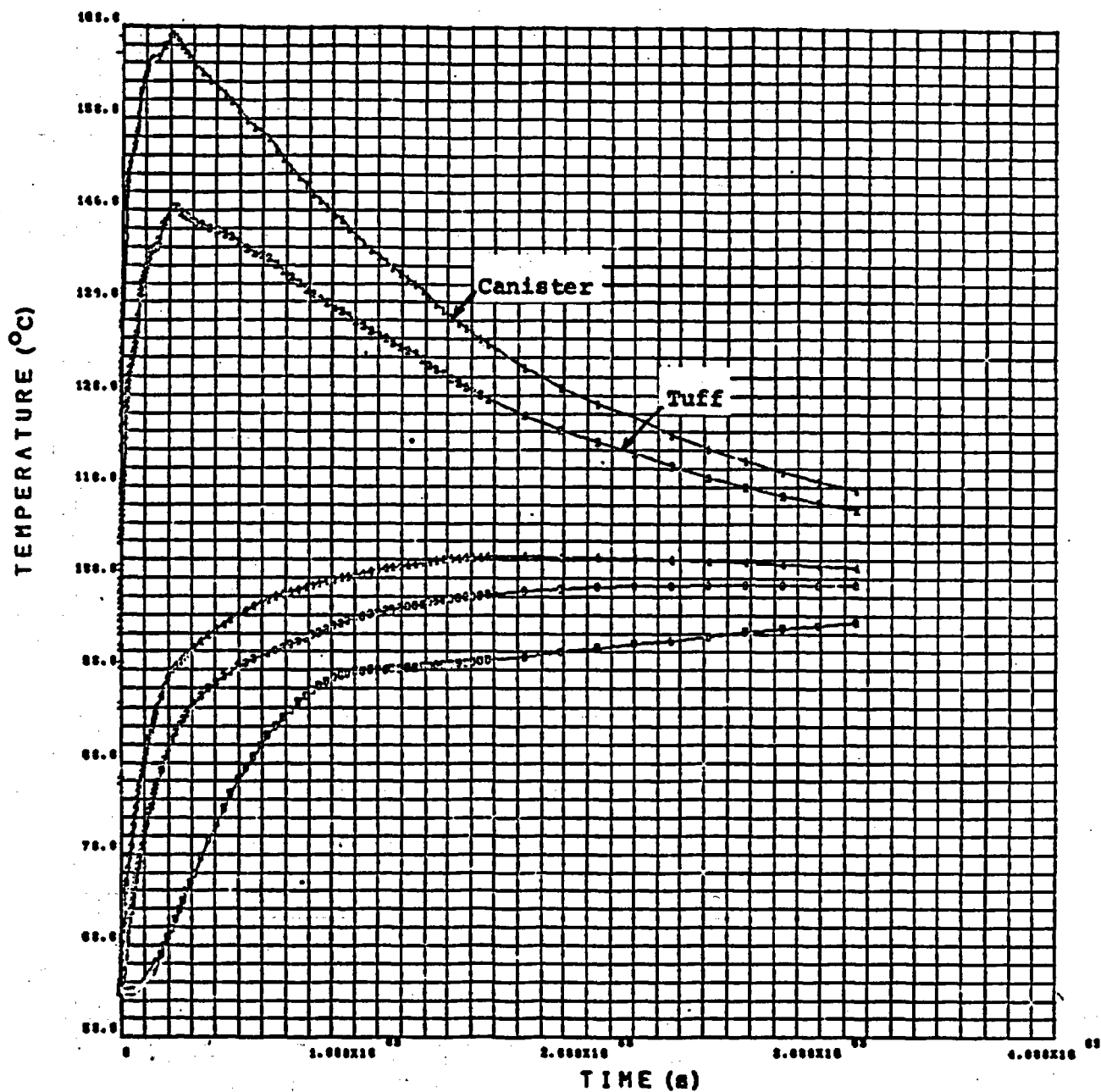


FIGURE 3c. Maximum Canister and Tuff Temperature, Nominal Case, Initial Output = 1.0 kW, 75 kW/acre, ER = 20%, Maximum Time = 100 years

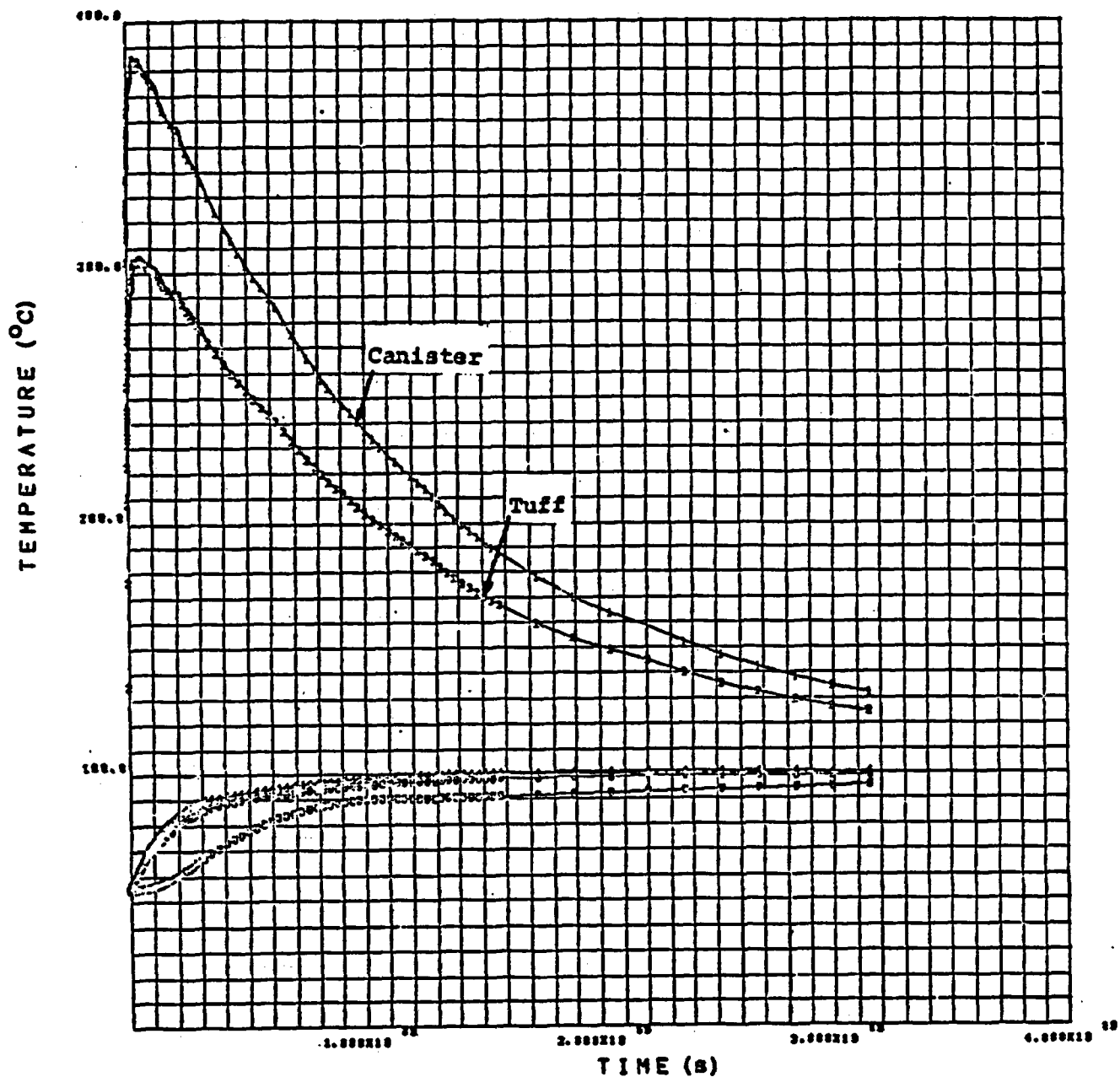


FIGURE 3d. Maximum Canister and Tuff Temperature, Nominal Case, Initial Output = 3.5 kW, 75 kW/acre, ER = 20%, Maximum Time = 100 years

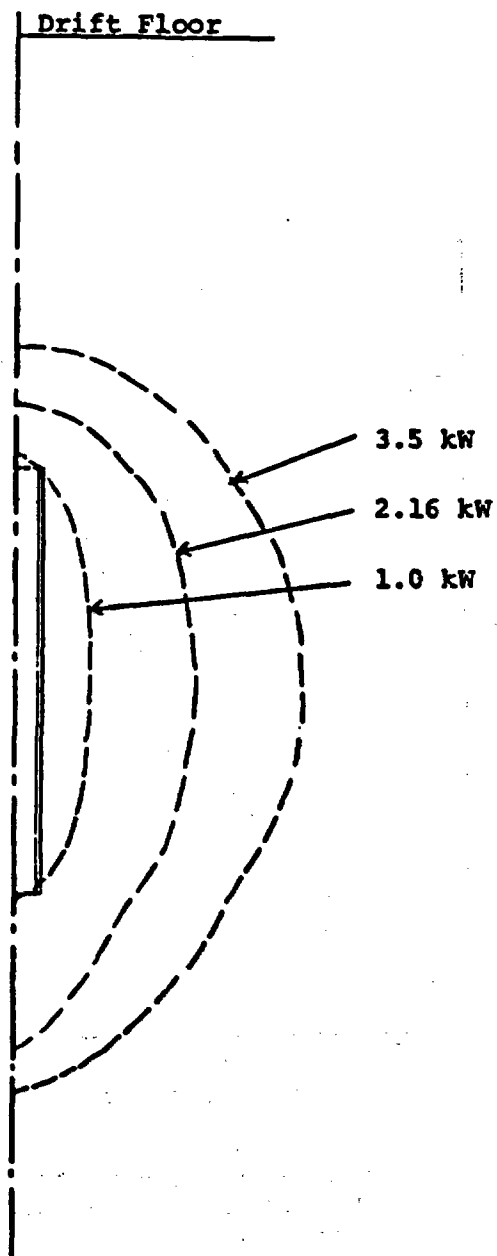


FIGURE 4. 100°C Isotherm for Nominal Case With Three Canister Outputs, Time = 2 years, 75 kW/acre, ER = 20%

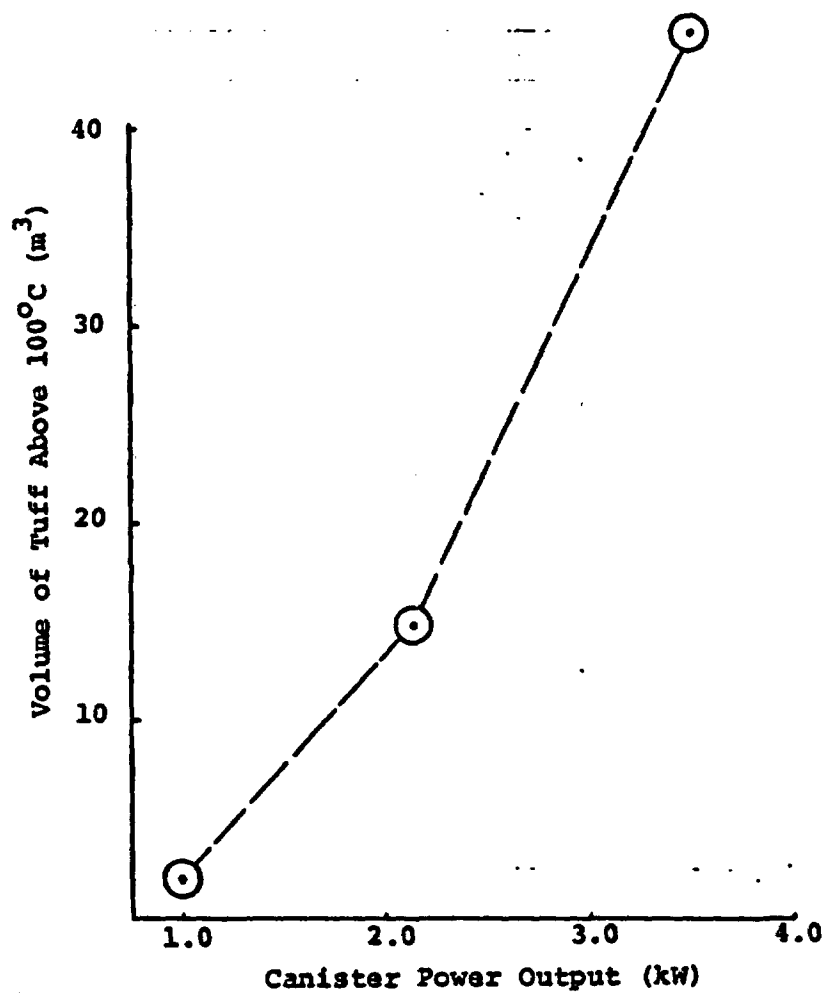


FIGURE 5. Volume of Unsaturated Tuff for Nominal Case, Time = 2 years, 75 kW/acre, ER = 20%

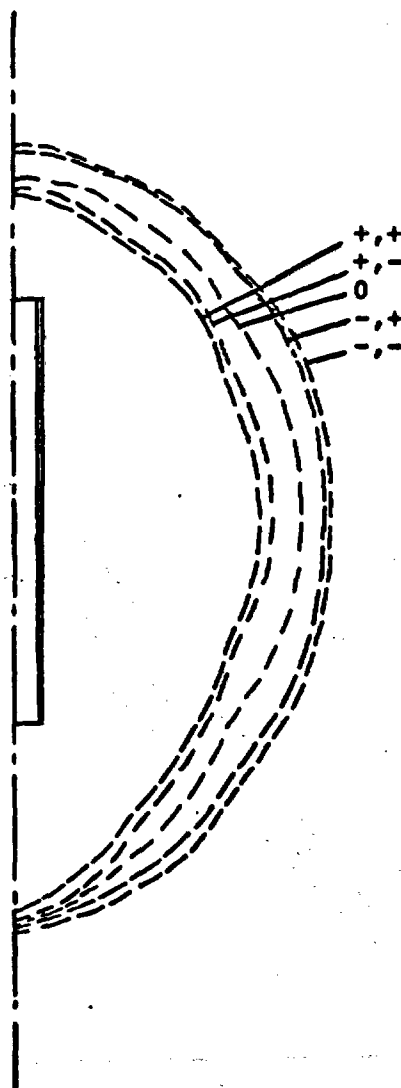


FIGURE 6. Effect of Tuff Conductivities on Location of 100°C Isotherm for Parametric Cases. Time = 2 years, 3.5 kW/can, 75 kW/acre, ER = 20%

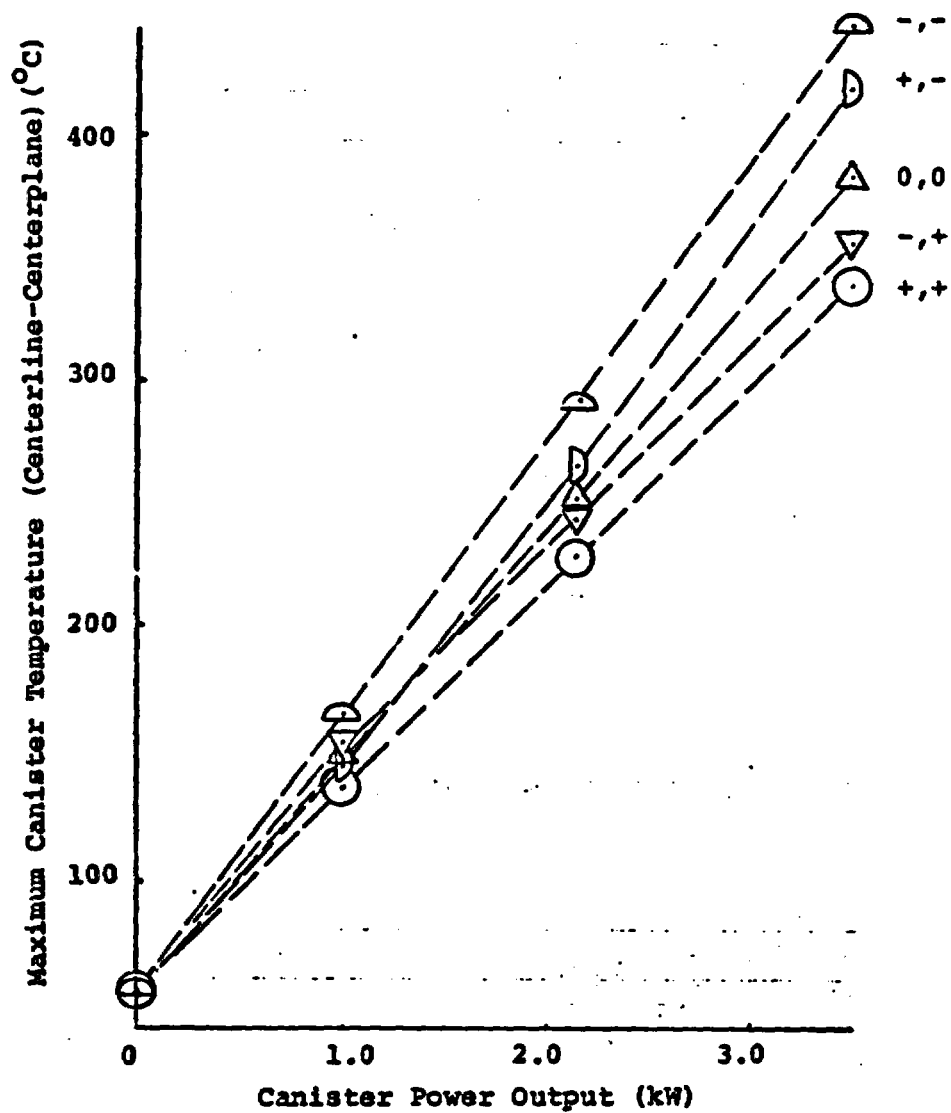


FIGURE 7. Effect of Tuff Conductivity on Maximum Canister Temperature, Time = 2 years, 75 kW/acre, ER = 20%

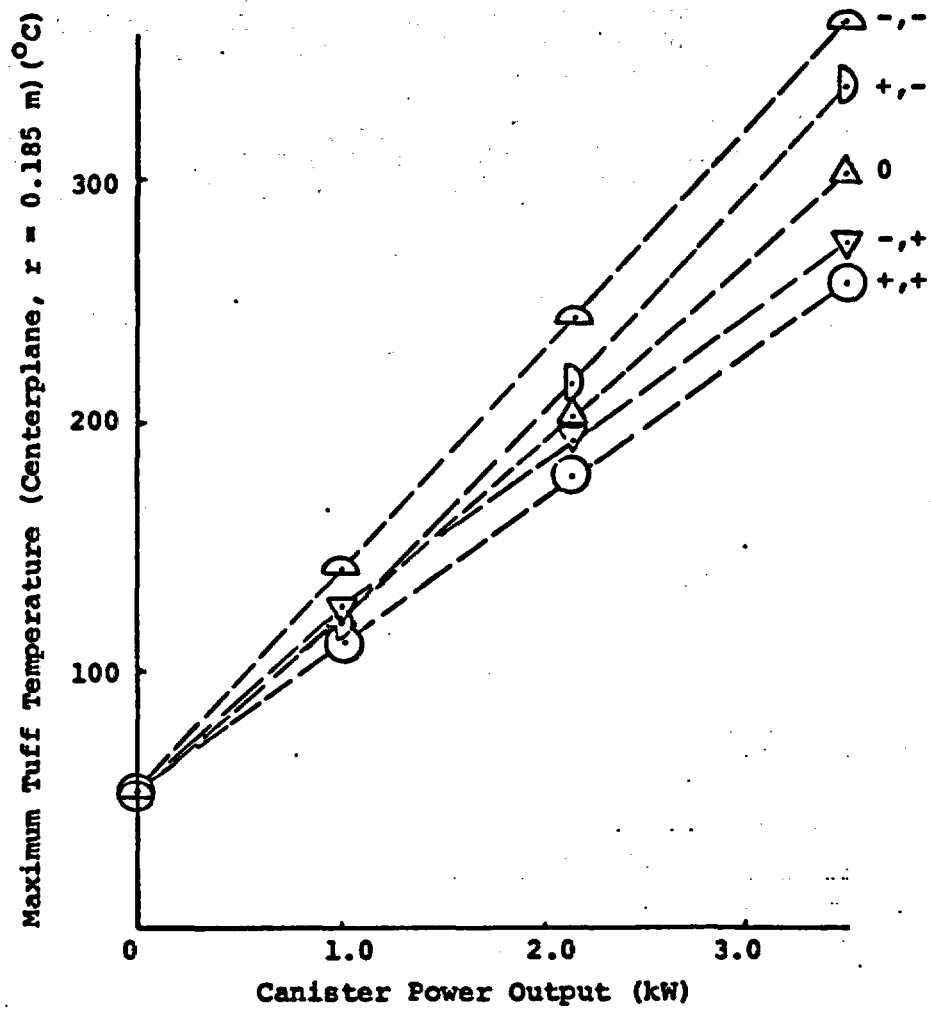


FIGURE 8. Effect of Tuff Conductivity on Maximum Tuff Temperature, Time = 2 years, 75 kW/acre, ER = 20%

Distribution

-5-

REFERENCES

1. D. K. Gartling, "COYOTE--A Finite Element Computer Program for Non-Linear Heat Conduction Problems," SAND77-1332, Sandia Laboratories, Albuquerque, NM, June 1978.
2. Memo, O. L. George, Jr., 5511, to D. F. McVey, 5511, dtd 1/4/80, subject: The Effect of Thermal Radiation in the Disposal of High Level Waste (HLW) in Tuff

Sandia Laboratories

Albuquerque, New Mexico
Livermore, California

date: May 12, 1980

to: Distribution


from: R. R. Eaton - 5511

subject: Single Canister Thermal Calculations to Estimate Canister and Very Near-Field Temperatures Resulting from Emplacement of High Level Waste (HLW) in Welded and Non-Welded Tuff

- Ref: 1. Memo, R. R. Eaton, 5511, to Dist. dtd 3/1/80.
Subject: Single Canister Thermal Calculations to Estimate Canister and Very Near-Field Temperatures Resulting from Emplacement of High Level Waste (HLW) in Welded Tuff in Initial Tuff Temperature of 55°C.
2. D. K. Gartling, "COYOTE - A Finite Element Computer Program for Non-Linear Heat Conduction Problems," SAND77-1332, Sandia Laboratories, Albuquerque, NM, June, 1978.
3. Memo, W. E. Wowak, 4541, to Dist. dtd 4/14/80.
Subject: Temperature Limits for Operations in a Welded Tuff Repository.

A preliminary thermal analysis is presented in Reference 1 for the very near-field of a single canister containing HLW (3.5, 2.16 and 1.0 KW) emplaced in welded tuff for an ER=20% and a repository loading of 75 KW/acre. This memo supplements those calculations by presenting the results for non-welded tuff. These calculations were made using the two-dimensional axisymmetric geometry and mesh system identical to that used in the welded tuff study (Fig. 1). The 1.0 KW/can case is considered. Material properties are given in Table 1. The COYOTE finite element heat conduction code² was used to generate time-dependent temperature solutions in the canister and tuff.

Figure 2 shows the time-dependent temperature profiles for the canister centerline, tuff next to the can and a tuff boundary location at $r=r_{\text{effective}}$. Both welded and non-welded results are given. The figure shows that the maximum canister and tuff temperatures for the non-welded material have increased by approximately 50% above those calculated for welded tuff. This is caused primarily by the thermal conductivity change from 2.4 to 1.1 for $T < T_{\text{boil}}$ and 1.65 to 0.74 for $T > T_{\text{boil}}$.

In the non-welded and welded tuff case the floor of the drift reaches a maximum temperature of 103°C and 98°C respectively. The maximum temperature cycle in the non-welded case exceeds the 100°C maximum rock temperature recommended by Worak¹.

RRE:5511:oma

Attachment (Table 1, Figures 1 & 2)

Distribution:

4530 D. Lynch
4537 R. Zimmerman
4537 B. Langkopf
4537 A. Lappin
4537 R. Shaw
4537 L. Tyler
4537 K. Johnstone
4541 B. Wowak
5500 O. E. Jones
5510 D. B. Hayes
5511 J. W. Nunziato
5511 D. K. Gartling
5520 T. B. Lane
5521 L. Davison
5521 B. K. Thomas
5530 W. Herrmann
5532 B. Olsson
5532 B. M. Butcher
5540 O. E. Jones (Actg)
5541 B. C. Luth
5812 C. Northrup

TABLE 1. Material Properties

Welded Tuff*	Non-Welded Tuff
$K = \begin{cases} 2.4 & T < T_{\text{boil}} \\ 1.65 & T > T_{\text{boil}} \end{cases}$	$K = \begin{cases} 1.1 & T < T_{\text{boil}} \\ 0.74 & T > T_{\text{boil}} \end{cases}$
$\rho C_p = \begin{cases} 3.64E6 & T < T_{\text{boil}} \\ 1.72E6 & T > T_{\text{boil}} \end{cases}$	$\rho C_p = \begin{cases} 3.72E6 & T < T_{\text{boil}} \\ 1.38E6 & T > T_{\text{boil}} \end{cases}$

Can

$$K = 1.21$$

$$\rho = 2995.0$$

$$C_p = 0.834E3$$

Tunnel (Air)

$$K = 25.0$$

$$\rho = 1.1$$

$$C_p = 1.6E3$$

$$T_{\text{boil}} = 100^{\circ}\text{C}$$

$$T_{\text{initial}} = 55^{\circ}\text{C}$$

Units:

$$K(\text{J/s}\cdot\text{m}^{\circ}\text{C}), \rho(\text{Kg/m}^3), C_p(\text{J/Kg}^{\circ}\text{C})$$

* Reference 1.

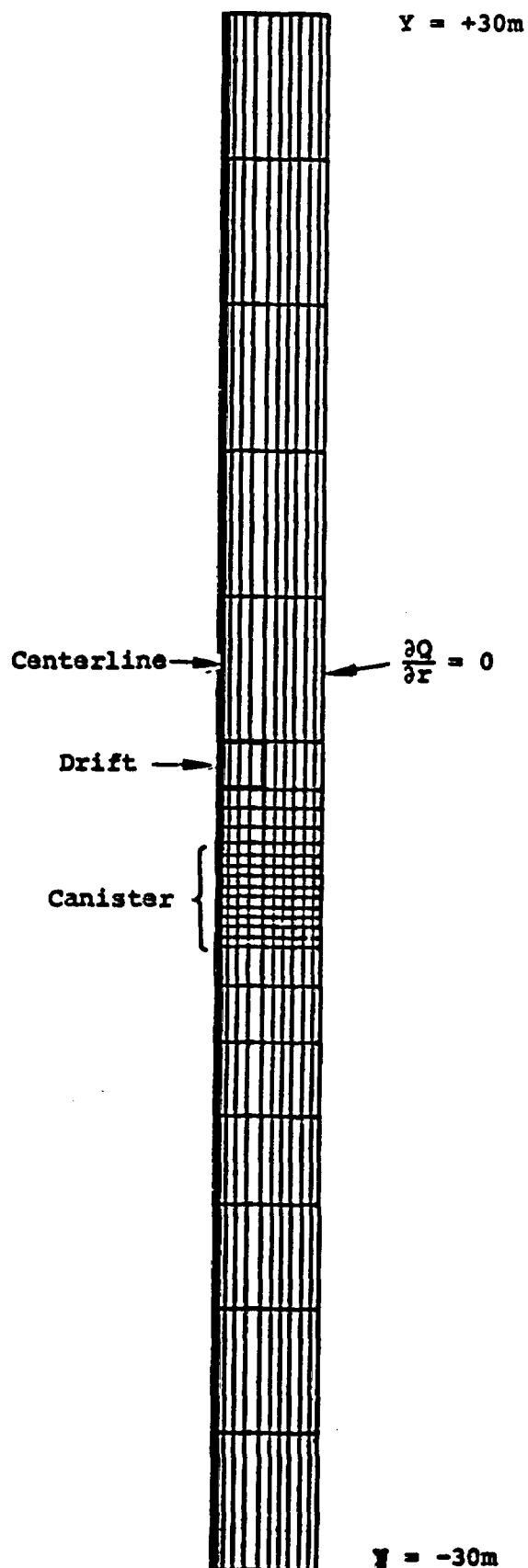


Figure 1.
Mesh Geometry

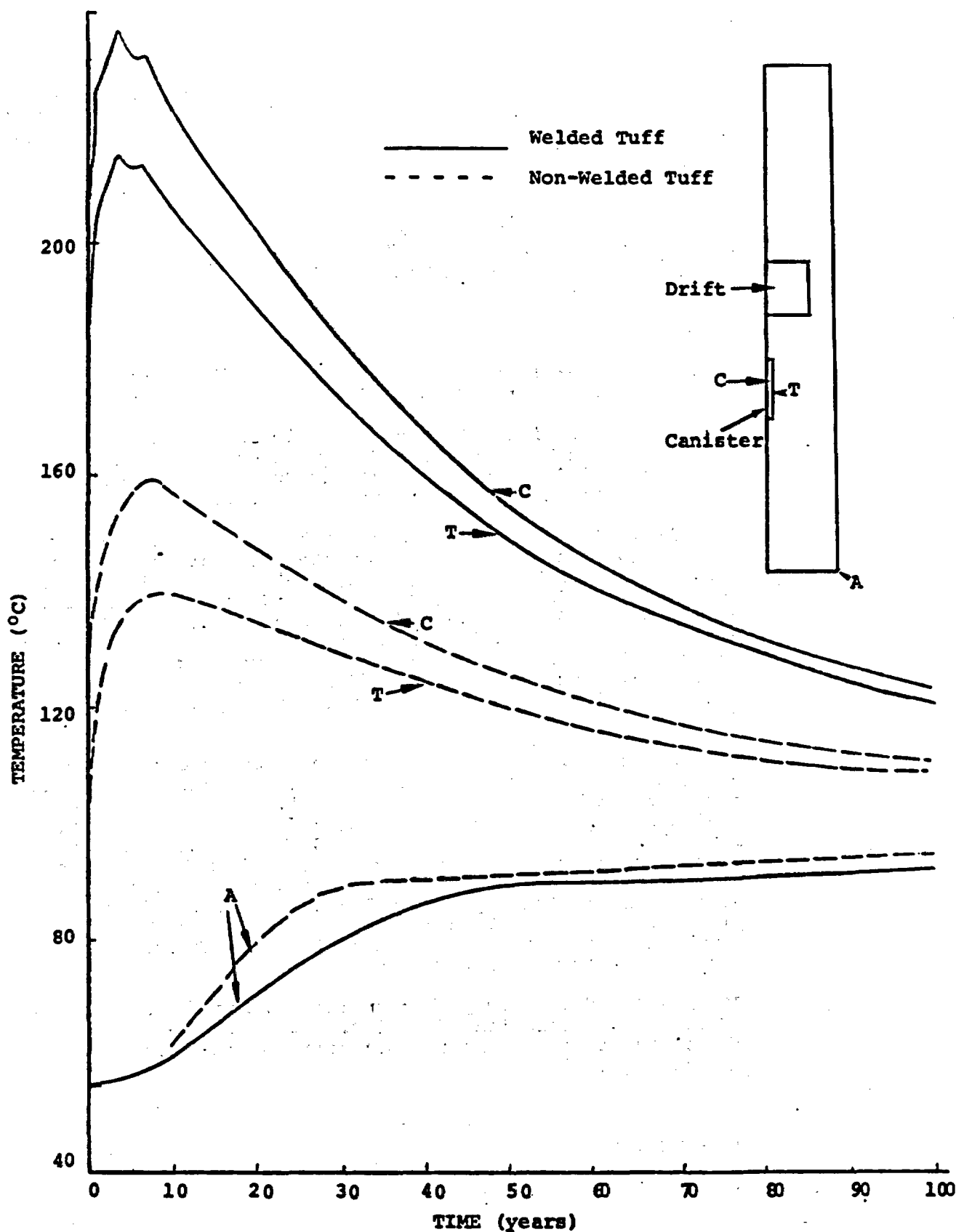


Figure 2. Canister, Tuff and Boundary Temperatures for Welded and Non-Welded Tuff, 1.0 KW/can

Sandia Laboratories

Albuquerque, New Mexico
Livermore, California

date: July 3, 1980

to: Distribution

J. J. Eaton *C. M. Korbin*
from: R. R. Eaton and C. M. Korbin - 5511

subject: Single Canister Thermal Calculations in Welded Tuff for an Initial Tuff Temperature of 35°C

Ref: Single Canister Thermohydrologic Calculations to Estimate Very Near-Field Temperatures, Pressures, and Boiling Regions Resulting From Emplacement of High Level Waste (HLW) in Welded Tuff

A preliminary thermal analysis has been made for the very near-field of a single nuclear waste canister containing 2.16 kW of High Level Waste (HLW) emplaced in welded tuff for an Extraction Ratio (ER) of 20% and repository loadings equal to 50, 75, and 100 kW/acre. The effective radius concept as discussed in the reference was used to determine the radial extent of the computational mesh grid, Table I. Additional specifications regarding capacitances, conductivities, geometry and densities are given in Table II.

The primary purpose of making these calculations was to predict the maximum canister and tuff temperatures and the times at which they occur. Figures 1, 2, 3, and 4 show canister midplane temperatures as a function of time for several radial locations. Figure 5 shows the effect of global canister loading (kW/acre) on maximum canister and tuff temperature. The maximum predicted temperatures are nearly linear with repository loading. Figures 6, 7 and 8 give radial distribution of temperatures along the centerplane of the canister at a time when the canister temperature is maximum.

Figures 9 and 10 show peak temperatures for the 50 and 100 kW cases as a function of radius. It should be noted that the times at which peak temperatures occur increases for increasing radius.

RRE;CMK;5511:lh

Distribution:
4530 Dick Lynch
4537 Roger Zimmerman
4537 Brenda Langkopf (5)
4537 Richard Shaw
4537 Al Lappin
4537 Lynn Tyler
4537 Keith Johnstone
4541 Bill Wowak
5511 Jace Nunziato
5511 Dave Gartling
5511 Roger Eaton
5511 Chris Korbin
5521 Lee Davison
5521 Bob Thomas
5532 Bill Olsson
5532 Barry Butcher
5541 Bill Luth
5812 Clyde Northrup

TABLE I

Case	R_{eff} (m)	$R_{drift} = H_{drift}$ (m)
1	7.45	3.3
2	6.09	2.7
3	5.27	2.4

TABLE II

$$K = \begin{cases} 2.4 & T < T_{\text{boil}} \\ 1.65 & T > T_{\text{boil}} \end{cases}$$

$$\rho C_p = \begin{cases} 3.64 \text{ E6} & T < (T_{\text{boil}} - 10^\circ\text{C}) \\ 1.72 \text{ E6} & T > (T_{\text{boil}} + 10^\circ\text{C}) \\ 2.5 \text{ E7} & (T_{\text{boil}} - 10^\circ\text{C}) < T < (T_{\text{boil}} + 10^\circ\text{C}) \end{cases}$$

Canister

$$K = 1.21$$

$$\rho = 2995$$

$$C_p = 0.834\text{E3}$$

$$T_{\text{boil}} = 100^\circ\text{C}$$

Units

$$K(\text{J/S} \cdot \text{m}^\circ\text{C}), \rho(\text{kg/m}^3), C_p(\text{J/kg}^\circ\text{C})$$

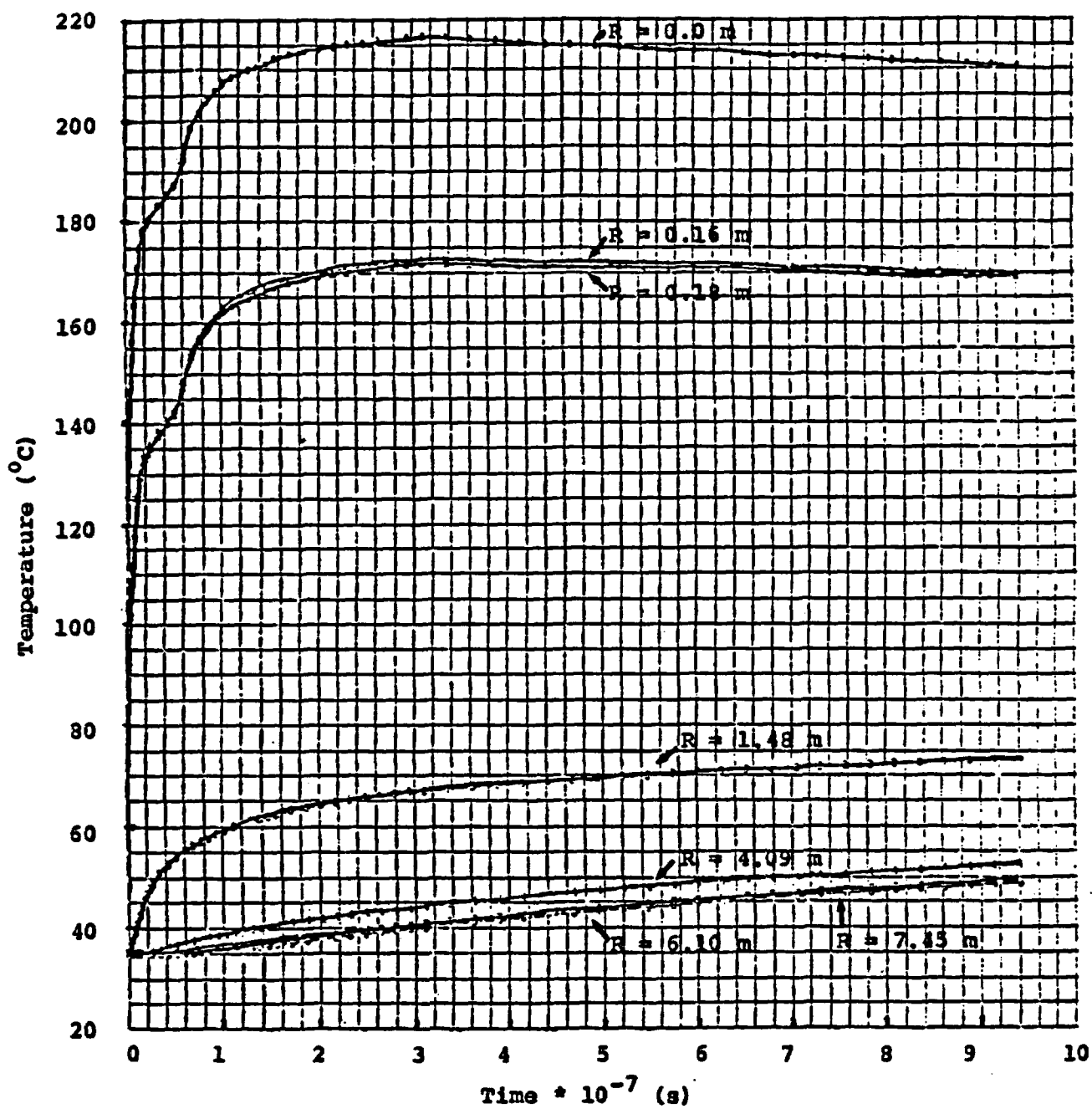


Figure 1. Canister and Tuff Temperatures at Several Radial Locations Along Centerplane of Canister: 50 kW/Acre, 2.16 kW/Can, 20% ER, Maximum Time = 9.5×10^7 s.

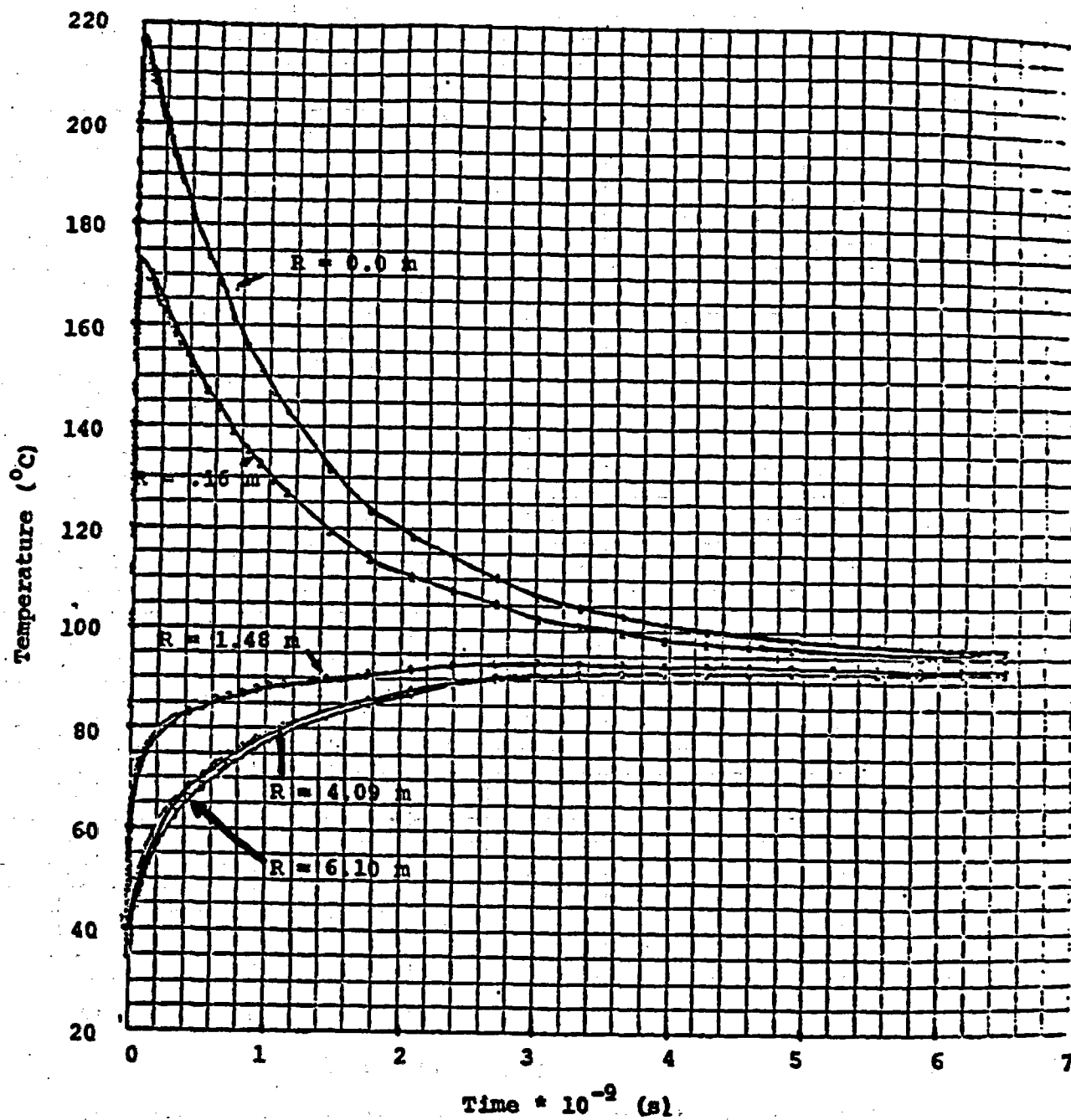


Figure 2. Canister and Tuff Temperatures at Several Radial Locations Along Centerplane of Canister: 50 kW/Acre, 2.16 kW/Can, 20% ER.

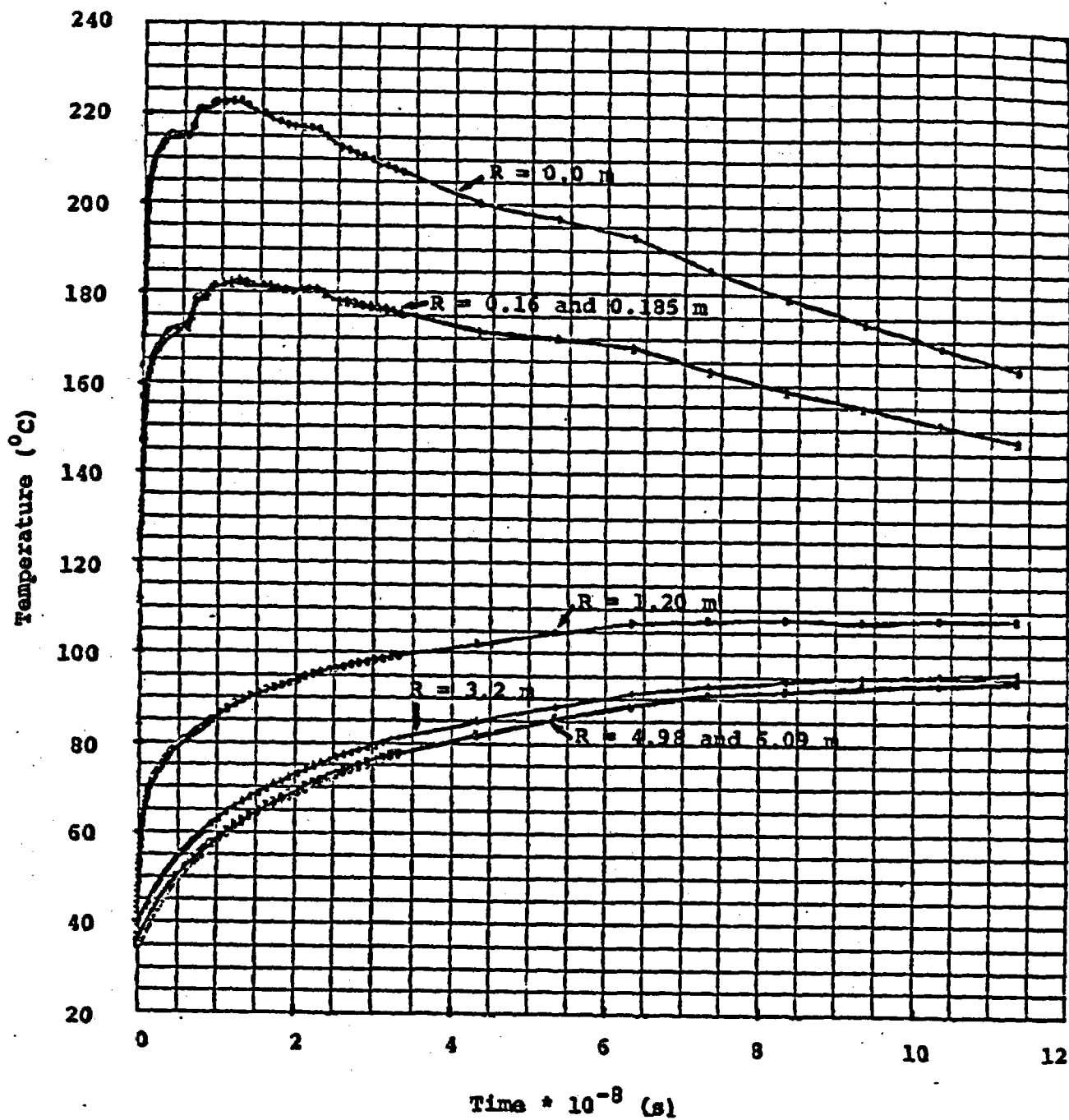


Figure 3. Canister and Tuff Temperatures at Several Radial Locations Along Centerplane of Canister: 75 kW/Acre, 2.16 kW/Can, 20% ER.

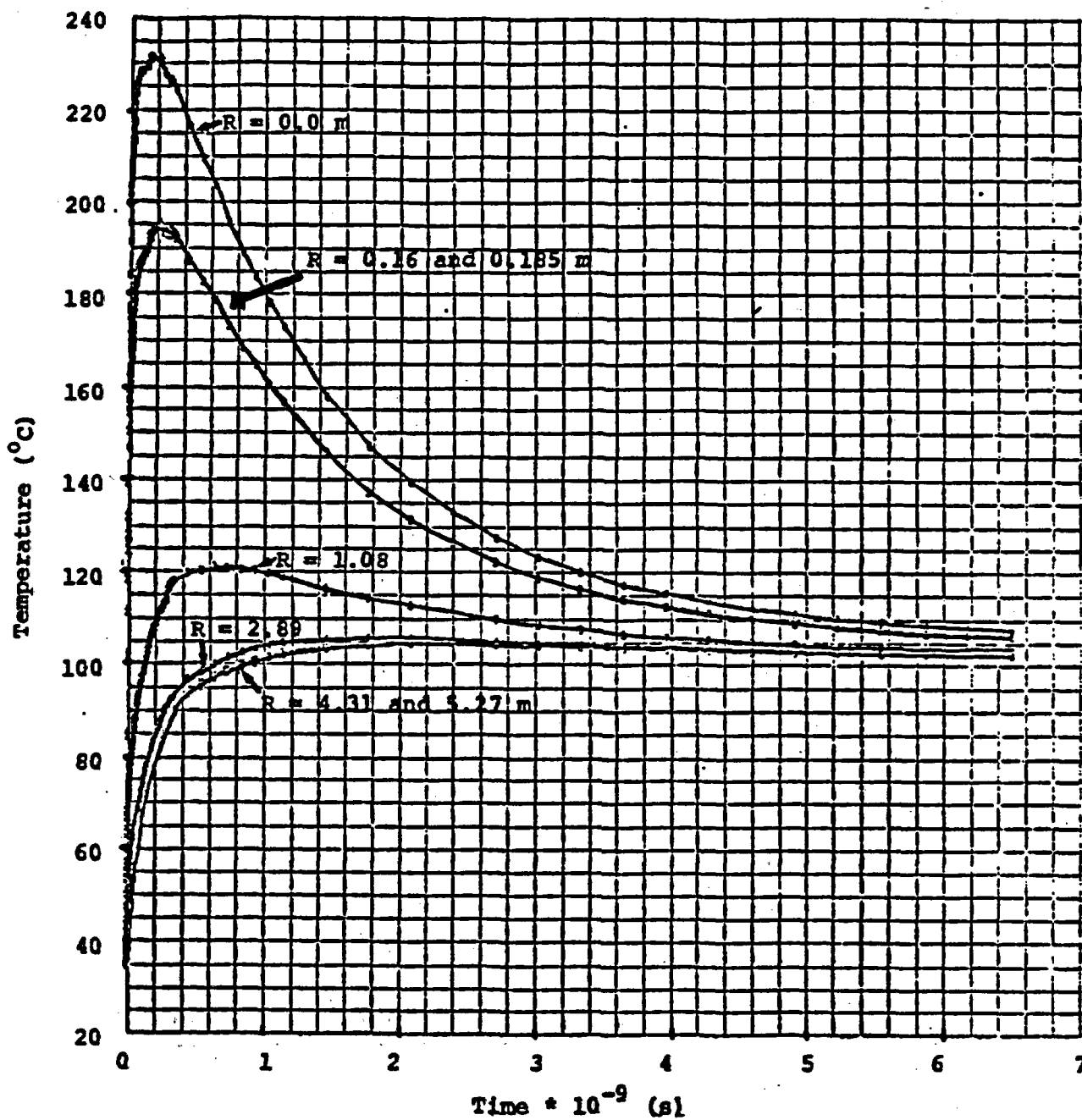


Figure 4. Canister and Tuff Temperatures at Several Radial Locations Along Centerplane of Canister: 100 kW/Acre, 2.16 kW/Can, 20% ER.

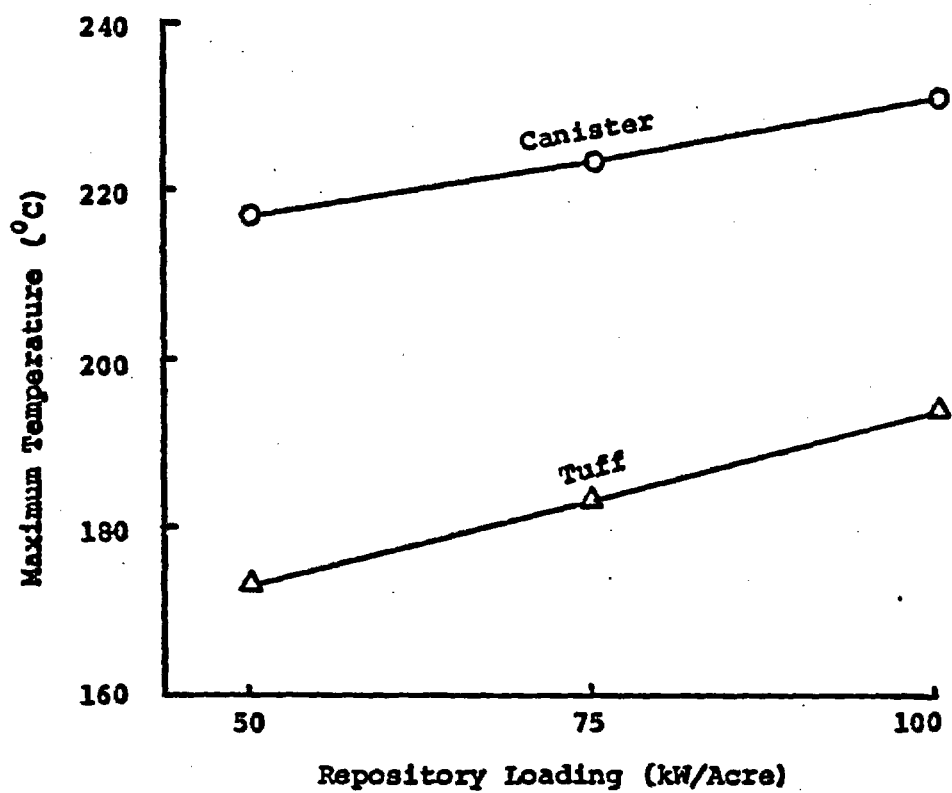


Figure 5. Effect of Repository Loading on Maximum Canister and Tuff Temperatures.

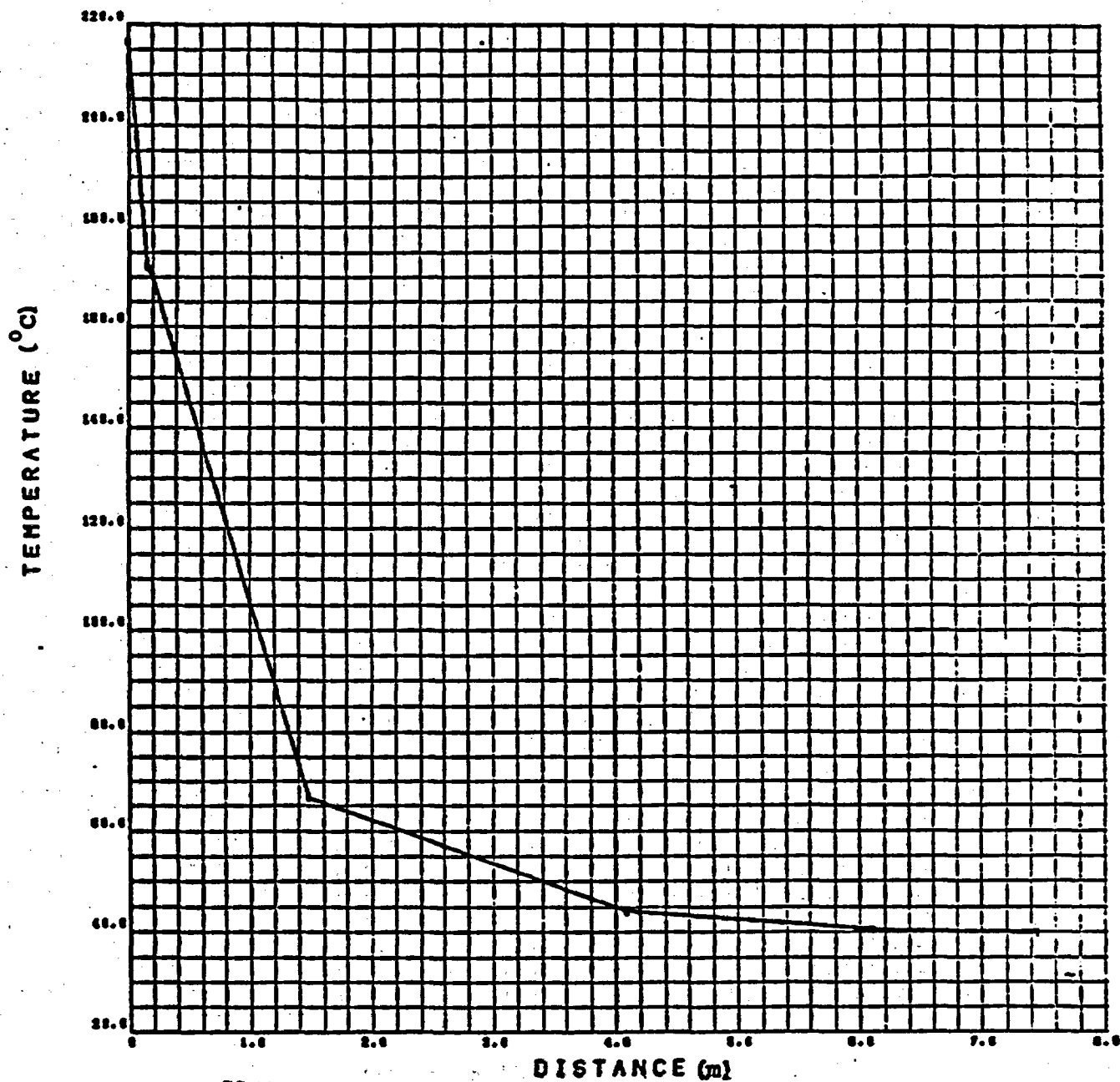


Figure 6. Temperature Distribution Through Canister Midplane at a Time When Canister Temperature is Maximum:
 $t = 3 \times 10^7$ s, 50 kW/Acre, 2.16 kW/Can, 20% ER.

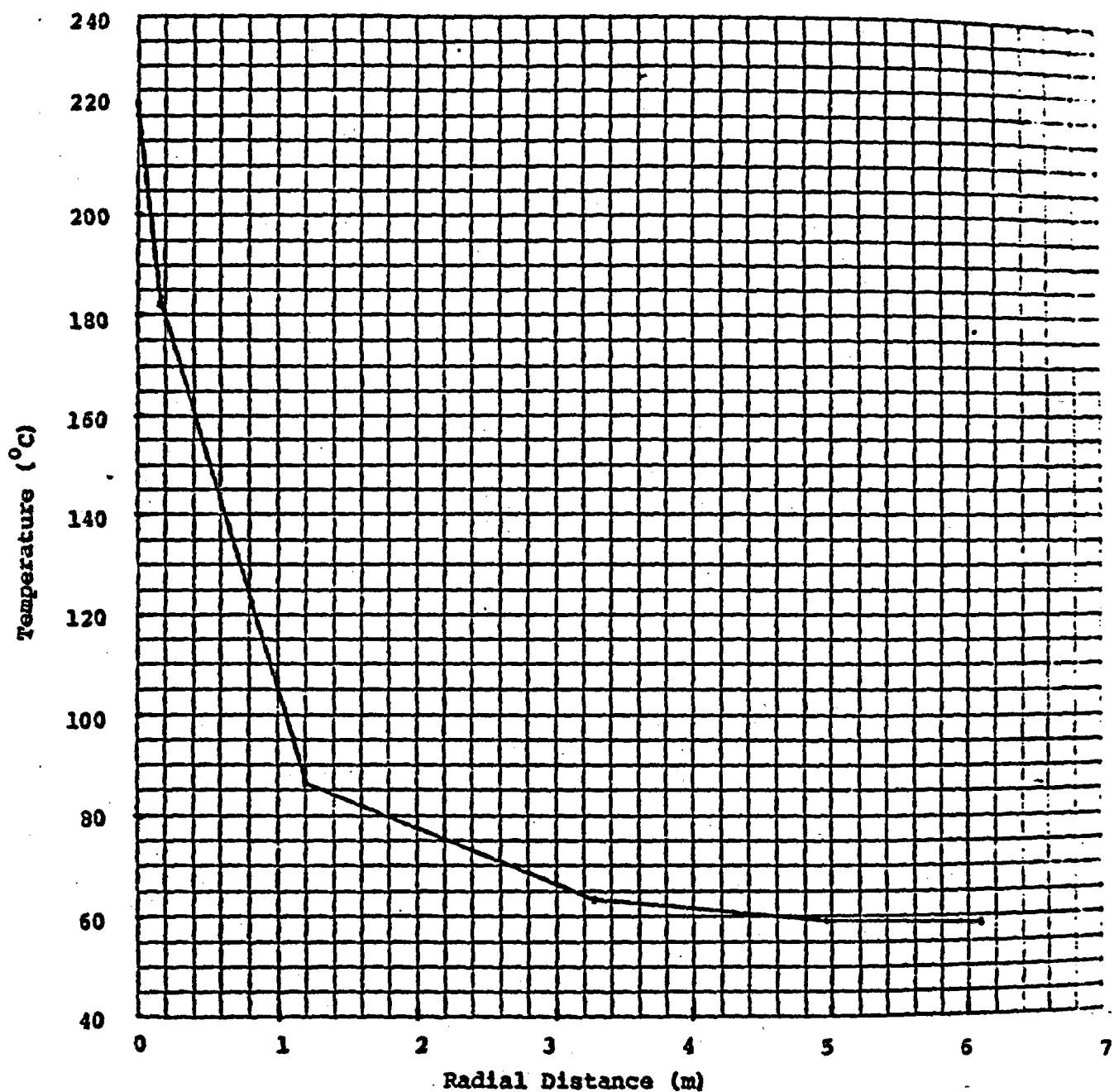


Figure 7. Temperature Distribution Through Canister Midplane at a Time When Canister Temperature is Maximum: $t = 1 \times 10^8$ s, 75 kW/Acre, 2.16 kW/Can, 20% ER.

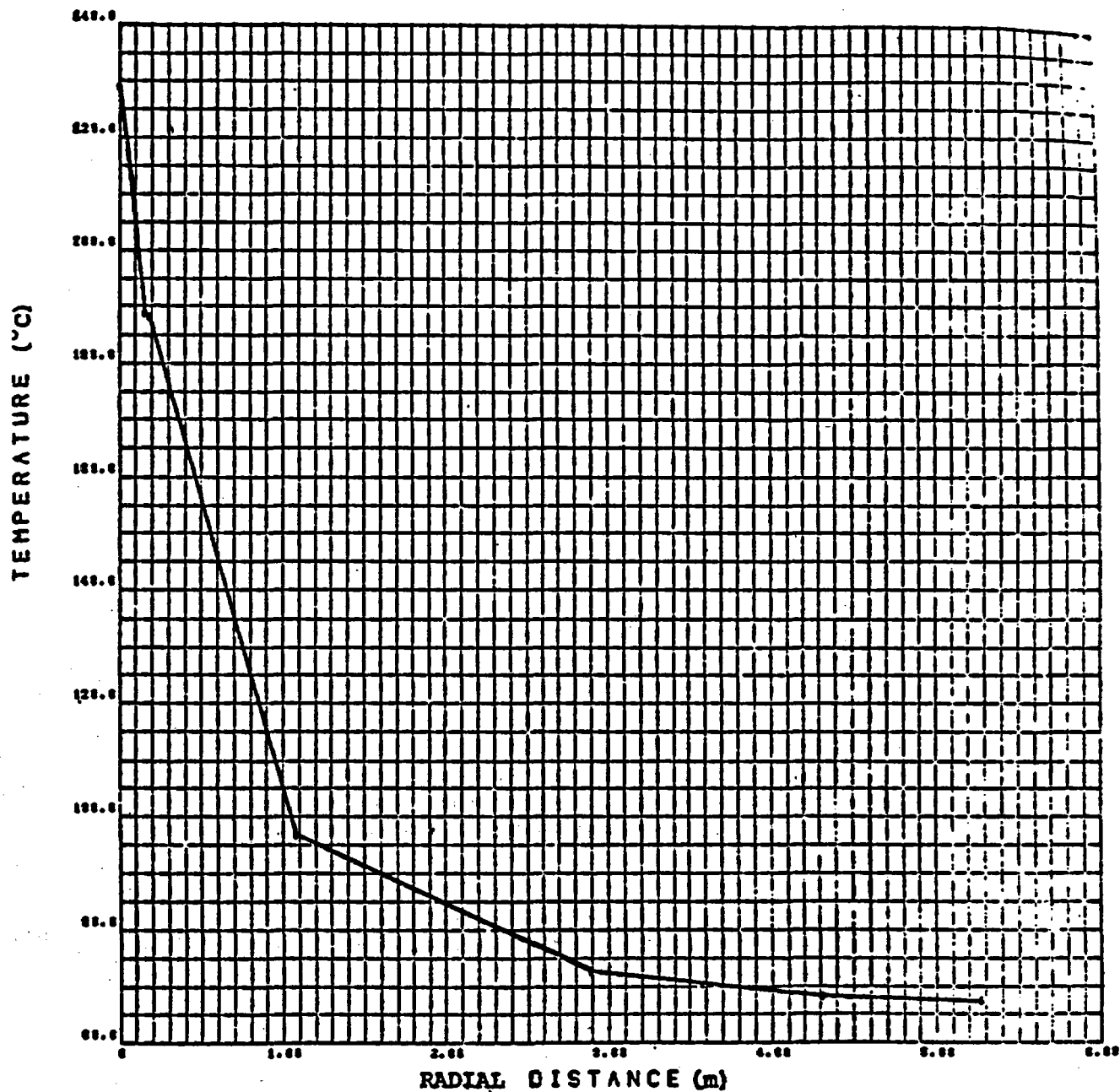


Figure 8. Temperature Distribution Through Canister Midplane at a Time When Canister Temperature is Maximum:
 $t = 2 * 10^8$ s, 100 kW/Acre, 2.16 kW/Can, 20% ER.

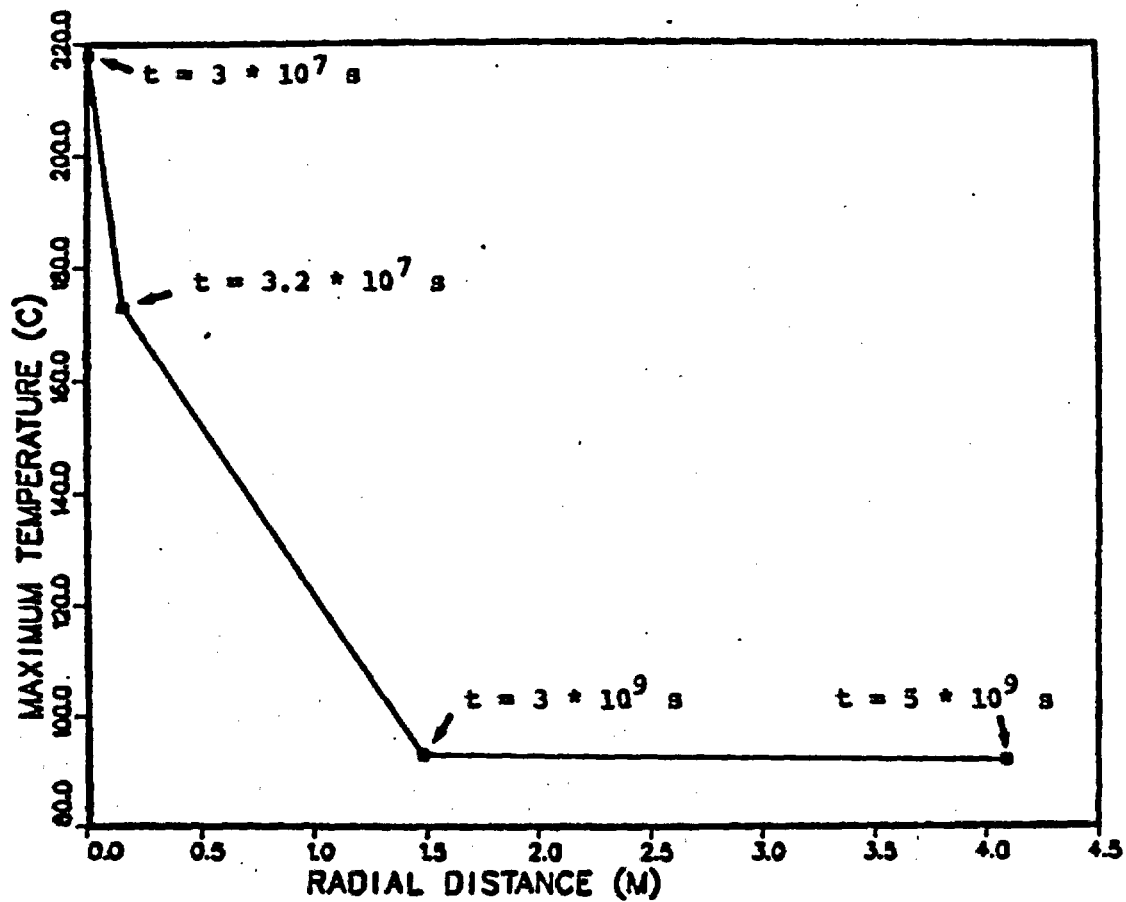


Figure 9. Radial Distribution of Maximum Temperatures Along Canister Centerplane: 50 kW/Acre, 2.16 kW/Can, 20% ER.

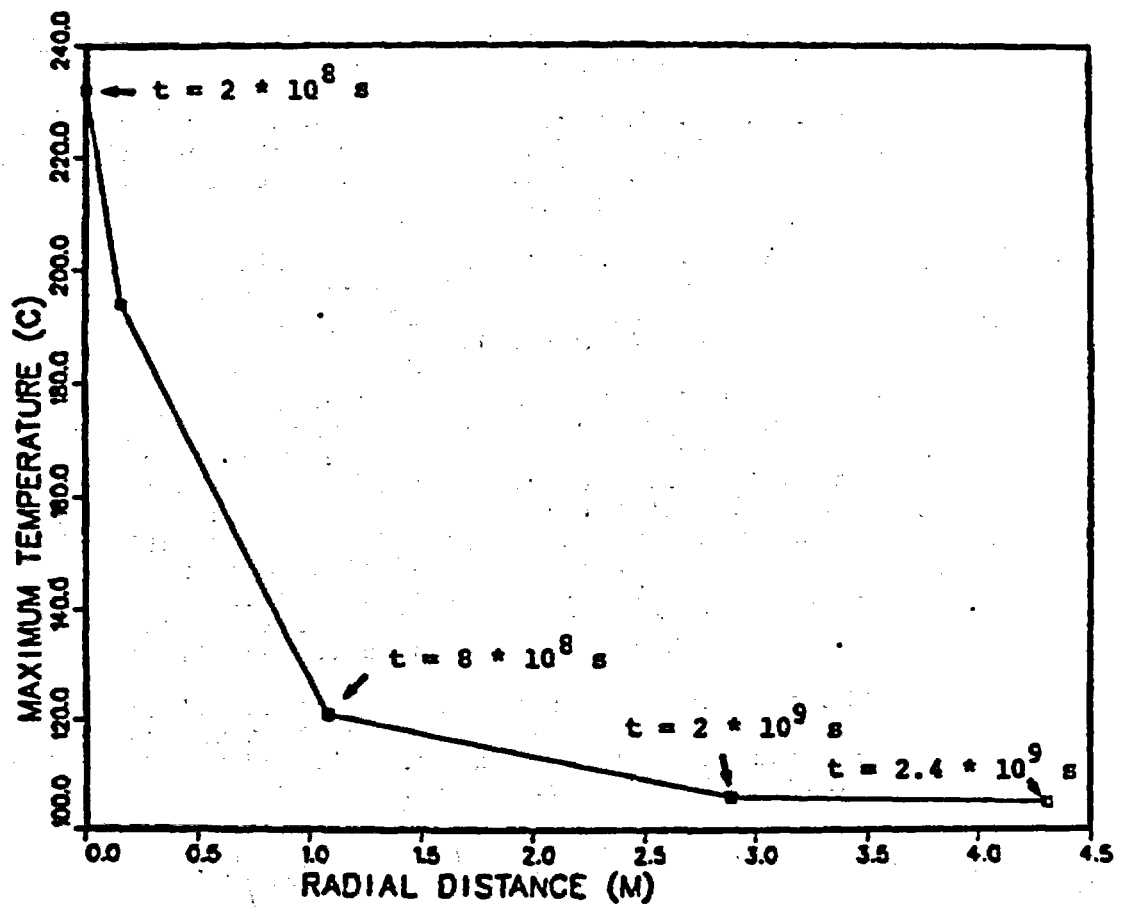


Figure 10. Radial Distribution of Maximum Temperatures Along Canister Centerplane: 50 kW/Acre, 2.16 kW/Can, 20% ER.

Sandia National Laboratories

Albuquerque, New Mexico 87185

date: November 12, 1980

to: Distribution

from: 
R. R. Eaton and R. K. Thomas - 5521

subject: Comparison of Effective Radius 2-Dimensional Thermal Simulation
With Full 3-Dimensional Results

Ref. 1. D. K. Gartling "Coyote - A Finite Element Computer Program for Non-Linear Heat Conduction Problems," SAND77-1322, Sandia Laboratories, Albuquerque, NM, June, 1978.

Ref: 2. K. J. Bathe, "ADINAT - A Finite Element Program For Automatic Dynamic Incremental Nonlinear Analysis of Temperatures," MIT Report 8 2 448-5, May, 1977 (Revised 1978).

This memo compares the results of two-dimensional effective radius (2-D)¹ and three-dimensional (3-D)² thermal analysis of the very near field of a simulated HLW heat source buried in tuff. Previously, numerous studies have been made using a two-dimensional effective radius model to simulate three dimensional problems. This 2-D model greatly simplifies the code set up procedure and significantly reduces the required computer run time. The intent of this memo is to document the details of this simplified model and to compare the results with a full 3-D conduction model.

The numerical nodalization for the two-dimensional axisymmetric model is based on an effective radius or unit cell concept where r_{eff} is the location of the far adiabatic boundary (see Figure 1 and 2),

$$r_{eff} = \left((h_1 \times h_2) / \pi \right)^{1/2}$$

The drift dimension was determined such that $\pi r^2 = h_1 \times W$ (equal floor area/can) and $2\pi r_d \times Z_d = 2 \times h_2 \times H$ (equal wall area/can). H equals the height of the drift. See Table 1 for material properties and problem dimensions. The vertical extent of the numerical zoning was $\pm 150m$ from the floor of the mine drift. From symmetry consideration, the 3-D model spans the cross-hatched region ($h_1/2$ by $h_2/2$).

The results of these two calculations are given in Fig. 3 and 4. All data is taken from the canister horizontal center plane location at various radial distances along the pitch line, Fig. 2a. The results show that temperatures calculated from the 3-D model are consistently higher, in the rear region of the canister, than those obtained from the 2-D effective radius model. Peak temperatures calculated by the effective radius model are approximately 10% lower than those obtained by the 3-D formulation. The times for the peak temperature to occur are within 0.5 years of each other.

The higher peak temperature for the 3-D case is in part a result of the adiabatic wall in the vicinity of the heat source. It is located at $Y = 1.7$ m for the 3-D model and $r = 5.27$ m for the 2-D case. An adiabatic wall in the near vicinity of the canister tends to result in higher temperatures because it greatly restricts heat release in the pitch direction.

The 2-D approximation is well suited for parametric type studies. The input code data cards for this geometry are reasonably easy to generate and the run times for the 2-D program are about one order of magnitude less than that required for the 3-D runs. However, if more accurate absolute temperatures are required, then the additional effort and expenses required for the 3-D runs are justified.

Distribution:

4530 D. Lynch
4537 K. Johnstone
4537 R. Zimmerman
4537 Brenda Langkopf (5)
4537 R. Shaw
4537 A. Lappin
4537 L. D. Tyler
5500 O. E. Jones
5510 D. B. Hayes
5511 J. W. Nunziato
5511 D. K. Gartling
5511 R. R. Eaton
5511 W. D. Sundberg
5520 T. B. Lane
5521 L. W. Davison
5521 B. Thomas

TABLE I

Material Properties

K_{Tuff}	=	2.4 J/s·m°C
K_{canister}	=	1.21 J/s·m°C
$K_{\text{airgap}} = K_{\text{tunnel}}$	=	25 J/s·m°C
$(\rho C_p)_{\text{tuff}}$	=	3.64E6 J/m ³ °C
$(\rho C_p)_{\text{can}}$	=	2.48E6 J/m ² °C

Problem Dimensions

Pitch	=	3.4 m
Drift c to c	=	23.8 m
Output	=	2.16 kW/can (HLW)
Loading	=	100 kW/acre

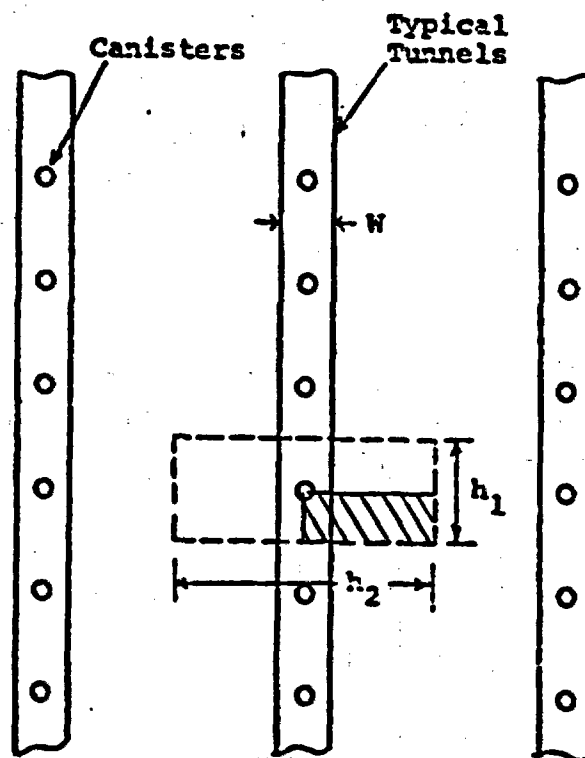


Figure 1. Plain view of Mine Drifts
Broken Lines Encompass Region
of Interest for 2-D model. The
3-D model encompasses the cross-
hatched domain.

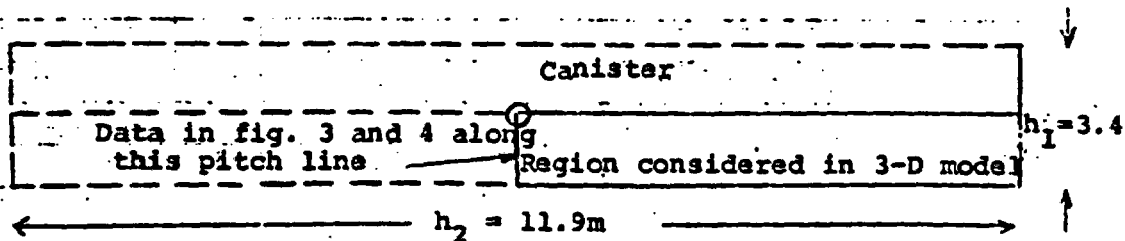


Fig. 2a Plain View of 3-D problem

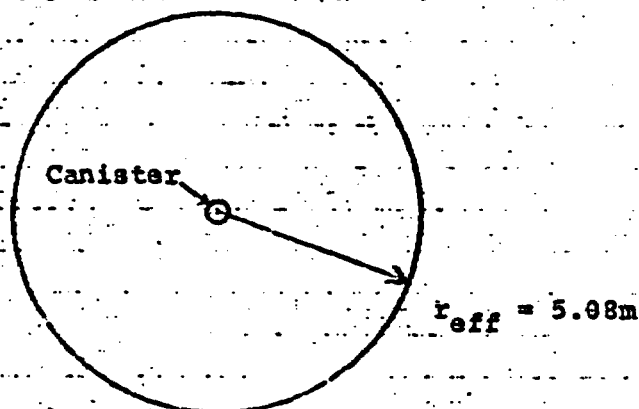


Fig. 2b Plain View of Effective-Radius, 2-D model

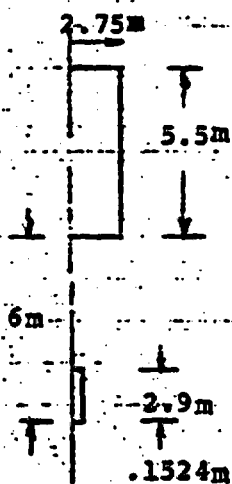


Fig. 2c Vertical View of drift and canister

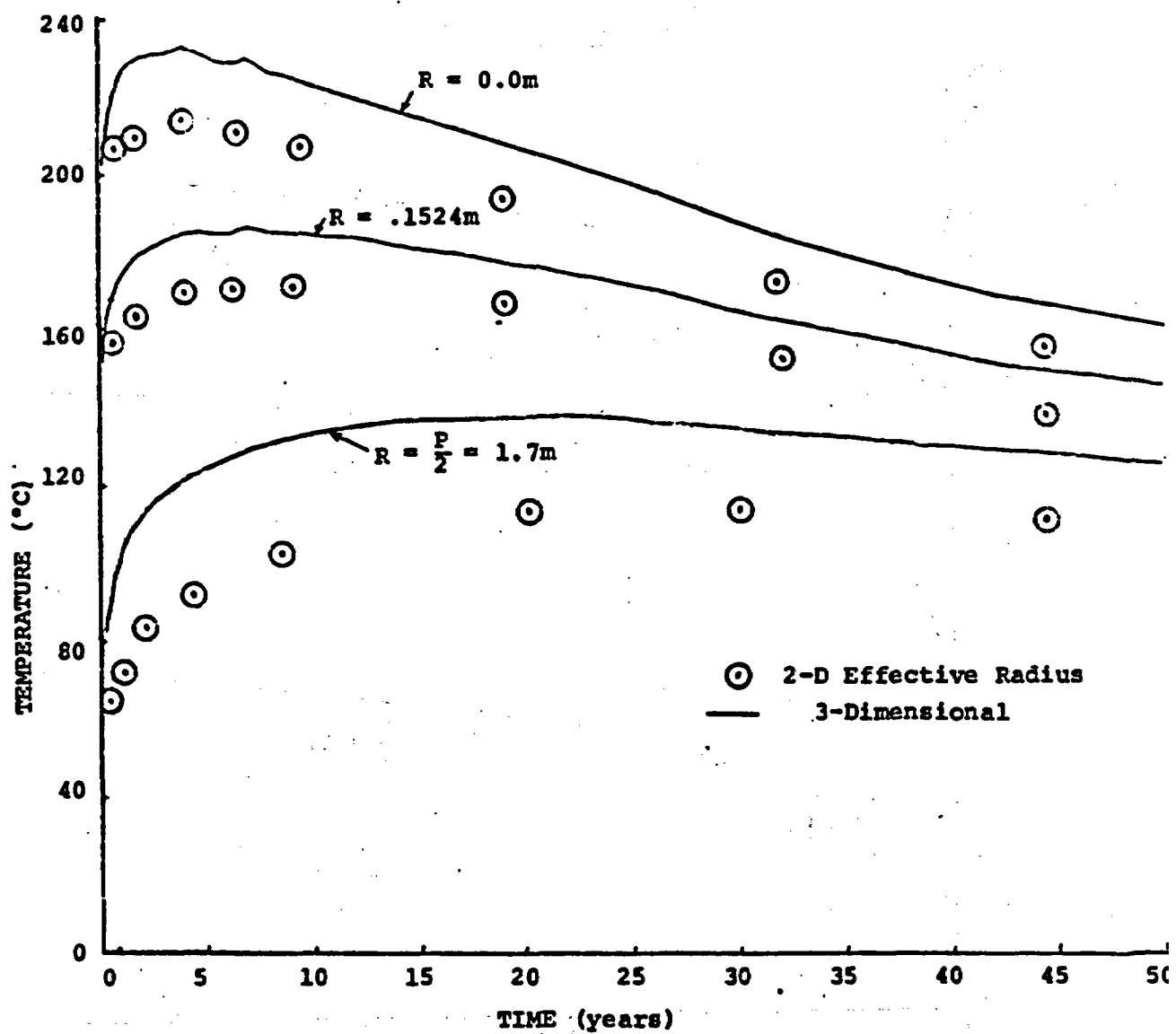


Fig. 3 Comparison of 2-D and 3-D Temperature Profiles, $t_{\text{max}} = 50$ yrs.

2-D Effective Radius
3-Dimensional

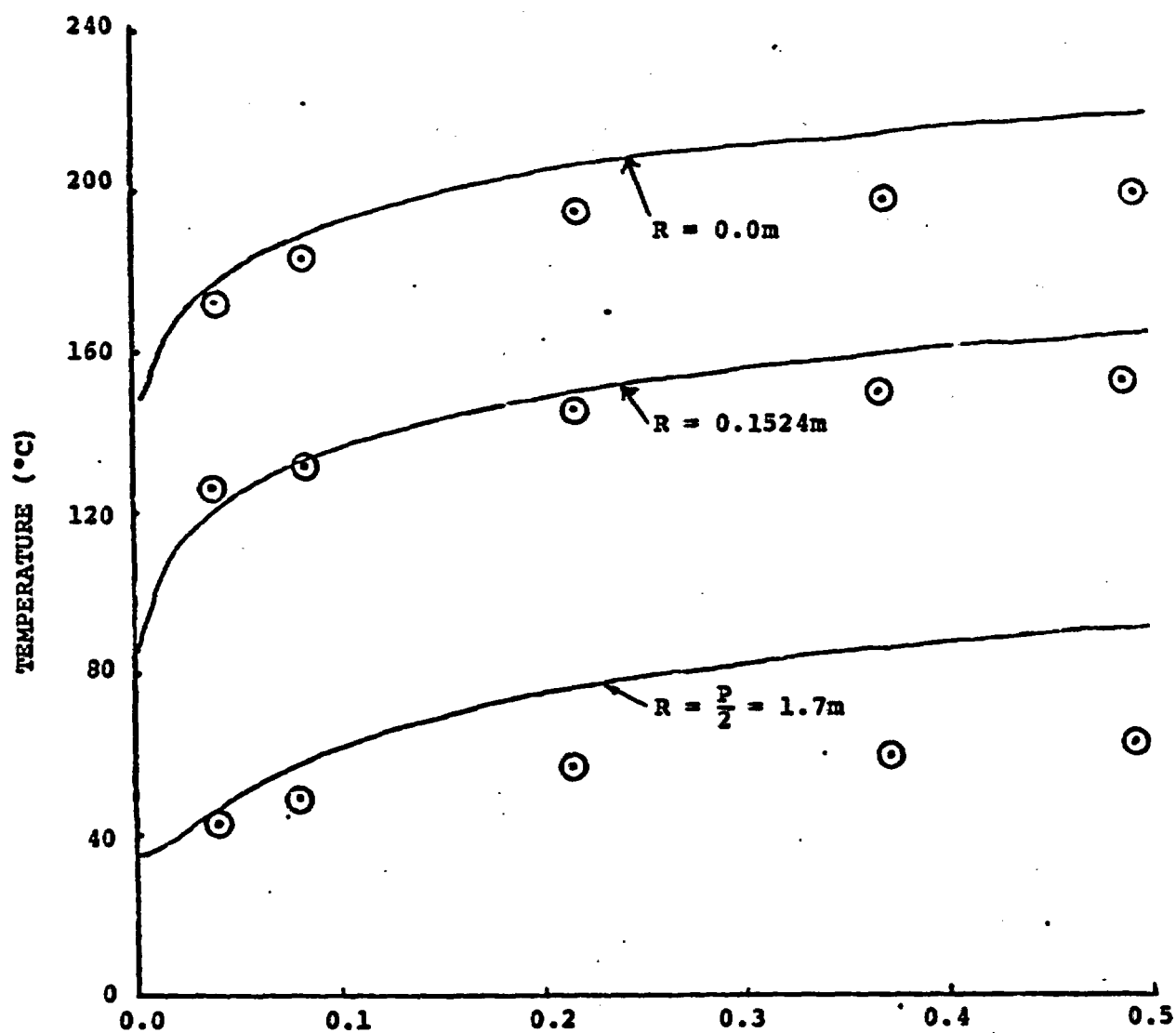


Fig. 4 Comparison of 2-D and 3-D Temperature Profiles
at three locations, see fig. 2, $t_{\max} = 0.5$ yr.

DISTRIBUTION:

U.S. Department of Energy
Assistant Secretary
for Defense Programs
MS SF-066
Washington, DC 20545
Attn: Duane C. Sewell (DP-1)

U.S. Department of Energy
Assistant Secretary
Nuclear Energy
MS 6E-098
Washington, DC 20545
Attn: G. W. Cunningham (NE-1)

U.S. Department of Energy
Office of Nuclear
Waste Management
MS B-107
Germantown, MD 20767
Attn: Sheldon Meyers (NE-30)
R. G. Romatowski (NE-30)
Colin A. Heath (NE-330)
D. L. Vieth (NE-332)
Ralph Stein (NE-330)
Carl R. Cooley (NE-330)
Mark W. Frei (NE-332)
G. P. Dix (EV-12)
Carl D. Newton (NE-30)

U.S. Department of Energy
Richland Operations Office
P.O. Box 550
Richland, WA 99352
Attn: Frank Standerfer
David J. Squires

U.S. Department of Energy
Albuquerque Operations Office
P.O. Box 5400
Albuquerque, NM 87115
Attn: D. T. Schueler, Jr.

U.S. Department of Energy
San Francisco Operations Office
1333 Broadway, Wells Fargo Bldg.
Oakland, CA 94612
Attn: L. Lanni

Rockwell International
Atomics International Division
Rockwell Hanford Operations
Richland, WA 99352
Attn: R. Deju
B. Dietz

U.S. Department of Energy
Nevada Operations Office
P.O. Box 14100
Las Vegas, NV 89114

Attn: M. E. Gates
R. W. Taft
R. W. Newman
J. B. Cotter
M. P. Kunich
H. L. Melancon
C. P. Bromley
R. H. Richards
F. C. Hood
A. J. Roberts
R. M. Nelson
D. F. Miller
P. J. Mudra
R. Marks, CP-1, MS 210
S. R. Elliott
B. W. Church
T. H. Blankenship
R. R. Loux (10)

U. S. Department of Energy
NTS Support Office
P.O. Box 435
Mercury, NV 89023
Attn: J. H. Dryden, MS 701
F. Huckabee, MS 701
L. P. Skousen, MS 701

Director of External Affairs
U.S. Department of Energy
DOE-IX
333 Market Street, 7th Floor
San Francisco, CA 94105
Attn: D. J. Cook

U. S. Department of Energy
National Program Office
505 King Avenue
Columbus, OH 43201
Attn: J. O. Neff

Nuclear Regulatory Commission
Washington, DC 20555
Attn: J. C. Malaro, MS SS-674
R. Boyle, MS P-522
D. Alexander, MS 905SS

Holmes & Narver, Inc.
P.O. Box 14340
Las Vegas, NV 89114
Attn: A. E. Gurrola, MS 158

Lawrence Livermore
National Laboratory
P.O. Box 808
Livermore, CA 94550

Attn: L. D. Ramspott, L-204
A. Holzer, L-209
L. B. Ballou, L-204
R. L. Wagner, L-1
K. Street, L-209
W. C. Patrick, L-204
A. B. Miller, L-204
D. J. Isherwood, L-224

Los Alamos Scientific Laboratory
University of California
P.O. Box 1663
Los Alamos, NM 87545
Attn: K. Wolfsberg, MS 514
L. S. Germain, MS 570
L. Lanham, MS 753
B. R. Erdal, MS 514
J. R. Smyth, MS 978

Westinghouse
P.O. Box 708
Mercury, NV 89023
Attn: A. R. Hakl, MS 703 (8)

Westinghouse - AESD
P.O. Box 10864
Pittsburgh, PA 15236
Attn: J. B. Wright (6)
W. R. Morris
T. E. Cross
R. J. Bahorich
C. R. Bolmgren
W. A. Henninger

Nuclear Fuel Cycle Research
University of Arizona
Tucson, AZ 85721
Attn: J. G. McCray

U.S. Geological Survey
National Center
Reston, VA 22092
Attn: G. D. DeBuchananne, MS 410
P. R. Stevens, MS 410
D. B. Steward, MS 959

U.S. Geological Survey
P.O. Box 25046
Federal Center
Denver, CO 80301
Attn: W. S. Twenhofel, MS 954
G. L. Dixon, MS 954

Geologic Society of America
3300 Penrose Place
Boulder, CO 80301
Attn: J. C. Frye

Kansas Geological Survey
University of Kansas
Lawrence, KS 66044
Attn: W. B. Hambleton

Battelle
Office of Nuclear Waste Isolation
505 King Avenue
Columbus, OH 43201
Attn: N. E. Carter
S. C. Matthews
W. M. Hewitt
R. J. Hall
S. J. Basham
G. E. Raines
N. J. Hubbard
J. E. Monsees
J. A. Carr
ONWI Library (5)
R. A. Robinson
W. A. Carbiener

State of Nevada
Capitol Complex
Carson City, NV 89710
Attn: Robert Hill
State Planning Coord.
Governor's Office of
Planning Coordination

Fenix & Scisson, Inc.
P.O. Box 498
Mercury, NV 89023
Attn: F. D. Waltman, MS 940

State of Nevada
Capitol Complex
Carson City, NV 89710
Attn: N. Clark
Department of Energy

Woodward-Clyde Consultants
No. 3 Embarcadero Center
San Francisco, CA 94111
Attn: Western Region Library

Department of Chemistry
Idaho State University
Pocatello, ID 83201
Attn: J. L. Thompson

Holmes & Narver, Inc.
P.O. Box I
Mercury, NV 890-23
Attn: G. E. Christensen, MS 605

J. A. Blume Enegineers
Sheraton Palace Hotel
130 Jessie Street
San Francisco, CA 94105
Attn: P. Yanev

Department of Earth Sciences
Harvard University
Cambridge, MA 02138
Attn: R. Siever

Department of Earth Sciences
Dartmouth College
Hanover, NH 03755
Attn: J. Lyons

Intl. Atomic Energy Agency
Division of Nuclear Power
and Reactors
Karntner Ring 11
P.O. Box 590, A-1011
Vienna, Austria
Attn: J. P. Colton

Fenix & Scisson, Inc.
P.O. Box 15408
Las Vegas, NV 89114
Attn: J. A. Cross, MS 514

Department of Civil Engineering
Princeton University
Princeton, NJ 07540
Attn: G. Pinder

California Energy Resources
Conservation & Development
Commission
1111 Howe Avenue
Sacramento, CA 95825
Attn: Art Soinski

Lawrence Berkeley Laboratory
Energy & Environment Division
University of California
Berkeley, CA 94720
Attn: P. Witherspoon

Hanford Engineering Development
Laboratory
P.O. Box 1970
Richland, WA 99352

Arthur D. Little, Inc.
Acorn Park
Cambridge, MA 02140
Attn: C. R. Hadlock

Department of Geological
Sciences
Brown University
Providence, RI 02912
Attn: Bruno Giletti

Center for Tectonophysics
Texas A&M University
College Station, TX 77840
Attn: J. Handin

Law Engineering Testing Co.
2749 Delk Road, SE
Marietta, GA 30067
Attn: Bud Woodward

Subcommittee on Energy
Research and Production
Room B-374
Rayburn House Office Bldg.
Washington, DC 20575
Attn: Steve Lanes, Staff Dir.

Bureau of Radiation Control
Dept. of Health & Environment
Forbes Field
Topeka, KS 66620
Attn: G. W. Allen, Director

Energy Research and Policy
State of Connecticut
80 Washington Street
Hartford, CT 06115
Attn: Ms. F. N. Brenneman

Executive Office
Lansing, MI 48909
Attn: William C. Taylor
Science Advisor

Director for Policy & Planning
Room 300, 325 West Adams Street
Springfield, IL 62706
Attn: Dr. Anthony Liberatore

Nuclear Projects Coordinator
Nuclear Energy Division
P.O. Box 14690
Baton Rouge, LA 70808
Attn: L. Hall Bohlinger

Oregon Department of Energy
Labor & Industries Bldg.
Room 111
Salem, OR 97310
Attn: Donald W. Godard

Radiation Protection Division
1000 Northeast 10th Street
P.O. Box 53551
Oklahoma City, OK 73152
Attn: R. L. Craig, Director

Reynolds Electrical and
Engineering Co., Inc.
P.O. Box 14400
Las Vegas, NV 89114
Attn: H. D. Cunningham, MS 555
W. C. Flangas, MS 615
G. W. Adair, MS 154
V. M. Milligan, MS 765
C. W. Dunnam, MS 745
R. L. Powell, MS 634
R. B. Land, MS 585

Radiation Health
Information Project
Environmental Policy Inst.
317 Pennsylvania Ave., SE
Washington, DC 20003
Attn: Ms. Elli Walters

Nuclear Safety Associates, Inc.
5101 River Road
Bethesda, MD 20016
Attn: J. A. Lieberman

Federal Agency Relations
1050 17th St., NW
Washington, DC 20036
Attn: O. H. Davis, Director

Environmental Prog. Supervisor
903 Ninth Street Office Bldg.
Richmond, VA 23219
Attn: Keith J. Buttleman

Energy Administration
Department of Natural Resources
Tawes State Office Bldg.
Annapolis, MD 21401
Attn: Paul Massicot, Actg. Dir.

State of Ohio Environmental
Protection Agency
Box 1049, 361 E. Broad St.
Columbus, OH 43216
Attn: J. F. McAvoy, Director

State of Connecticut
House of Representatives
One Hundred and Sixth District
24 Rock Ridge Road
Newtown, CT 06470
Attn: J. W. Anderson

Missouri Department
of Natural Resources
P.O. Box 176
Jefferson City, MO 65102

Mississippi Department
of Natural Resources
Suite 228, Barefield Complex
455 North Lamar Street
Jackson, MS 39201
Attn: P. T. Bankston

Tennessee Energy Authority
Suite 708 Capitol Blvd. Bldg.
Nashville, TN 37219
Attn: J. A. Thomas, Assoc. Dir.

Council Member
374 South Rock River Drive
Berea, OH 44017
Attn: Dr. G. A. Brown

Public Law Utilities Group
One American Place, Suite 1601
Baton Rouge, LA 70825
Attn: Ms. D. Falkenheier,
Assistant Director

Associate Dean for Research
Georgia Institute of Technology
Atlanta GA 30332
Attn: Richard Williams

Fenix & Scisson, Inc.
P.O. Box 498
Mercury, NV 89023
Attn: D. A. Robins, MS 940

Reynolds Electrical &
Engineering Co., Inc.
P.O. Box 14400
Las Vegas, NV 89114
Attn: E. H. Weintraub, MS 625

U.S. Department of Energy
Division of Waste Isolation
Germantown, MD 20767
Attn: J. W. Rowen, DP-342
M. E. Langston, ME-512

Energy Facility Site
Evaluation Council
820 East Fifth Avenue
Olympia, WA 98504
Attn: N. D. Lewis

University of Texas at Austin
University Station, Box X
Austin, TX 78712
Attn: E. G. Wermund

Department of Human Resources
73 Tremont Street
Boston, MA 02108
Attn: Dr. L. Morgenstern

Department of Environmental
Regulation
Twin Towers Office Bldg.
2600 Blair Stone Road
Tallahassee, FL 32301
Attn: D. S. Kell

Holmes & Narver
P.O. Box I
Mercury, NV 89023
Attn: V. L. Angell, MS 605

Westinghouse
P.O. Box 708
Mercury, NV 89023
Attn: R. L. Malloy, MS 703

EG&G, Inc.
P.O. Box 295
Mercury, NV 89023
Attn: W. C. Roper, MS 570/N24

Office of Nuclear Waste Isolation
505 King Avenue
Columbus, OH 43201
Attn: M. J. Golis

Hanford Engineering
Development Laboratory
P.O. Box 1970
Richland, WA 99352
Attn: D. L. Garland

Rockwell Hanford Operations
P.O. Box 800
Richland, WA 99352
Attn: D. A. Turner

Westinghouse Electric Corp.
P.O. Box 40039
Albuquerque, NM 87196
Attn: D. I. Hulbert

Oak Ridge National Laboratories
P.O. Box X
Oak Ridge, TN 37830
Attn: H. C. Claiborne

Rockwell Hanford Operations
Energy Systems Group
P.O. Box 800
Richland, WA 99352
Attn: K. R. Hoopingarner
Manager, Master Planning

Battelle Pacific Northwest
Laboratory
P.O. Box 999
Richland, WA 99352
Attn: J. L. McElroy

RE/SPEC, Inc.
P.O. Box 725
Rapid City, SD 57709
Attn: J. D. Osnes

Science Applications, Inc.
P.O. Box 843
Oak Ridge, TN 37830
Attn: L. D. Rickertsen

E. I. DuPont de Nemours & Co.
Savannah River Laboratory
Aiken, SC 29801
Attn: N. E. Bibler

Nuclear Environmental
Application Branch
Mail Station E-201 (Gtn)
U.S. Department of Energy
Washington, DC 20545
Attn: R. W. Barber, Actg. Chief

Gesellschaft fur Strahlen-und
Umweltforschung MBH Munchen
Institut fur Tieflagerung
3392 Clausthal-Zellerfeld
Berliner Strasse 2
Federal Republic of Germany
Attn: Klaus Kuhn

Hahn-Meitner-Institut fur
Kernforschung
Glienicker Strasse 100
1000 Berlin 39
Federal Republic of Germany
Attn: Klaus Eckart Maass

Bundesanstalt fur
Geowissenschaften und
Rohstoffe
Postfach 510 153
3000 Hannover 51
Federal Republic of Germany
Attn: Michael Langer

Kernforschung Karlsruhe
Postfach 3640
7500 Karlsruhe
Federal Republic of Germany
Attn: Reinhard Kraemer

Physikalisch-Technische
Bundesanstalt
Bundesallee 100, 3300 Braunschweig
Federal Republic of Germany
Attn: Helmut Rothemeyer

Bundesministerium fur Forschung
und Technologie
Postfach 200 706
5300 Bonn 2
Federal Republic of Germany
Attn: Rolf-Peter Randl

Georgia Institute of Technology
School of Nuclear Engineering
Atlanta, GA 30332
Attn: Melvin Carter

4530 R. W. Lynch
4537 L. D. Tyler (25)
4537 B. S. Langkopf
4537 A. R. Lappin
4537 R. M. Zimmerman
4537 R. Shaw
5500 O. E. Jones
5510 D. B. Hayes
5511 J. W. Nunziato
5511 D. K. Gartling
5520 T. B. Lane
5521 L. W. Davison
5521 N. D. Gilbertsen
5521 C. M. Stone
5521 R. K. Thomas
5522 R. L. Johnson
5530 W. Herrmann
5531 M. L. Blanford
5532 B. M. Butcher
5532 W. A. Olsson
5541 W. C. Luth
3141 L. J. Erickson (5)
3151 W. L. Garner (3)
For DOE/TIC (Unlimited Release)
DOE/TIC (25)
(J. Hernandez 3154-4)
8266 E. A. Aas

[illegible]